

UC Santa Barbara

UC Santa Barbara Electronic Theses and Dissertations

Title

The exceptional columbine: exploring the genetic basis of three ecologically important traits in a high alpine plant, *Aquilegia jonesii*

Permalink

<https://escholarship.org/uc/item/5fj638md>

Author

Johns, Jason

Publication Date

2023

Peer reviewed|Thesis/dissertation

UNIVERSITY OF CALIFORNIA

Santa Barbara

The exceptional columbine: exploring the genetic basis of three ecologically important traits
in a high alpine plant, *Aquilegia jonesii*

A dissertation submitted in partial satisfaction of the
requirements for the degree Doctor of Philosophy
in Ecology, Evolution, and Marine Biology

by

Jason Wells Johns

Committee in charge:

Professor Scott Hodges, Chair

Professor Evangeline Ballerini

Professor Ruth Finkelstein

Professor Thomas Turner

September 2023

The dissertation of Jason Wells Johns is approved.

Evangeline Ballerini

Ruth Finkelstein

Thomas Turner

Scott Hodges, Committee Chair

September 2023

The exceptional columbine: exploring the genetic basis of three ecologically important traits
in a high alpine plant, *Aquilegia jonesii*

Copyright © 2023
by
Jason Wells Johns

ACKNOWLEDGEMENTS

My first expression of gratitude goes to my advisor, Prof. Scott Hodges. Scott humbly led me from someone who knew very little about genetics to someone who actually passes for a geneticist. He gave me room to explore, fail, and succeed. Prof. Anji Ballerini graciously gave me her annotated code and guided me through QTL analysis. She commiserated with me, showed me some of her favorite field sites, and was a powerful advocate. I can't imagine anyone knowing more about plant molecular biology than Prof. Ruth Finkelstein. She is a true master of her craft, and I'm fortunate to have been able to learn (and forget) much from her. Thank you for never making me feel dumb, Ruth. You had many opportunities. Thank you, Prof. Tom Turner, for pushing committee meetings forward and for your kind encouragement.

I worked with all kinds of high quality people in the lab, a few of which showed me the ropes when I first showed up, including Dr. Zac Cabin, Alex Primo, and Jasen Liu. Nathan Derieg wrote much of the code I used, set up our lab computer ('Enemion'), and gave me useful guidance before my qualifying exam. The efforts, creativity, and personalities of undergraduates that I had the privilege of working with were invaluable. I was fortunate to spend significant time with Austin Reynolds, Alexis Guenther, Diego Orellana, Anthony O'Dea, Nina Suzuki, Lauren Harris, Taylor Bouknight, Josey Jaramillo, Lucas Funaro, and Jack/Yining Huang. Gavin Thatcher, thank you for teaching me more in a week than anyone ever has. I'm especially grateful for Josey's efforts on the California Conservation Genomics Project (CCGP) and in mentoring and training undergraduates. Lucas and Jack, I couldn't have asked for better buds to cross the finish line with. Thank you to Prof. Elena Kramer, Dr. Molly Edwards, and Dr. Minya of the Kramer Lab for your camaraderie, guidance, and collaboration.

I am grateful to many staff members who made the experience possible for me, including Azure Stewart, Andi Jorgensen, Cathy Arnold, Haley Martin, and Wendy Devlin. Thank you to the Wyoming Native Plant Society, the Alpine Garden Society, the Worster Family, and the UCSB URCA, FRAP, and Eureka programs for funding my work.

I have better friends than I deserve, including colleagues such as Natalie Love, Sevan Esaian, Tadeo Ramírez, Cameron Hannah-Bick, Kai Kopecky, Sam Bogan, Krista Kraskura, Olivia Isbell, Rebecca Varney, and Joey Peters. Cameron is the reason any of my plants survived and Krista kept us in shape during 'quarantine'. I'm nothing without the boys: Ryan Buckley, Mikey Giugni, Gregory Mundia (Jr., Sr., & brother), Dom Carmassi, Juan Roca, Mark Fischer, Skip Kanemaki, Jimmy Shaner, Dan Monteverde, Blaze Syka, Kevin Krisfield, Alex McQuiston, Ramey Dallimonti, Reverend Gabriel Ruzzier-Gaul, Carl Holm. Jobinas: Berenice Saint-Saens Buckley, Gina Giugni, Giana Roca, Jaime Holm, Veronica McQuiston, Roxy. Thank you, Zach Sawaya, for putting me on such great waves and fish at the islands. A special thank you goes to President Anne McCall for your mentorship, friendship, and generosity. Thank you to my Cooper Rd. neighbors for substantially improving the quality of my daily life. Thank you to my '96 Tacoma that always broke down in the most convenient places. Thank you to the UCSB Gospel Choir for including me for the last couple quarters. It was by far the most joyful experience I had on campus.

Derek Thoele passed a few weeks before I defended, but his influence and love persists. I'm so grateful for your true friendship, D. My grandfather, Major Gene Johns ended his 99 year career in December 2022. He was my most outspoken advocate.

I'm blessed with a top shelf family. Thank you, Uncle Mike, for sparking and funding my love of fishing. Thank you, Grandma Peg, for your support, love, and friendship. I have a wonderful mother (Shawn Beese) and father (Milton Johns), and even scored a bonus dad in Glenn Beese. Thank you all for everything you've done for me. Thank you to my sisters, Jori and Jenna, for reminding me that I'm not cool or handsome. Thank you to my brother-in-law to be, P.J. for balancing that out. Dana Cook's family has been a wonderful addition of my life the past 5 years, including Taylor Cook, Chuck Cook, Eric Romer, Melissa Bishop, Mike Sullivan, and Jim Churchill.

I owe my curiosity about the natural world to Prof. Matt Ritter. Enrolling in your class as an 18-year-old business major was a lottery win, Matt, and I somehow tricked you into mentoring me the past several years. My thanks will never account for my gratitude to you. Prof. Jenn Yost was also there from the beginning as my TA in Bio114, co-advisor for my master's program, and now mentor and friend.

The two beings that impact my life the most are Dana Cook and Blue dog. Blue has been my best friend for 12 years and has known me as a wine salesman, a biologist, and everything in between. Thank you Blue, for your unconditional love and for keeping me in shape. Dana Cook is the most all around high quality person I know. Everything she interacts with substantially improves, myself included. Thank you, my love.

VITA OF JASON WELLS JOHNS

September 2023

EDUCATION

University of California Santa Barbara September 2023
Ecology, Evolution, and Marine Biology, M.A. & PhD.

Cal Poly, San Luis Obispo, Biological Sciences January 2017
Biological Sciences, M.S.

Cal Poly, San Luis Obispo December 2010
Business Administration (International Business), B.S.
Biology Minor

PROFESSIONAL EMPLOYMENT

Teaching Assistant | various courses in EEMB

Instructor of Record | Introduction to Genetics (EEMB 129), Winter 2021

Graduate Student Researcher | California Conservation Genomics Project (CCGP): June
2020 – September 2023

Website Manager | MarineOmics working group: November 2022 – present

PUBLICATIONS

Johns, J. W., Yost, J. M., Nicolle, D., Igic, B. and Ritter, M. K. (2017), Worldwide
hemisphere-dependent lean in Cook pines. *Ecology*, 98: 2482–2484.

In Press

Bogan, S., Johns, J., Griffiths, J.,...Silliman, K. MarineOmics: A living web resource for
robust and reproducible genomic research in marine and non-model species. *Methods in
Ecology & Evolution*.

In Preparation

Johns, J., Ya, M., Ballerini, E., Kramer, E. and Hodges, S. The genetic architecture of
staminode development in columbines (*Aquilegia*).

Johns, J., Bouknight, T., Funaro, L., Hodges, S. Quantitative Trait Locus (QTL) analysis
reveals a candidate gene for amphistomaty *AqSPEECHLESS*, in the alpine plant
Aquilegia jonesii.

Johns, J., Escalona, M., Hodges, S. The de-novo genome assembly for the marine flowering
plant surfgrass (*Phyllospadix torreyi*). *Journal of Heredity*

Johns, J., Escalona, M., Hodges, S. A new de-novo genome assembly for the serpentine
columbine (*Aquilegia eximia*). *Journal of Heredity*

Johns, J., Escalona, M., Hodges, S. The de-novo genome assembly for the widespread
California manroot (*Marah fabacea*). *Journal of Heredity*

Johns, J., Escalona, M., Hodges, S. The de-novo genome assembly for the thimbleberry
(*Rubus parviflorus*). *Journal of Heredity*

Johns, J., Escalona, M., Hodges, S. The de-novo genome assembly for the winter annual baby blue eyes (*Nemophila menziesii* var. *menziesii*). *Journal of Heredity*
*All genome assembly publications for the CCGP have been preemptively accepted to the Journal of Heredity

INFORMATION PAGES & TUTORIALS

February 2023 | Published an information page to the MarineOmics.io website with an accompanying template for creating a new page for a GitHub Pages website with R Markdown

In Progress | Information page and accompanying tutorial for building genetic maps and performing Quantitative Trait Locus (QTL) analysis in non-model systems MarineOmics.io website

SCHOLARSHIPS AND AND GRANTS

December 2022 | Mentor for Undergraduate Research and Creative Activities, \$750

May 2020 | California Conservation Genomics Project for *Aquilegia*, \$120,000

June 2020 | California Conservation Genomics Project for *Rubus*, *Marah*, & *Nemophila*, \$149,000

June 2020 | California Conservation Genomics Project for *Phyllospadix*, \$56,000

May 2019 | Worster Award, \$4700

March 2019 | Individualized Professional Skills Grant, \$500

October 2018 | Mentor for Undergraduate Research and Creative Activities, \$750

July 2018 | North American Rock Garden Society, \$2500

June 2018 | Mentor for Undergraduate Research and Creative Activities, \$750

May 2018 | Alpine Garden Society Hendry Fund, \$2250

May 2018 | Wyoming Native Plant Society, \$750

January 2018 | California Native Plant Society Conference Student Grant, \$380

PRESENTATIONS

August 2023 | Public Defense (Exit Seminar) of PhD | UCSB, CA - The exceptional columbine: exploring the genetic basis of three ecologically important traits in a high alpine plant, *Aquilegia jonesii*

January 2023 | Twist Biosciences webinar - Genetic map construction and Quantitative Trait Locus (QTL) analysis using a skim sequencing approach in the plant genus *Aquilegia* (columbines)

February 2021 | Ecology, Evolution, and Marine Biology Graduate Student Symposium | UCSB, CA - The anomalous columbine

March 2019 | California Botanical Society Student Research Symposium | San Luis Obispo, CA - The genetic basis of alpine dwarfism in columbines

February 2018 | Ecology, Evolution, and Marine Biology Graduate Student Symposium | UCSB, CA - Synopsis of both past and current research

POSTER

January 2023 | Plant and Animal Genomes Conference (PAG) | San Diego, California - The genetic basis of alpine adapted, economically important traits in the plant genus *Aquilegia* (columbines)

PARTICIPATION IN PROFESSIONAL ASSOCIATIONS AND ORGANIZATIONS

Graduate Student Advisory Committee-EEMB (Chair) | Urban Forest Institute (UFI) board member | Design & Review Committee-UCSB (Graduate Student Representative) | Graduate Student Association-UCSB (Graduate Student Representative) | MarineOmics working group (web manager) | Graduate Student Symposium Organizing Committee (Chair) | UCSB Plant Club (Vice President) | California Native Plant Society, California Botanical Society | Botanical Society of America | Northern California Botanists | Alpine Garden Society | North American Rock Garden Society

TEACHING EXPERIENCE

Introductory Genetics (EEMB 129): Instructor of record | UCSB
Plant Evolution & Genomics (EEMB 595PE): Teaching Assistant | UCSB
Introductory Biology Lab (EEMB 3L, EEMB 2LL): Head Teaching Assistant | UCSB
Introductory Genetics (EEMB 129): Teaching Assistant | UCSB
Principles of Evolution (EEMB 131): Teaching Assistant | UCSB
Plant Biology & Biodiversity (EEMB 127): Teaching Assistant | UCSB
Plant Biology & Biodiversity Lab (EEMB 127L): Teaching Assistant | UCSB
Intro to Ecology (EEMB 120): Teaching Assistant | UCSB
Plant Diversity and Ecology Lab (BIO 114): Teaching Assistant | Cal Poly, San Luis Obispo
General Botany (BOT 121): Teaching Assistant | Cal Poly, San Luis Obispo
Plants, People, and Civilization (BOT 311): Teaching Assistant | Cal Poly, San Luis Obispo

MENTORSHIP EXPERIENCE & AWARDS

2021-2023 | Supervised one lab technician and seven undergraduate research assistants for the California Conservation Genomics Project
2020 | Excellence in Mentoring Undergraduates in Scientific Research Award, Center for Science and Engineering Partnerships
2018, 2019, 2022, 2023 | Secured grants for and supervised five Undergraduate Research Creative Activities (URCA) projects
Summer 2019 | EUREKA program mentor
Summer 2019 | Summer Institute in Mathematics & Science (SIMS) program mentor for four incoming freshmen

ABSTRACT

The exceptional columbine: exploring the genetic basis of three ecologically important traits
in a high alpine plant, *Aquilegia jonesii*

by

Jason Wells Johns

Our understanding of the molecular mechanisms governing plant traits and development is largely restricted to a few model taxa which represent a small fraction of plant biodiversity. As such, these model systems lack the variation necessary to investigate many traits, especially adaptations to extreme environmental conditions. A suite of traits is common among high alpine plants which allow them to mitigate environmental stressors, including dwarfism and the production of stomata on both sides of a leaf (amphistomaty). The blue limestone columbine (*Aquilegia jonesii*) exemplifies both of these traits. The ability to cross this species with a non-alpine relative, along with an annotated reference genome, gives us an opportunity to fill a significant gap in our understanding of these adaptations at the genetic level. In addition, *A. jonesii* is unique among columbine species by having lost an otherwise novel floral organ, staminodes, which allows us to dissect aspects of their development.

In this dissertation, I present my research investigating the genetic basis and phenotypic nuance of these three exceptional traits in *A. jonesii* using Quantitative Trait Locus (QTL) analysis. My results demonstrate that staminode loss is not complete in *A. jonesii*, and the genetic basis of its partial loss is complex. Dwarfism in *A. jonesii* is similarly complex, likely involving multiple hormonal pathways, in contrast to model taxa where dwarfism is most often caused by a single gene. In contrast, amphistomaty is

controlled primarily by a single major-effect QTL. I will show that this QTL is very likely due to cis-regulatory variation at the ortholog of a master stomatal development gene (*AqSPEECHLESS*). These studies together demonstrate the varying levels of complexity in the mechanisms by which nature selects for adaptive traits.

TABLE OF CONTENTS

Chapter I: Loss of staminodes in <i>A. jonesii</i> reveals a fading stamen-staminode boundary	1
Introduction.....	1
Methods	5
Results.....	8
Discussion.....	19
Supplemental Figures & Tables	30
References.....	41
Chapter II: A complex genetic basis for adaptive dwarfism in a high alpine plant, <i>Aquilegia jonesii</i>	45
Introduction.....	45
Methods	48
Results.....	50
Discussion.....	57
Supplemental Figures & Tables	65
References.....	69
Chapter III: A simple genetic basis for amphistomaty and stomatal density in an alpine columbine, <i>Aquilegia jonesii</i>	74
Introduction.....	74
Methods	77
Results.....	82
Discussion.....	92
Supplemental Figures & Tables	100
References.....	107

LIST OF FIGURES

Chapter I

Figure 1.1. Floral phenotypes of ‘Origami’ and <i>A. jonesii</i>	9
Figure 1.2. Examples of phenotype scores of subtraits	11
Figure 1.3. Phenotypic stamen/staminode gradient by phenotype in the parents and F2	13
Figure 1.4. QTL maps for each subtrait and whorl.....	16

Chapter II

Figure 2.1. Plant stature and leaf comparisons of parents	51
Figure 2.2. Histograms of each dwarfism trait in the F2 population and parents.....	51
Figure 2.3. QTL maps and effect plots for each dwarfism related trait.....	55

Chapter III

Figure 3.1. Parental phenotypes.....	83
Figure 3.2. Distributions of SI in F2 population and parents, and correlation between SI_{AB} and SI_{AD} in $F2_{AM}$ plants	85
Figure 3.3. QTL maps for amphistomaty, SI and SR and their effect plots	88
Figure 3.4. Bivariate plot of SI_{AB} and SI_{AD} in $F2_{AM}$ plants	89
Figure 3.5. <i>SPCH</i> polymorphisms fixed and unique to <i>A. jonesii</i>	91

LIST OF TABLES

Chapter I

Table 1.1. QTL results for each subtrait and whorl.....	16
---	----

Chapter II

Table 2.1. Correlation matrix across dwarfism traits in F2 plants.....	53
Table 2.2. QTL results for each trait.....	55

Chapter III

Table 3.1. Mean values for dorsiventral stomatal patterning (DSP) traits	84
Table 3.2. Correlation matrix across DSP traits in F2 plants	86
Table 3.3. QTL results for each trait.....	88

Chapter I: Loss of staminodes in *Aquilegia jonesii* reveals a fading stamen-staminode boundary

Introduction

Flowers are by far the most evolutionarily successful means of reproduction for plants (Magallón and Castillo, 2009). Originally modified from leaves, subsequent modifications to every floral organ have produced a broad array of floral morphologies across angiosperms (Meyerowitz et al., 1989; Bowman et al., 1991). Modifications to stamens have occurred in at least one species of ca. 30% of plant families (Walker-Larsen and Harder, 2000; Decraene and Smets, 2001). Often these modified stamens are rudimentary, but in some cases they maintain and/or gain some function (Walker-Larsen and Harder, 2000). The most common stamen modifications are ones that aid directly in pollination, such as becoming showy or developing a mechanical function like catapulting pollen onto a pollinator (Eyde and Morgan, 1973; Walker-Larsen and Harder, 2000). Many stamen modifications result in their sterility, on a gradient from producing pollen without viable sperm to not producing anthers at all (Decraene and Smets, 2001). These modified stamens are referred to generally as staminodes (staminodia).

Well-developed and whorled staminodes are absent in the Ranunculaceae except in a single clade encompassing the genera *Aquilegia*, *Semiaquilegia* and *Urophysa* (Wang and Chen, 2007; Huang et al., 2017; Qin et al., 2020). These genera have organs constituting a novel, fifth floral whorl, modified from the two stamen whorls closest to the carpels (Tucker and Hodges, 2005; Voelckel et al., 2010; Sharma and Kramer, 2013). Staminodes differ from stamens by loss of anthers and flattening and fringing of the filament. Occasionally weakly chimeric organs develop, where a wild-type staminode has a reduced, apparently

sterile anther (Voelckel et al., 2010; Meaders et al., 2020). In *Aquilegia*, staminodes develop lignification on their adaxial side and neighboring staminodes are often fused, representing more extensive modification (Meaders et al., 2020). After anthesis the outer floral organs senesce and abscise, yet the fused staminodes persist in a sheath around the developing carpels and are eventually sloughed off as the carpels expand (Kramer, 2009; Voelckel et al., 2010). In addition, many genes associated with anti-herbivory and anti-microbial functions are upregulated in staminodes compared to the other floral whorls (Voelckel et al., 2010). These features together suggest that staminodes may be adapted to provide defense against herbivory or microbial pathogens, although this has yet to be demonstrated directly (Tucker and Hodges, 2005; Voelckel et al., 2010; Meaders et al., 2020).

Aquilegia jonesii Parry, the only species of columbine lacking staminodes, presents a natural variant that we use here to investigate the genetic basis of staminode development (Parry, 1874). *A. jonesii* is nested well within the *Aquilegia* clade indicating that staminodes were lost in this species (Munz, 1946; Whittall and Hodges, 2007). Despite this loss, no other obvious difference in floral organ identity, such as carpel number, distinguishes *A. jonesii* from other species of *Aquilegia*, suggesting that staminodes have been reverted to stamens.

An initial candidate gene for staminode loss would be an organ identity gene. In *Aquilegia*, there are three functional paralogous copies of the MADS-box B-class floral identity gene *APETALA3* (*AP3*): *AqAP3-1*, *AqAP3-2* and *AqAP3-3*, all of which can heterodimerize with *AqPISTILLATA* (*AqPI*; Kramer et al., 2003; Kramer et al., 2007). *AqAP3-3* has been subfunctionalized to petal development (Kramer et al., 2007; Voelckel et al., 2010; Sharma and Kramer, 2013; Cabin et al., 2022). *AqAP3-1* and *AqAP3-2* are both

expressed in the primordia of stamens and staminodes but their expression diverges with *AqAP3-2* becoming concentrated in stamens and *AqAP3-1* becoming concentrated in staminodes (Kramer et al., 2007; Voelckel et al., 2010; Sharma and Kramer, 2013). *AqAP3-1* continues to be upregulated in staminodes compared to other organs late in development, suggesting it has neo-functionalized activity specific to staminode development and function (Voelckel et al., 2010; Sharma and Kramer, 2013). Knockdown of *AqAP3-1* in *Aquilegia* results in the conversion of staminodes to carpels and/or a chimeric carpel-stamen organ, making it a less-likely candidate gene for staminode loss in *A. jonesii*. Knockdown of *AqAP3-2* results in the loss of anthers in stamens but has no obvious effect on staminodes (Sharma and Kramer, 2013).

Genes not specific to organ-identity may also be involved with differentiating stamens and staminodes. In an early study using expression arrays, Voelckel et al. (2010) found upregulation of genes involved with lignification in staminodes of late pre-anthesis flowers (stage 12 from Min and Kramer, 2017), in concert with the cellular patterning later discovered by Meaders et al. (2020). Additionally, given that stamens and staminodes have been shown in other taxa to differ in expression of genes involved with abaxial/adaxial polarity (de Almeida et al., 2014), Meaders et al. (2020) explored this possibility in *Aquilegia* using histology, RNAseq, and in-situ hybridization. They showed that staminodes differ from stamen filaments in the position and expression level of several developmental polarity genes known to be involved in laminar expansion, including the YABBY gene family transcription factors *AqCRABS CLAW* and *AqFILAMENTOUS FLOWER/YABBY1*. They also found upregulation in staminodes compared to stamens of two genes known to be

involved in organ adhesion in *Arabidopsis*, *AqHOTHEAD* and *AqDEFECTIVE IN CUTICULAR RIDGES* (Krolkowski et al., 2003; Panikashvili et al., 2009).

In addition to or in concert with modifications to the genetic pathway specific to staminode development, a potential explanation for a loss of staminodes in *A. jonesii* could be its relatively few floral whorls. When comparing species of *Aquilegia* and close relatives, Tucker and Hodges (2005) found a positive correlation between stamen and staminode number, as *A. ecalcarata* flowers with only 10 stamens (2 whorls) had only 1-3 staminodes (less than 1 whorl), and other species with 40-60 stamens (8-12 whorls) made 10 staminodes (2 whorls). Given that *A. jonesii* flowers are relatively small with fewer whorls of stamens than most other columbine species, we also investigated whether the number of stamen organs is correlated with staminode production.

The natural variant *A. jonesii* gives an opportunity to further explore key genes in staminode development. We sought to determine if the loss of staminodes in *A. jonesii* was due to a simple genetic change, such as a change in *AqAP3-1/2* activity, or if it involved other and potentially novel pathways. To identify regions of the genome harboring causal genes, we used QTL analysis with an F2 population generated by crossing *A. jonesii* and a staminode producing variety of *Aquilegia*, *A. coerulea* 'Origami', henceforth referred to as 'Origami'. In addition to using photographs of whole organs to identify the morphological nuances in transition from stamens to staminodes, we also used histological analysis to characterize the cellular morphology of staminodes in the parents and in the F2 population. Together, these analyses uncover more phenotypic and genotypic complexity for staminode development than previously reported, and identify new candidate genes that could be involved in the trait.

Methods

Crossing experiment

Pollen from an *A. jonesii* plant collected from a wild population (Hunt Mtn Rd, WY) was used as the paternal parent and an *A. coerulea* ‘Origami’ plant as the maternal parent to produce the F1 generation. This F1 plant was self-pollinated to produce an F2 population. F1 and F2 seeds were soaked in 100 μ M gibberellic acid overnight prior to planting to induce germination.

Plants were germinated and grown in a custom soil mix (4 parts pumice, 2 parts perlite, 2 parts Foxfarm™ potting soil, 1 part vermiculite, 0.5 parts sand, 0.01 parts fertilizer) at 18°C with a 12/12 light schedule. Seeds were germinated in individual 2” pots then grown to a point where we determined that they were strong enough to transfer to 4” pots. Plants were further grown to near reproductive maturity and transferred to 1 gallon pots. To induce flowering, all F2 individuals were vernalized at 4°C for ca. 12 weeks.

Phenotyping

We phenotyped flowers by first removing the petals and sepals, counting stamens as they were removed, and scoring staminodes as we removed them. If organs came off of the flower together when dissected, they were considered fused (Fig. 2, Supp. Fig. 3). Four photographs were taken of each flower: whole, petals and sepals removed, stamens removed, and staminodes removed. Phenotypes were later confirmed from photographs. When two flowers were measured for a plant, we averaged the values of each subtrait, which is why some plants have non-integer values. As phenotypes were categorical and ordered, we used polychoric correlation tests.

Genotyping

Genomic DNA (gDNA) was isolated from young leaves of all F2 individuals with a lab based method using Qiagen reagents and the BioSprint 96 (Qiagen; see Cabin et al., 2022). Genomic DNA quantities were verified via Qubit. Whole genome libraries were prepared using 1/2 reactions with the iGenomx Riptide 96-plex kit (now TWIST biosciences), analyzed on a Bioanalyzer at the UCSB Bio-Nanostructures Laboratory, multiplexed, then sequenced (~1x) at UC Davis DNA Technologies Core on one lane of a Novaseq S6 with 150PE reads. Sequence data for the *A. jonesii* parent were generated on an earlier run, where gDNA was isolated via the above method, a library was prepared using a 1/2 reactions of the NEBNext Ultra II DNA Library Prep Kit for Illumina (New England Biolabs), and was sequenced with other samples on a Novaseq S6 at the UC Davis DNA Technologies Core.

Sequencing data were demultiplexed by the UC Davis DNA Technologies Core, then paired-end reads were aligned to the *Aquilegia coerulea* 'Goldsmith' V3 reference genome (Filiault et al., 2018) using the Burrows-Wheeler Aligner (see Filiault et al., 2018 for parameters and details). F2 sequence data were aggregated to create a .bam file of the F1 parent. SNPs were called across this file using Samtools (v1.8) mpileup with options -q 30 -B -u -v -f and vcf files were created with bcftools (v1.10.1) call with options -vm -f GQ (see Ballerini et al., 2020 for genotyping details). As we only had deep-coverage sequence for the *A. jonesii* parent we used the 1,039,650 SNPs heterozygous in the F1 and homozygous in the *A. jonesii* parent to genotype F2s. We called SNPs across these usable sites for each F2 using the above method. Allele frequencies for each F2 were calculated across 693 marker bins ranging from 50kb to 1Mb using custom scripts (see Ballerini et al., 2020 for custom

scripts). We used smaller bin sizes in regions of higher recombination (chromosome ends) and in areas where there was discordance between the physical and genetic maps (see below).

Genetic map

We made a genetic map using the recommended protocol from the R/qtl package (Broman et al., 2003). In several regions across our genetic map, there were particular markers that had a recombination event in almost all individuals. Similar to previous crosses using *Aquilegia* (Ballerini et al., 2020; Filiault et al., 2018; Edwards et al., 2021), we determined that this was due to either mis-assemblies in the reference genome or structural differences between the reference genome and the taxa in our cross. We manually reconstructed our genetic map in these regions, moving markers according to parsimony.

QTL analysis

QTL analysis was performed using the R/qtl package (Broman et al., 2003). We first ran the ‘scanone’ analysis to independently test whether each marker has a QTL and identify general regions of the genome associated with the trait. We then ran ‘scantwo’, which looks at each possible pair of markers and determines whether each of them holds a QTL. The significance cutoffs for QTL were determined by 1000 random permutations of the data to determine the highest LOD score produced by random chance. Using the results of scanone and scantwo, we used ‘multipleqtl’ to predict the best model and used ‘refineqtl’ to determine the most likely locations for each QTL given the model as a whole. The model that explained the most variation and had the highest overall LOD score was chosen. Any

loci that did not increase the overall LOD score by more than the significance threshold were excluded from the final model.

Candidate gene analysis

Genes were searched in the ‘Araport11’ *Arabidopsis* genome by keyword using Phytozome (Cheng et al., 2017; <https://phytozome.jgi.doe.gov>) and compared to the *Aquilegia* proteome using the ‘Protein Homologs’ tool. Results were then filtered based on sequence similarity and alignment length.

Histology

Developing flower buds (1-3 cm) were harvested, photographed, measured, and dissected from 10 individuals representing an array of staminode phenotypes and genotypes at the various QTLs. See Meaders et al. (2020) for the histology protocol.

Results

Staminode phenotypes

‘Origami’ makes well developed staminodes that completely lack anthers, and have flattened and fringed filaments that fuse together to form a sheath around the carpels (Fig. 1.1A,B). Furthermore, there is a sharp boundary between staminodes and the next outer whorl, which are stamens with anthers and round, unfused filaments (Fig. 1.1C,D). While *A. jonesii* has lost canonical staminodes, some staminode-like characteristics can remain in the stamens (Fig. 1.1E-H, Supp. Figs. 1.1,1.2). In the two innermost whorls of stamens, where staminodes normally develop in other *Aquilegia* species, the stamens make normal anthers

but the filaments are often somewhat flattened and sometimes fringed, increasingly so proximally, and to a greater degree in the innermost whorl (Fig. 1.1E-H, Supp. Figs. 1.1,1.2). Furthermore, we observed that in the whorls extending outward to the petals, the filaments gradually become more stamen-like with any flattening reduced to the proximal end (Supp. Figs. 1.1,1.2). Thus, stamens of *A. jonesii* can show a degree of being chimeric with staminodes with a decreasing gradient away from the carpels, representing a fading stamen-staminode boundary.

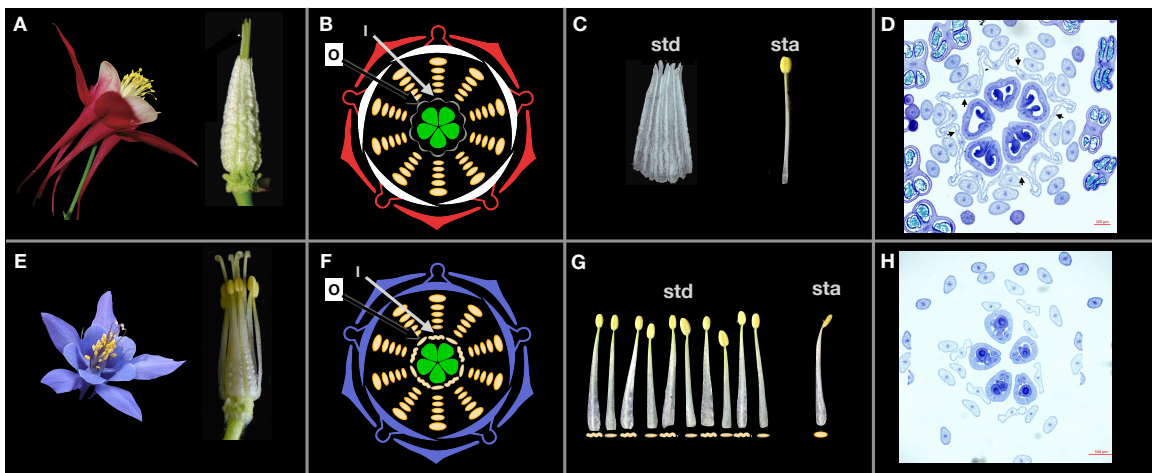


Figure 1.1. Floral phenotypes of ‘Origami’ (A-D) and *A. jonesii* (E-H). A,E whole flowers and after dissection to just the inner two staminode/stamen whorls and carpels. B,F floral diagrams with the inner-most whorl (I) to the carpels and the next outer whorl (O) indicated. For *A. jonesii*, morphological variation between the I-whorl (wavy symbol) and the O-whorl (flattened) is depicted. C,G, dissected staminodia and stamens. Symbols under organs in (G) depict chimeric organs in *A. jonesii*. Scores for the *A. jonesii* flower are indicated in Supp. Fig. 2 (AjBB3a). Scores for the ‘Origami’ flower are all maximal staminode-like scores (Fig. 2). For ‘Origami’ staminodes, the inner and outer whorls are identical other than their directionality of folding, thus the inner whorl organs are indicated with arrows in panels B&D. D,H Toluidine blue stained sections of young floral buds at stage 12 (Min & Kramer, 2017). D arrows indicate inner whorl organs. H image is from an F2 flower with the same phenotype as *A. jonesii*. Scale bars = 500µm.

We observed variation within and among *A. jonesii* individuals in the extent of flattening and fringing of filaments in outer stamen whorls (Supp. Fig. 1.2), although we did not have enough flowers available to quantitatively characterize this variation. By the time we became aware of the gradient in *A. jonesii*, the pollen donor for our cross was

unavailable for phenotyping, and therefore we do not know the degree to which it displayed flattening and fringing of its stamen filaments. We dissected a flower from the same population as the pollen donor (Hunt Mntn. Rd., WY), which had weakly chimeric stamen-staminode organs extending to stamen whorls (Supp. Fig. 1.1). Regardless, by far the largest phenotypic difference between ‘Origami’ and *A. jonesii* was in the two whorls closest to the carpels (Fig. 1.1C-D,G-H).

Similar to *A. jonesii*, variation among F2 flowers revealed that two whorls closest to the carpels sometimes differed in their phenotypes, indicating variation in the boundary of organ identity. We refer to the whorl closest to the carpels as the “inner (I)” whorl and the next whorl out as the “outer (O)” whorl (Fig. 1.1B-D,F,H). Staminode or chimeric staminode-stamen organs were largely confined to these whorls and therefore we restricted our analysis to them and phenotyped them separately (Supp. Figs. 1.3,1.4). Only 22 out of 400 flowers from 19 plants had any amount of flattening and fringing beyond this region.

Chimeric organs were complex and appeared to vary continuously. We chose to phenotype these organs using three subtraits: presence/absence of anthers (AN), flattening/fringing of filaments (FR), and +/- fusion of neighboring filaments (FU; Fig. 1.2). For instance, organs ranged from making no anther at all, to small, shriveled anthers, to pollen producing anthers of various sizes (Supp. Fig. 1.3). We did not measure the level of pollen viability of anthers, but focused our analysis to anther production of any kind with a binary score of presence/absence (Fig. 1.2). Filament fringing was similarly continuous, varying from relatively round filaments to completely flattened and fringed (Supp. Figs. 1.3, 1.4). When the degree of FR varied within a filament, it always decreased from the proximal to the distal end. Given this variation in FR along the length of the filament, we scored FR

with four ordered bins (Supp. Fig. 1.3, Fig. 1.2): round or flattened, but not fringed (0), flattened and fringed less than halfway up the filament (1), flattened and fringed halfway up the filament (2), and flattened and fringed more than halfway up the filament (3). The degree of FU also varied somewhat continuously, but we scored the trait using a binary presence/absence of fusion (Supp. Fig. 1.3, Fig. 1.2).

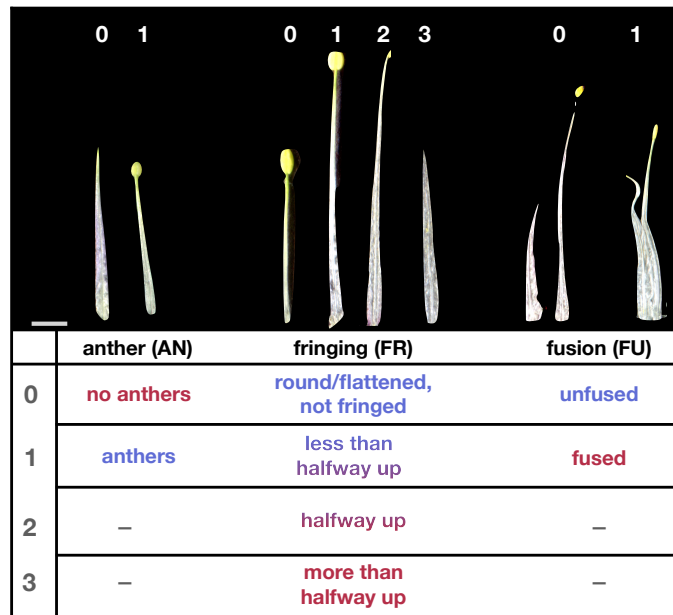


Figure 1.2. Examples of phenotype scores of subtraits. Organs were dissected from F2s representative of each phenotype score. Red text indicates an ‘Origami’-like (staminode-like) score and blue text indicates a *A. jonesii*-like (stamen-like) score. Text with both colors are varying levels of intermediate between the two parents, with more blue indicating more *A. jonesii*-like and more red indicating more ‘Origami’-like. Scale bar = 2mm.

We phenotyped either one (62 plants) or two (169 plants) flowers per plant for a total of 400 flowers. Most often the two flowers from the same plant had identical phenotypic scores. For AN, 139 plants (82%) had the same score across both flowers in both the inner and outer whorls (Supp. Table 1.1). Of the 50 plants with variation between flowers, 20 differed only in the inner whorl, 20 differed only in the outer whorl, and 10 differed in both whorls. Scores between flowers were also highly consistent for FR, where the same score

was observed in 139 plants (82%) for the inner whorl and 123 plants (73%) for the outer whorl (Supp. Table 1.2). Only four plants had flowers differing by a score of 3 in either whorl for FR. FU was the most consistent trait across flowers within a plant, where 154 plants (91%) had the same phenotype (Supp. Table 1.3). Thus, for the QTL analysis, we averaged scores across plants with two flowers phenotyped.

Correlations were relatively high among subtraits using one flower from each of 231 plants (polychoric correlations; Supp. Table 1.4). For correlation tests, we randomly chose one flower per plant to maintain the independence of each measurement. Mirroring the parental phenotypes, AN was negatively correlated with both FU and FR in both whorls (polychoric correlations ranged from -0.57 to -0.77), although these correlations were weaker than the positive correlations between FR and FU (0.88 to 0.95; Supp. Table 1.4). The near perfect positive correlation of FR and FU is expected as FU can only occur with some amount of FR (Supp. Fig. 1.3, Supp. Fig. 1.4; Meaders et al., 2020).

The F₂ plants varied in the degree of morphological difference between inner and outer whorls. We used one randomly chosen flower per plant for comparisons between whorls. The majority of plants reflected ‘Origami’ where the inner and outer whorls had the same phenotype (horizontal lines Fig. 1.3A-F, Supp. Table 1.5). This was especially true for AN, where 72% had the same phenotype in both whorls and 28% produced anthers only in the outer whorl (Fig. 1.3B, Supp. Table 1.5). FR was less consistent across whorls, where just over half (54%) of flowers had the same phenotype in both whorls and 46% had different phenotypes between whorls (Fig. 1.3D, Supp. Table 1.6). Similar to *A. jonesii*, when the two whorls of a flower differed, the inner whorl was always more staminode-like (Fig. 1.3B,D).

In addition, flowers with a strongly staminode-like inner whorl were more likely to have a staminode-like outer whorl (Fig. 1.3B,D, Supp. Tables 1.5,1.6).

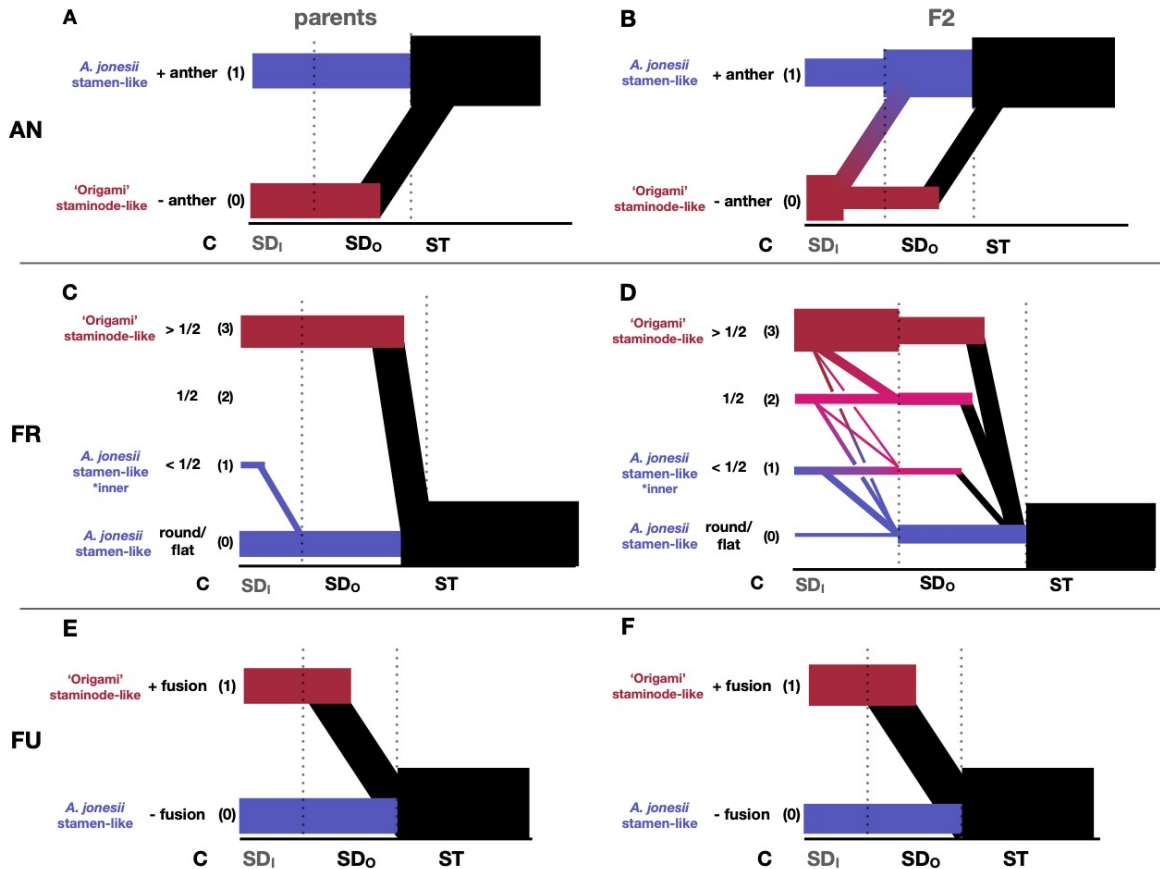


Figure 1.3. The phenotypic stamen/staminode gradient by phenotype in the parents (left) and F2 (right). The proportions of plants in a given category are indicated with numbers line thickness. Horizontal lines indicate no change in phenotype between whorls, diagonal lines indicate a change in phenotype between whorls. Red lines indicate an ‘Origami’-like (staminode-like) score and blue lines indicate a *A. jonesii*-like (stamen-like) score. Black lines depict the stamen whorl. The magenta color in FR represents an intermediate phenotype between the parents observed in the F2, and doesn’t reflect either parent directly. Parental phenotypes are based on the 5 *A. jonesii* and 5 ‘Origami’ flowers observed. C: carpels, SD₁: staminode inner whorl, SD₀: staminode inner whorl, ST: stamen whorls.

Histological cross sections of one flower from each of ten plants also revealed continuous variation among F2 plants in FR and FU, in addition to occasional variation between whorls (Supp. Fig. 1.4). As sections were taken ca. halfway down the flower bud,

AN phenotypes were not visible. The inner whorl, in the row alternating with the carpels, was always more staminode-like (Supp. Fig. 1.4).

While the number of sepals, petals, and carpels is almost always five across both parents, ‘Origami’ flowers have many more stamens ($\bar{x} = 60.6$, $s = 5.6$, $n = 44$) plus the two whorls of staminodes than *A. jonesii* flowers ($\bar{x} = 34.2$, $s = 4.9$, $n = 12$; $t = -16.4$, $p \ll 0.001$; Supp. Fig. 1.5). Thus, we sought to determine if floral organ number (FON) is correlated with staminode production, and if this varies for the inner versus outer whorl. Logistic regression revealed that FON was significantly correlated [odds ratio (OR) = 0.97, $p = 0.001$, $\alpha = 0.05$] with all three subtraits, though given that the ORs are all near 1.0, the effect of FON is very small (Supp. Fig. 1.5A-C & Supp. Table 1.7). Whorl identity had a much larger effect on AN and FR than FON, where the outer whorl is more likely to make anthers [OR (outer whorl): 2.83, $p < 0.001$, $\alpha = 0.05$] and was less fringed [OR (outer whorl): 0.35, $p < 0.001$; Supp. Fig. 1.5A,B & Supp. Table 1.7]. The interaction term between FON and whorl was not included in the final models for AN or FR as it was not significant. Whorl was not included in the FU model, as fusion occurs between whorls, and thus cannot differ between them. While there were significant correlations, there was nearly complete overlap in trait values among FON counts (Supp. Fig. 1.5A-C) indicating that little variation in staminode development is explained from FON (Supp. Table 1.7).

Genotypic data

We identified 849,724 SNPs across 599 marker bins (see Methods) spanning the genome. Of the 334 plants, 5 did not have enough coverage to genotype, leaving 329 individuals to assemble a genetic map. The genetic map had similar ordering of marker bins

to their physical order in the *A. coerulea* ‘Goldsmith’ V3 reference genome (Goodstein et al., 2012). However, there was some discordance between the physical and genetic marker positions, mostly in pericentromeric regions, similar to the findings in other crosses of *Aquilegia* (Supp. Fig. 1.6; Filiault et al., 2018; Ballerini et al., 2020; Xie et al., 2020; Edwards et al., 2021). Recombination rates were higher toward the ends of chromosomes (Supp. Fig. 1.6). Patterns of transmission distortion varied across the seven chromosomes, with distortion favoring the ‘Origami’ allele in some regions and the *A. jonesii* allele in others (Supp. Fig. 1.7).

QTL analysis

Overall, we identified 9 independent QTL (non-overlapping 1.5 LOD intervals) across the three subtraits and two whorls (Table 1.1 & Fig. 1.4). Full models explained 44-53% of the total percent variation explained (PVE). We found one ‘major effect’ QTL, defined as having greater than 25% PVE, for FR in the outer whorl on Chr3 (FR_{OU}-Q3, 25.5 PVE). Multiple QTL were identified for each subtrait, many of which had overlapping 1.5 LOD intervals across both whorls within and across subtraits, suggesting pleiotropic effects for genes within these QTL. For instance, the 1.5 LOD intervals overlap for QTL for nearly all three subtraits across both whorls on Chr3 (excluding FR_{IN}-Q3). Similarly, the intervals for a Chr2 QTL overlap across most subtraits in both whorls (excluding AN_{OU}-Q2, FR_{IN}-2.1,2.2). We did not detect any significant interactions between QTL. As FON never explained more than 3% of the variation, it was not included as a covariate in final QTL models.

Table 1.1. QTL results for each subtrait and whorl. “inner” & “outer” refer to the staminode whorls. Abbreviations: chr, chromosome; 1.5 LOD int, 1.5 LOD interval; PVE, Percent Variance Explained. Additive effects are in terms of the ‘Origami’ allele.

subtrait	chr	name	1.5 LOD int (cM)	1.5LOD marker	peak position (cM)	LOD	PVE	total PVE	additive effect	dominance deviation	degree of dominance
anther, inner	2	AN _{IN} -Q2	22.7 - 44.6	2.52 - 2.74	33.0	7.0	7.3	50.8	-0.19	-0.04	0.21
	3	AN _{IN} -Q3	24.4 - 27.6	3.093 - 3.116	26.1	19.8	23.8		-0.29	-0.19	0.66
	5	AN _{IN} -Q5	14.3 - 22.9	5.1 - 5.17	16.0	11.2	12.3		-0.23	0.02	0.09
anther, outer	2	AN _{OU} -Q2	3.2 - 37.2	2.05 - 2.69	16.9	3.8	4.4	44.3	-0.13	0.04	0.31
	3	AN _{OU} -Q3	15.9 - 29.2	3.023 - 3.125	26.1	8.9	10.8		-0.22	0.02	0.09
	5	AN _{OU} -Q5	16.0 - 25.0	5.12 - 5.18	21.9	7.9	9.5		-0.15	-0.11	0.73
	6	AN _{OU} -Q6	0.0 - 46.9	6.01 - 6.44	34.2	4.0	4.6		-0.14	-0.07	0.50
fringing, inner	2	FR _{IN} -Q2.1	8.6 - 28.0	2.09 - 2.61	21.4	4.1	4.0	53.0	0.27	0.22	0.81
	2	FR _{IN} -Q2.2	47.2 - 56.3	2.76 - 2.84	54.8	8.9	9.2		0.39	0.21	0.54
	3	FR _{IN} -Q3	31.7 - 34.8	3.126 - 3.129	33.8	16.1	17.8		0.47	0.34	0.72
	5	FR _{IN} -Q5	42.2 - 46.7	5.58 - 5.63	44.9	5.1	5.1		0.55	0.45	0.82
fringing, outer	2	FR _{OU} -Q2	38.8 - 44.6	2.7 - 2.74	41.2	19.4	23.3	50.8	0.79	0.39	0.49
	3	FR _{OU} -Q3	24.4 - 27.1	3.093 - 3.08	26.7	21.0	25.5		0.87	0.30	0.34
fusion	1	FU-Q1	37.2 - 51.8	1.54 - 1.69	42.3	4.3	4.4	50.7	-0.16	0.02	0.13
	2	FU-Q2	38.8 - 44.6	2.7 - 2.74	40.9	18.4	21.9		0.29	0.16	0.55
	3	FU-Q3	24.4 - 29.2	3.093 - 3.125	26.7	16.1	18.7		0.29	0.09	0.31

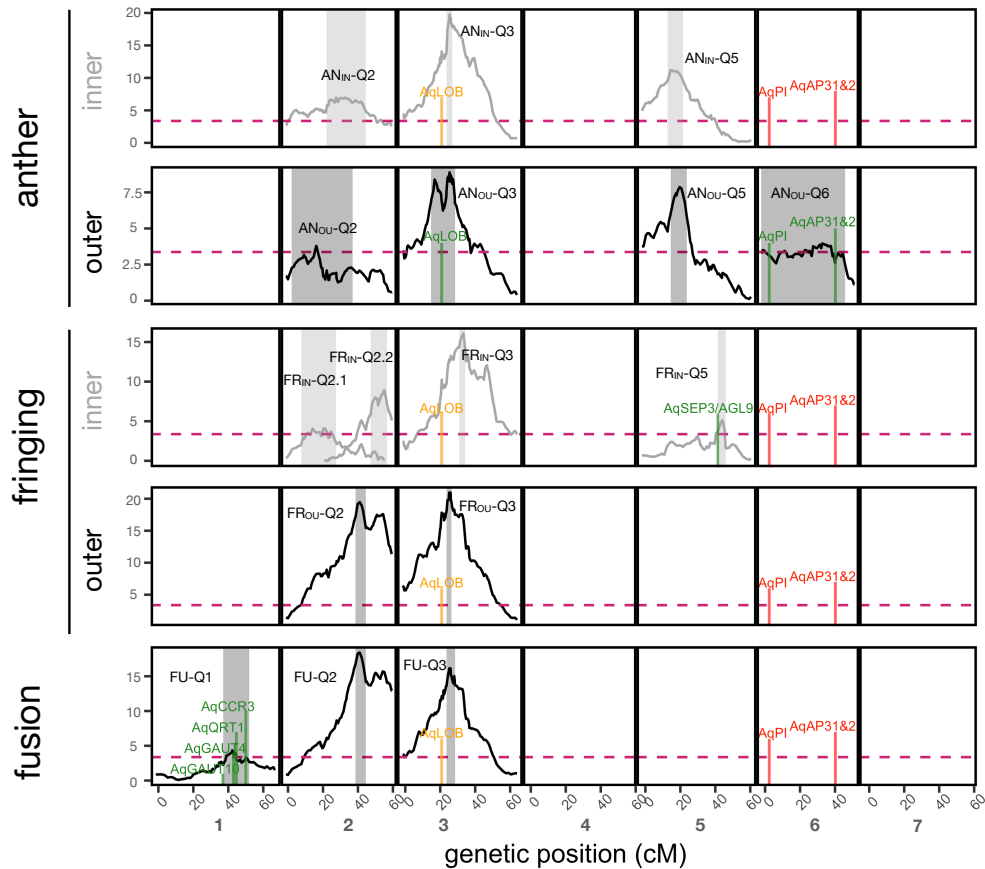


Figure 1.4. QTL maps for each subtrait and whorl. LOD profiles reflect the best multiple QTL model associated with each subtrait and whorl. Shaded areas represent 1.5 LOD intervals for each QTL peak. Dashed line represents the significance LOD threshold for each trait of 3.37. For the two traits where whorls were measured separately, grey = inner & black = outer. FU is black, where whorls were measured together. Green indicates genes within QTL 1.5 LOD intervals. Orange indicates where LOB is just outside the QTL 1.5 LOD interval. Red indicates where B-class genes are not within QTL 1.5 LOD intervals.

For all QTL except one, we observed parental divergence where F2s with alleles for a given parent were more likely to make organs with the same phenotype as the parent (e.g., for *A. jonesii*, AN = 1, FU = 0, FR = 0; Table 1.1, Supp. Figs. 1.8-1.10). The only exception was FU-Q1, where individuals homozygous for the *A. jonesii* allele were more likely to be fused than individuals heterozygous or homozygous for the ‘Origami’ allele. However, this is a minor effect QTL, defined as having less than 10 PVE, with 4.4 PVE (Table 1.1, Supp. Fig. 1.10). A simple QTL sign test assuming equal effects (QTLST-EE; see Methods & Discussion) was significant ($p = 0.03$). Most traits showed additive patterns of inheritance for the parental alleles, although ‘Origami’ alleles were dominant slightly more often than *A. jonesii* alleles (Table 1.1; Supp. Figs. 1.8-1.10).

Anther (AN)

The best fit model for AN identified three QTL for the inner whorl (AN_{IN}) and four QTL for the outer whorl (AN_{OU}; Table 1.1, Fig. 1.4), with 51 and 44 total PVE, respectively. Across the three QTL common to both whorls, AN_{IN} had higher LOD scores than AN_{OU}. Among the subtraits, AN had the most consistent QTL across the two whorls, with their 1.5 LOD intervals overlapping on chromosomes 2, 3 and 5. Q3 explained the most variation for both AN_{IN} (24%) and AN_{OU} (11%). A minor effect QTL for AN_{OU} was detected on Chr6 (4.6 PVE). While *AqAP3-1&2* are within this QTL, it is of minor effect and the 1.5 LOD interval covers most of the chromosome, indicating these genes play a minor role, if any, in *A. jonesii*'s gain of anthers. Q5 does not overlap across AN and FR indicating that it does not have pleiotropic effects across subtraits. *A. jonesii* alleles for AN QTL always promoted

anther presence (Table 1.1, Supp. Fig. 1.8). FON only explained 0.9% of the variance, suggesting it plays a minimal role in this subtrait, and was not included in the final model.

We focused our candidate gene search for AN on homologs of genes and gene families implicated in anther development, the establishment of ab-adaxial polarity, and organ boundaries. We did not find any genes known to be involved in anther development or ab-adaxial polarity within the 1.5 LOD intervals of all QTL (henceforth referred to as “within QTL”). We did find a homolog of a gene involved in the establishment of organ boundaries in plants, *LATERAL ORGAN BOUNDARIES (LOB)*, which was within AN_{OU}-Q3 and just outside AN_{IN}-Q3 (Fig. 1.4; Supp. Table 1.8). *AqPI*, *AqAP3-1*, and *AqAP3-2* all fell within AN_{OU}-Q6, although it was a minor effect QTL and the 1.5 LOD interval covered 90% (in cM) of the chromosome (Fig. 1.4, Table 1.1, Supp. Table 1.8).

Fringing (FR)

The best fit models for FR revealed four QTL for the inner whorl (53% PVE) and two QTL for the outer whorl (51% PVE; Table 1.1, Fig. 1.4). For both whorls, the largest effect QTL was on Chr3, although the 1.5 LOD regions did not overlap between whorls (Table 1.1, Fig. 1.4). We detected two QTL for FR_{IN} and one QTL for FR_{OU} on Chr2. ‘Origami’ alleles always produced more flattened/fringed organs (Table 1.1, Supp. Fig. 1.9). FON only accounted for 1.6 PVE in FR_{IN} and 1.9 PVE in FR_{OU}, and was not included in the final models.

For FR specific candidate genes, we considered homologs of genes and gene families previously implicated in floral organ identity, ab-adaxial polarity, organ boundaries, and laminar expansion of stamens (Supp. Table 1.8). The only notable gene we found was

AqSEPALLATA3/AGAMOUS-LIKE9 (AqSEP3/AGL9), which fell within FR_{IN}-Q5; unique to FR for the inner whorl (Fig. 1.4, Table 1.1, Supp. Table 1.8).

Fusion (FU)

The best fit model for FU identified three significant QTL, which explain 51% of the variance (Table 1.1, Fig. 1.4). The LOD profiles of FU-Q2 and FU-Q3 were nearly identical to that of FR_{OU}-Q2 and FR_{OU}-Q3. We detected moderate effect QTL, defined as having 10-25 PVE, on Chr2 and Chr3, where FU-Q2 had the largest effect (22 PVE). Although FU-Q1 was narrowly significant, explaining an estimated 4.9% of the variance, it was unique to FU, suggesting it may harbor genes specific to organ adhesion. However, FU-Q1 was the only QTL for FU where plants with ‘Origami’ alleles were less likely to be fused (Table 1.1, Supp. Fig. 1.10). FON explained more variation for FU than for AN or FR, however it was marginal (3 PVE), so it was not included in the final model.

We searched for genes and gene families known to be involved with fusion and organ adhesion in other taxa and found candidates for staminode fusion in *Aquilegia* (Supp. Table 1.8) within FU QTL. Of particular interest were genes within FU-Q1, as this QTL was unique to FU. It happened to be the only QTL within which we found FU specific candidates, including a paralog of *CR4*, *CRINKLY-RELATED3 (CCR3)* and three galacturonosyltransferase homologs (*GAUT4*, *10*, & *12*; Fig. 1.4, Supp. Table 1.8).

Discussion

Using *A. jonesii* in a QTL experiment to dissect the genetic basis of staminode development, we found a complex pattern of morphological variation among the F2

population involving multiple QTL, with some QTL affecting specific subtraits of staminode morphology (Table 1.1, Fig. 1.4). We found that the two whorls comprising normal staminode development can differ phenotypically and while the two whorls have largely overlapping QTL, they also have whorl-specific QTL. Finally, we found that while *A. jonesii* has functionally lost staminodes, some of its stamens retain remnants of staminode morphology which display a gradual boundary beyond the normal position of staminodes (Fig. 1.1, Supp. Figs.1.1,1.2). Thus it appears that staminode development, and its loss in *A. jonesii*, involves multiple genetic factors controlling identity and organ boundaries.

Fading boundary between stamens and staminodes in A. jonesii

Upon close examination, we found that *A. jonesii*'s loss of staminodes is not absolute. Instead, there is often some amount of flattening and fringing of stamen filaments, decreasing in a gradient outward from the carpels (Supp. Figs. 1.1,1.2). The degree of this gradient varied among the flowers we examined, but the strongest difference was always between the “inner” and “outer” whorls where staminodes normally develop in other species (Fig. 1.1, Supp. Figs. 1.1,1.2). Unfortunately, we did not observe this phenomenon while we had access to the plant we used as the pollen donor for the F2 population. Within F2 plants, stamens with flattening and fringing were almost always restricted to the two whorls where staminodes normally develop (Supp. Fig. 1.3), suggesting that the *A. jonesii* parent may have had a relatively strong boundary between the normal staminode whorls and the stamens. Although F2 plants generally did not have the same extent of fading boundary into the outer stamens as observed in *A. jonesii* (Supp. Fig. 1.3), the leaky stamen-staminode boundary observed in the whorls closest to the carpels of F2 plants allowed us to analyze the

differential genetic architectures of stamen-staminode identity as development continues toward the carpels.

This gradient in staminode organ identity and incomplete loss of staminodes in *A. jonesii* contrasts the floral homeotic mutants found in populations of *A. coerulea*, which exhibit a complete loss of petals (Eastwood, 1897; Irwin, 1998; Cabin et al., 2022). *A. jonesii*'s gradient is more reminiscent of the “fading boundaries” observed in many basal angiosperms, which has been attributed to gradients in B-class organ identity gene expression across whorls (Buzgo et al., 2004; Kim et al., 2005; Soltis et al., 2006; Chanderbali et al., 2009; Luo et al., 2011). While *A. jonesii*'s gradient differs from basal angiosperms in that it only involves stamen whorls, it may be similarly attributed to gradients in the expression of B-class genes such as *AqAP3-1*. Interestingly, QTL analysis reveals that *A. jonesii*'s staminode loss is due to mutations in genes with up- and/or downstream activity of the B-class genes rather than to the B-class genes themselves.

Organ loss via changes to multiple genes of minor/moderate effect

Changes to a single or few early acting developmental genes can lead to the loss or conversion of an organ, even when the organ is relatively complex (Coen and Meyerowitz, 1991; Averof and Patel, 1997; Géant et al., 2006; Cabin et al., 2022). However, we found multiple QTL for each subtrait and only one had a marginally large (>25% PVE) effect (Table 1.1, Fig. 1.4), suggesting that the loss of staminodes in *A. jonesii* was likely polygenic and complex. We found nine QTL with non-overlapping 1.5 LOD scores in total, some of which were unique to a particular subtrait and others which affect multiple subtraits. QTL associated with multiple subtraits may hold genes with epistatic effects, such that the

activity of subtrait-specific genes (e.g. genes responsible for pollen development) depend on the upstream activity of genes which establish the stamen/staminode boundary. Additionally or alternatively, genes in these QTL may interact with floral identity genes (i.e. B-class transcription factors) upstream of subtrait specific genes. Detecting a significant epistatic interaction between QTL requires a strong interaction due to the additional degree of freedom for the interaction term (Broman et al., 2003). Thus, while we did not find any significant QTL x QTL interactions in this study, future studies with a larger sample size should not discount the possibility that QTL common to multiple subtraits act epistatically to subtrait specific QTL.

Notably, when QTL for a trait appeared in both whorls, the effect sizes varied between the inner and outer whorls. For AN, the inner whorl had consistently larger LOD scores and tighter 1.5 LOD intervals (Table 1.1, Fig. 1.4), suggesting that the genes responsible for anther development in *A. jonesii*'s two whorls closest to the carpels have a greater effect once the stamen/staminode boundary is more established. In contrast for FR, QTL had consistently larger and tighter LOD peaks in the outer whorl (Table 1.1, Fig. 1.4), suggesting that genes important for FR may have a greater effect before or during the establishment of the stamen/staminode boundary. Notably, for each of these traits, the whorl with fewer QTL in its respective 'multipleqtl' model also had greater PVE, which inherently inflates the PVE of each QTL compared to models with more QTL terms. However, when we only included the two QTL with the highest PVE for AN and FR in both whorls, the differences in effect sizes between whorls remained. Thus, while genes under the majority of QTL appear to affect staminode development in both whorls, the degree of their effect depends on where the boundary between stamens and staminodes is established.

Across three QTL present in both whorls for AN (Q2, Q3, Q5), LOD intervals overlapped nearly completely. As the Chr5 QTL is unique among subtraits to both whorls of AN (Table 1.1, Fig. 1.4), this region is likely to harbor genes specific to anther development. We did not identify any genes previously implicated in anther development or ab-adaxial polarity establishment within this QTL, suggesting it may hold gene(s) with functions upstream of anther development itself and/or anther development genes that have yet to be discovered in model taxa.

During early floral meristem development in *Aquilegia*, anthers appear before filaments (Tepfer, 1953; Tucker and Hodges, 2005). Thus, the genetic pathways affecting *A. jonesii*'s retention of anthers in the staminode whorls could be at least partially epistatic to processes affecting filament morphology in the FR and FU subtraits. We identified *AqLATERAL ORGAN BOUNDARIES* (*AqLOB*) as a plausible candidate for stamen/staminode boundary establishment, as it was within the largest QTL for AN_{OU} on Chr3 and just outside the 1.5 LOD intervals for AN_{IN}-Q3, FR_{OU}-Q3, and FU-Q3 (Supp. Table 1.8, Table 1.1, Fig. 1.4). While *LOB* has mostly been directly implicated in vegetative organ boundary establishment, it is expressed in early floral buds in *A. thaliana*, suggesting it may play a role in floral organ boundary establishment (Shuai et al., 2002; Majer and Hochholdinger, 2011; Xu et al., 2016). Additionally, ectopic *LOB* expression in *A. thaliana* causes misshapen, chimeric organs and sterility (Shuai et al., 2002). As *AqLOB* is also expressed in early floral buds in *Aquilegia* (Min and Kramer, 2020), it could be involved in establishing the transition between stamens and staminodes.

Although there can be substantial variation between whorls in the extent of FR, we would expect FR in both whorls to be controlled by the same genes. Surprisingly, there were

substantial inconsistencies across whorls in QTL maps for FR, where none of the 1.5 LOD intervals for any QTL overlapped (Table 1.1 & Fig. 1.4). Therefore it appears that the morphology of these two whorls are at least partially influenced by different genes. Flowers on the same F2 plant were more likely to differ in FR_{OU} than FR_{IN} (Supp. Table 1.2), suggesting that there may be more of an environmental and/or stochastic effect on FR in the outer whorl. The presence of both more variation and larger and tighter QTL in the outer whorl seems contradictory, as we would expect more non-genetic variation to weaken QTL. However, this would make biological sense if genes that positively regulate staminode identity and/or negatively regulate stamen identity have a greater effect before the stamen/staminode boundary is established. In the context of a fading boundary with a gradient of stamen/staminode gene expression, there is likely more competition with stamen identity genes in the outer whorl, and thus more phenotypic variation.

The QTL on Chr5 was unique to FR (non-overlapping with AN) for the inner whorl, and includes *AqSEP3* (Table 1.1, Fig. 1.4, Supp. Table 1.8). *SEPALLATA* genes, which are E-class genes in the canonical ABCE model of floral development, have undergone lineage-specific duplication and diversification in the Ranunculaceae (Soza et al., 2016). In *Arabidopsis*, *SEPALLATA3/AGAMOUS- LIKE9* (*SEP3/AGL9*) forms a heterotetramer complex with *AG*, *AP3*, and *PI* (*PISTILLATA*) to control stamen development. While *SEP3* appears to be largely involved in gynoecium development in *Thalictrum thalictroides* (Ranunculaceae), its knockdown caused chimeric organs across all three floral organs (*Thalictrum* lacks petals; Soza et al., 2016). Given *SEP3*'s involvement in floral development and its occurrence under FR_{IN}-Q5, it may be involved in causing fringing in *Aquilegia* staminode filaments.

The LOD profiles for FU and FR_{OU} were nearly identical (Table 1.1, Fig. 1.4), which was expected given the near perfect correlation values between the two traits (Supp. Table 1.4). Thus, it is difficult to conclude from these data whether FU is under unique genetic control or whether it is a spatial result of the fringing and bending patterns of neighboring organs. As the degree of fusion varies across *Aquilegia* species (Meaders et al., 2020), this could be further examined by crossing columbine species that make fused and unfused staminodes to identify loci responsible for FU itself. A notable difference between FU and FR is the Chr1 QTL unique to FU (Table 1.1, Fig. 1.4), and genes within this region may harbor candidates for FU specific processes.

Fusion of neighboring staminodes involves adhesion of epidermal cells, which is a process often mediated by interactions between pectin molecules within the cuticle (Du et al., 2022). Homogalacturonan (HG), which is polymerized by galacturonosyltransferases (*GAUTs*), is an abundant pectin molecule in plant cell walls. Given the direct involvement of *GAUT* genes in pectin biosynthesis and their previous implication in cell-cell adhesion (Mouille et al., 2007), the three *GAUT* homologs found within the 1.5 LOD interval of FU-Q1 are interesting candidates for staminode fusion (Fig. 1.4, Supp. Table 1.8). Finally, while *CCR3* has not been directly implicated in organ fusion to our knowledge, it is a paralog of *CRINKLY4* (*CR4*), which is involved in cuticle formation and *cr4* mutants have abnormal fusion of epidermal cells (Lolle et al., 1998). Together, these homologs of cuticle biosynthesis genes under the Chr1 QTL unique to FU are promising candidates for a genetic pathway associated with the fusion of neighboring staminodes in *Aquilegia*.

Variation in B-class genes not responsible for staminode loss

Previously, *AqAP3-1* and *AqPISTILLATA (PI)* were the only genes shown to have a functional effect on staminode development, with *AqAP3-1* apparently neofunctionalized to staminodes (Kramer et al., 2007; Sharma and Kramer, 2013). Thus, we hypothesized that *A. jonesii*'s loss of staminodes was due to variation in one of these B-class genes. However, while both of these genes colocalize with AN_{OU}-Q6, this QTL is of minor effect and covers 90% of the chromosome, providing weak evidence for their involvement in *A. jonesii*'s staminode loss (Fig. 1.4, Supp. Table 1.8). If changes to any of these genes do play a role, it is minor compared to genes within larger QTL that likely function up or downstream of B-class floral identity genes.

Importantly, although mutations in *A. jonesii*'s B-class genes did not lead to staminode loss, this does not negate their involvement in staminode development. Knockdown of *AqAP3-2* causes loss of anthers of stamens (but does not affect filaments) in staminode producing *Aquilegia* (Sharma and Kramer, 2013). Thus, *AqAP3-2* expression may not wane in the staminode whorls of *A. jonesii* as it does in staminode-producing plants. *AqAP3-2* also colocalizes with AN_{OU}-Q6, but as this QTL has a very weak effect on anther production, our results may be partially explained by a trans-acting factor(s) associated with another AN QTL that affects *AqAP3-2* expression. If the AN QTL have effects downstream and/or independent of *AqAP3-2*, then we might expect to see similar *AqAP3-2* expression profiles in plants with and without anther production.

In contrast, *AqAP3-1* and *AqPI* knockdowns convert staminodes to carpels and have minor effects on the 1-2 anther whorls adjacent to the normal staminode whorls, including anther necrosis and carpel-chimera (Kramer et al., 2007; Sharma and Kramer, 2013). Thus,

reduction in *AqAP3-1* or *AqPI* expression is unlikely to explain our results. Regardless, it would be informative to compare the expression profiles of *AqAP3-1*, *AqAP3-2*, and *AqPI* in early developing flowers with and without staminodes. This would have to be done using F2s, as *A. jonesii* produces inflorescences with a single flower which appear emerging from the rosette well-past the stage of early floral development when these genes are expressed. Differential expression patterns of these B-class genes between phenotypes would further implicate their role in determining stamen/staminode identity, and may inform whether genes driving QTL act up or downstream of the B-class genes.

Floral organ number plays little to no part in A. jonesii's staminode loss

Most phylogenies place *Aquilegia* and *Semiaquilegia* as sister species, with *Urophysa* as an outgroup (Wang and Chen, 2007; Bastida et al., 2010; Fior et al., 2013). Given that *Aquilegia* and *Urophysa* both make well developed staminodes, they were most likely reduced in the lineage leading to *Semiaquilegia adoxoides* (*S. guangxiensis* has more developed staminodes; Huang et al., 2017), and lost in the lineage leading to *A. jonesii*. It has been suggested that the two staminode whorls in *Aquilegia* could have evolved as a result of the large number of stamen whorls, which provided the “raw material” for the evolution of the novel organ (Min et al., 2022). *Semiaquilegia* has very small flowers compared to *Aquilegia*, *A. jonesii* has relatively small flowers compared to many other columbine species, and both species make relatively few stamens; *S. adoxoides* only make 8-14 stamens (Supp. Fig. 1.5; Tucker and Hodges, 2005). Given the positive correlation between stamen and staminode number found in *Aquilegia* (Tucker and Hodges, 2005), we

hypothesized that loss of staminodes in *S. adoxoides* and *A. jonesii* could be due to producing fewer stamens.

Our phenotypic data suggest FON plays a significant, but quite minor role in staminode development given the small odds ratios across subtraits (OR = 0.97-1.07; Supp. Fig. 1.5 & Supp. Table 1.7). This was corroborated by multiple QTL analysis models where FON was considered as a covariate but never included, as it did not account for more than 3 PVE compared with the 44-53 PVE from QTL. In addition, two close relatives of *A. jonesii*, *A. saximontana* and *A. laramiensis* make even smaller flowers than *A. jonesii* and also make fully developed staminodes (Munz, 1946). Thus, *A. jonesii*'s loss of staminodes is due to changes in genes specific to staminode development itself.

Is A. jonesii's loss of staminodes fitness related?

Although there is no empirical evidence of a fitness increase attributable to staminodes in columbines, several lines of evidence suggest they may be adaptive, and microbial and/or herbivory defense is the most common hypothesis (Tucker and Hodges, 2005; Sharma and Kramer, 2013; Meaders et al., 2020). If staminodes indeed evolved to protect the carpels from specific herbivores and microbes, perhaps these pests do not occur in *A. jonesii*'s environment, thus relaxing the selective pressure to maintain them. Furthermore, *A. jonesii* makes relatively few stamens compared to other columbines, so selection may favor the functional tradeoff of producing fertile stamens rather than staminodes if they are not useful.

The QTL analysis results add another line of evidence that selection may have driven *A. jonesii*'s staminode loss. For 8 out of 9 QTL, the *A. jonesii* allele causes more stamen-like

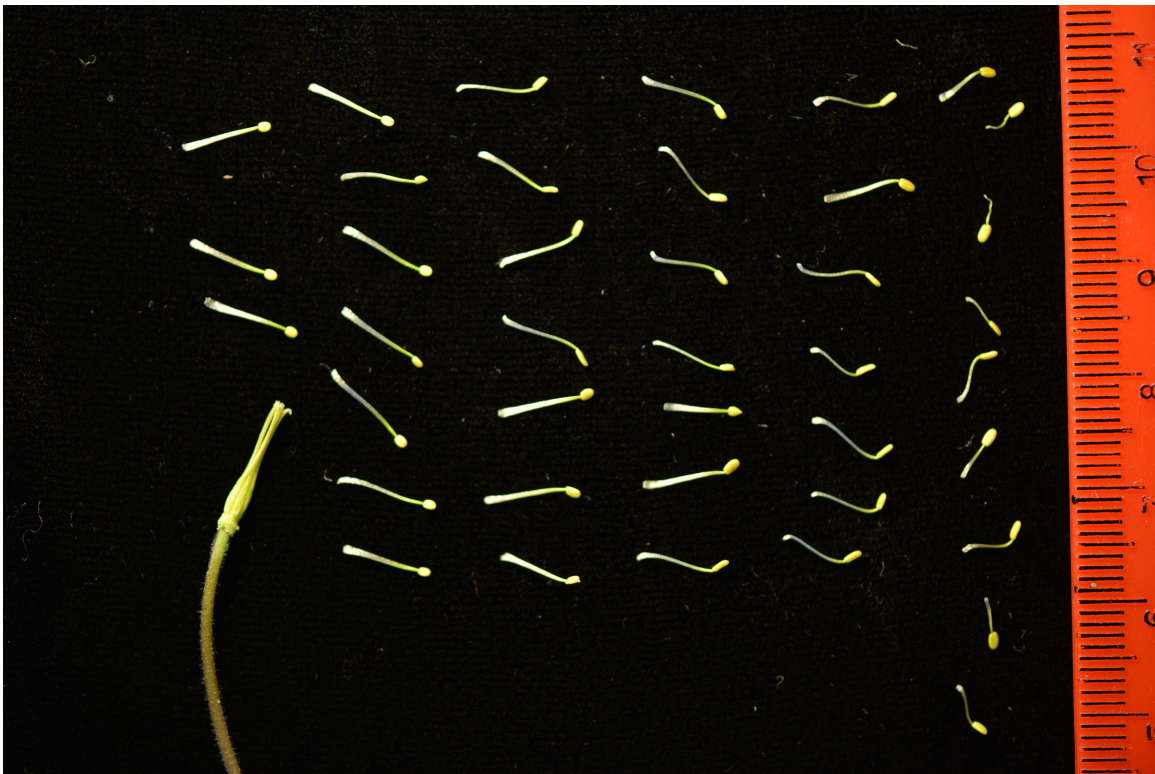
organs while the ‘Origami’ allele causes more staminode-like organs, yielding a significant QTL sign test assuming equal effects (QTLST-EE; Table 1.1, Supp. Fig. 1.8-1.10). If *A. jonesii*’s loss of staminodes was due to drift, it is more likely that alleles for functional staminodes would randomly increase in frequency in *A. jonesii*, such as the Chr1 QTL for FU (Orr, 1998; Rieseberg et al., 2002). While there is some evidence that the evolution of staminodes and subsequent loss in *A. jonesii* was selection driven, we cannot rule out the possible effect of drift. A QTLST, which accounts for the distribution of QTL effect sizes would be preferable given the inflated false discovery rate of the QTLST-EE when there is high variance in effect sizes (Rice and Townsend, 2012). Although we had enough independent QTL (≥ 6) to perform the test, some of our QTL affected multiple whorls and subtraits, making it difficult to determine a single effect size for each QTL. A more comprehensive test of selection’s role in *A. jonesii*’s staminode loss would be to compare the effects of staminodes on herbivory and/or disease vectors using *A. jonesii* and one of its co-occurring relatives such as *A. flavescens* or *A. brevistyla*.

Conclusion

As staminode development involves multiple modifications to normal stamens, we expected the genetic basis of the trait to be relatively complex. That said, the loss of staminodes in *A. jonesii* could have been caused by mutation to a master organ boundary establishment or organ identity gene. However, the crossing experiment with *A. jonesii* and a species that makes normal staminodes (‘Origami’) reveals a polygenic basis both for the evolutionary development and subsequent loss of staminodes in *Aquilegia*. While previous reverse genetic approaches focused on ABC floral development genes (i.e. *AqAP3-1*), our

forward genetic approach reveals evidence of the likely involvement of other genetic pathways. With significant correlation between the phenotypes and thus QTL, there is likely some amount of pleiotropy across subtraits. Finally, closer observation of staminode organs in *A. jonesii* revealed important caveats to its loss, uncovering a previously unrealized porosity between the stamen/staminode boundary in *Aquilegia*. Further investigation of this dynamic in *Aquilegia* and other taxa with chimeric organs will bolster our understanding of the evolution of novel organs and their developmental boundaries.

Supplemental Figures and Tables



Supplemental Figure 1.1. Photograph of an *A. jonesii* flower with all stamen whorls dissected and the carpels attached to the pedicel. Stamens are placed from inner (L) to outer (R). Filaments show some flattening and fringing toward the base, especially in inner whorls. The flower was dissected from a greenhouse grown plant grown from seed collected from Hunt Mntn. Rd., the same population as the pollen parent. Scale is mm.

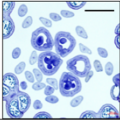
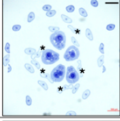
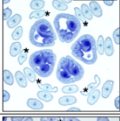
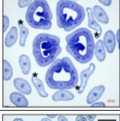
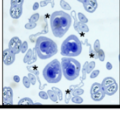
plant	selection of organs across all stamen whorls	staminode whorls	anther		fringing		fusion
			inner	outer	inner	outer	-
AjDM4b			1	1	1	0	0
AjBB4a			1	1	0	0	0
AjDM4a			1	1	0	0	0
AjBB3a *from Fig. 1			1	1	1	0	0

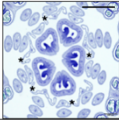
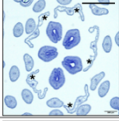
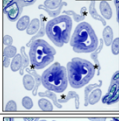
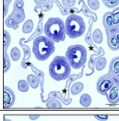
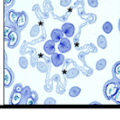
Supplemental Figure 1.2. Variation in stamen morphology of 4 *A. jonesii* flowers. Column 2: scans of dissected organs from the stamen whorls (outside of the two 'staminode' whorls) from inner (L) to outer (R) whorls. Column 3: scans of organs from the inner (grey bars) and outer 'staminode' whorls. Columns 4-8: subtrait scores for each flower. The 4 flowers were dissected from 3 different greenhouse grown plants grown from seed collected from two different populations.

plant	selection of organs across all stamen whorls	staminode whorls	anther		fringing		fusion
			inner	outer	inner	outer	-
23			1	1	2	0	0
292			1	1	2	0	0
89			0	1	3	0	0
272			0	1	3	0	0
78			0	1	3	1	0
107			0	1	3	2	1
214			0	0	3	3	0
331			0	1	3	3	1
2			0	1	3	3	1
163			0	0	3	3	1

Supplemental Figure 1.3. Variation in stamen and inner and outer 'staminode' morphology in F2 plants. Column 2: Scans of dissected organs from the stamen whorls (outside of the 'staminode' whorls) from inner (L) to outer (R) whorls. Column 3: Scans of organs from the inner (grey bars/arrows) and outer 'staminode'

whorls. Columns 4-8: subtrait scores for the inner two whorls of each flower. See Fig. 2 for details of scoring. Scale: each ruler tick is 1 mm.

plant	histological section	anther		fringing		fusion
		inner	outer	inner	outer	-
237		1	1	0	0	0
51		1	1	1	0	0
8		0	1	3	2	1
68		1	1	1	0	0
32		1	1	2	0	0

plant	histological section	anther		fringing		fusion
		inner	outer	inner	outer	-
125		0	1	3	1	0
117		0	1	1	1	0
41		0	0	2	1	0
130		1	1	2	1	1
44		0	0	3	3	1

Supplemental Figure 1.4. F2 toluidine blue-stained transverse histological sections from pre-anthesis flower buds. The inner whorl organs are between carpels and marked with an asterisk where distinguishable. Subtrait scores for the inner two whorls of each flower. See Fig. 2 for details of scoring. Scale bar = 500µm.

Supplemental Table 1.1. Comparison of anther (AN) scores for plants with two flowers measured, by whorl. The number of plants with a given pair of scores is given with the proportions of flowers in a given category in parentheses.

scores (flw1, flw2)	diff	inner	outer
0, 0	0	77 (0.46)	34 (0.20)
1, 1	0	62 (0.37)	105 (0.62)
total		139 (0.82)	139 (0.82)
0, 1	1	30 (0.18)	30 (0.18)
total		30 (0.18)	30 (0.18)

Supplemental Table 1.2. Comparison of fringing (FR) scores for plants with two flowers measured, by whorl. The number of plants with a given pair of scores is given with the proportions of flowers in a given category in parentheses.

scores (flw1, flw2)	diff	inner	outer
0, 0	0	4 (0.02)	36 (0.21)
1, 1	0	15 (0.09)	10 (0.06)
2, 2	0	17 (0.10)	12 (0.07)
3, 3	0	103 (0.61)	65 (0.38)
total		139 (0.82)	123 (0.73)
0, 1	1	6 (0.04)	10 (0.06)
1, 2	1	8 (0.05)	11 (0.07)
2, 3	1	12 (0.07)	17 (0.10)
total		26 (0.15)	38 (0.22)
0, 2	2	0 (0.00)	2 (0.01)
1, 3	2	3 (0.02)	3 (0.02)
total		3 (0.02)	5 (0.03)
0, 3	3	1 (0.01)	3 (0.02)
total		1 (0.01)	3 (0.02)

Supplemental Table 1.3. Comparison of fusion (FU) scores for plants with two flowers measured, by whorl. The number of plants with a given pair of scores is given with the proportions of flowers in a given category in parentheses.

scores (flw1, flw2)	diff	count
0, 0	0	60 (0.35)
1, 1	0	94 (0.56)
total		154 (0.91)
0, 1	1	15 (0.09)
total		15 (0.09)

Supplemental Table 1.4. Matrix of polychoric correlations between subtraits by whorl. “IN” & “OU” refer to the staminode whorls. We randomly chose 1 flower per plant for plants with two flowers measured to maintain independence of each measurement.

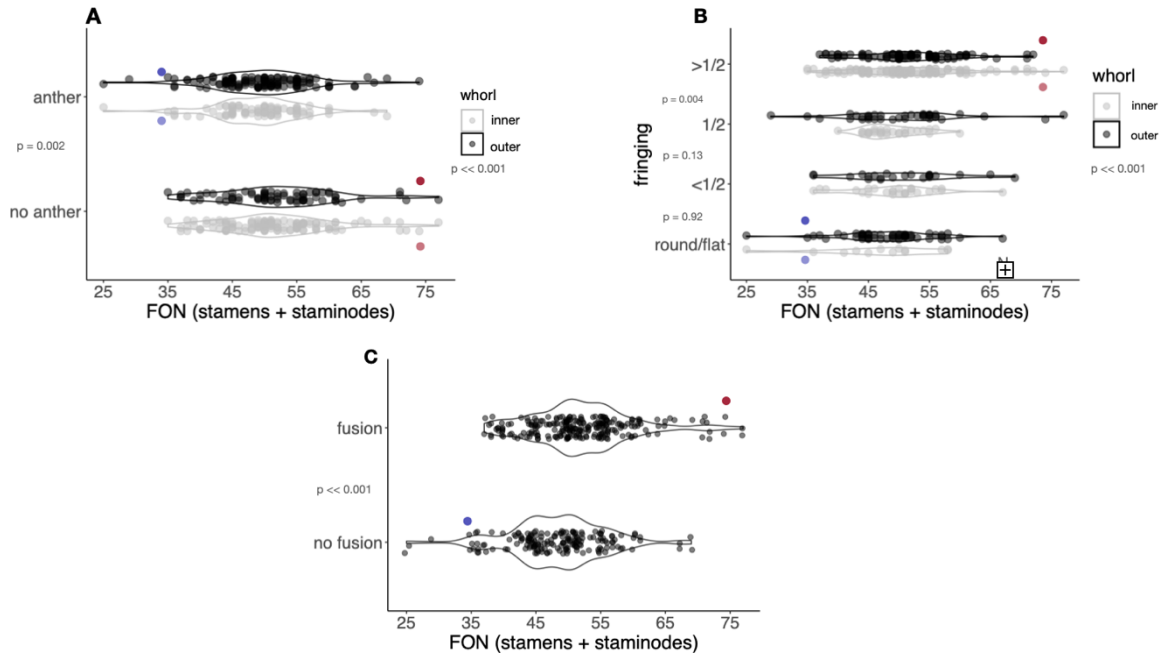
	AN_{ou}	FR_{IN}	FR_{ou}	FU
AN_{IN}	0.9954	-0.7696	-0.6542	-0.6885
AN_{ou}		-0.5748	-0.6332	-0.6353
		FR_{IN}	0.9205	0.8836
			FR_{ou}	0.9475

Supplemental Table 1.5. Comparison of anther (AN) scores within flowers between ‘staminode’ whorls. We randomly chose 1 flower per plant for plants with two flowers measured to maintain independence of each measurement. The number of plants with a given pair of scores is given with the proportions of plants in each category in parentheses.

		outer whorl		total
		presence (1)	absence (0)	
inner whorl	presence (1)	92 (0.40)	0 (0.00)	92 (0.40)
	absence (0)	65 (0.28)	74 (0.32)	139 (0.60)
total		157 (0.68)	74 (0.32)	

Supplemental Table 1.6. Comparison of flattening/fringing (FR) scores within flowers between ‘staminode’ whorls. We randomly chose 1 flower per plant for plants with two flowers measured to maintain independence of each measurement. The number of plants with a given pair of scores is given with the proportions of plants in each category in parentheses.

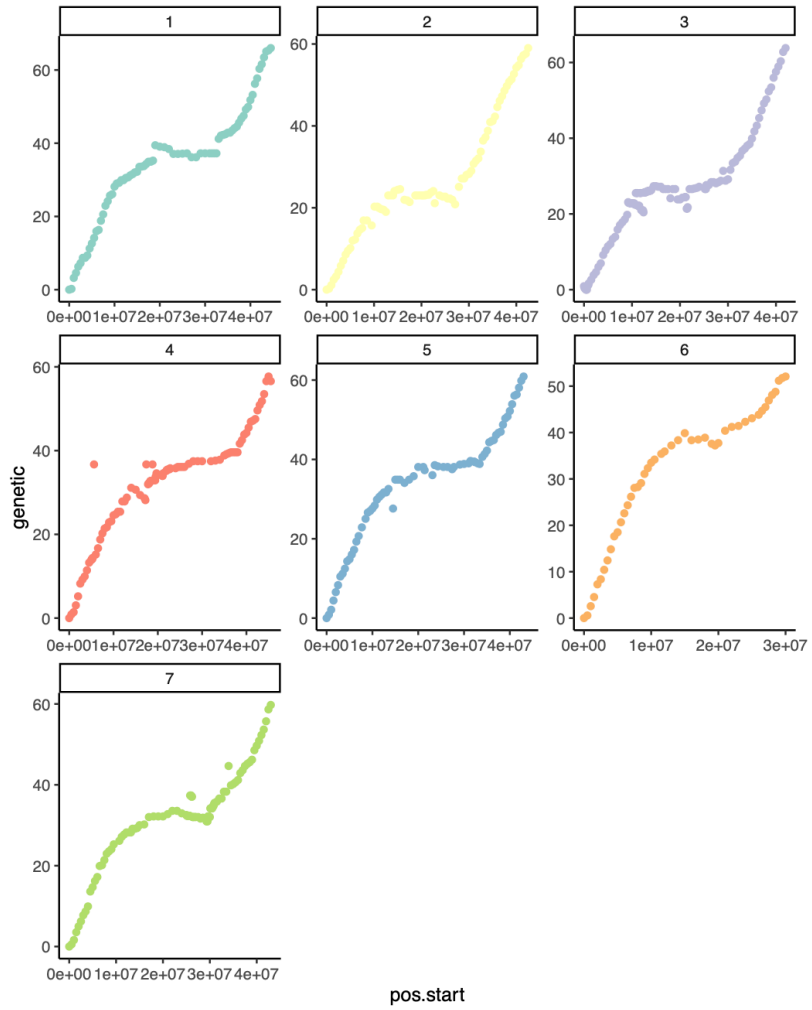
		outer whorl				total
		none (0)	< halfway (1)	halfway (2)	> halfway (3)	
inner whorl	none (0)	13 (0.06)	0 (0.00)	0 (0.00)	0 (0.00)	13 (0.06)
	< halfway (1)	26 (0.11)	4 (0.02)	0 (0.00)	0 (0.00)	30 (0.13)
	halfway (2)	16 (0.07)	10 (0.04)	9 (0.04)	0 (0.00)	35 (0.15)
	> halfway (3)	11 (0.05)	9 (0.04)	35 (0.15)	98 (0.42)	153 (0.66)
total		66 (0.29)	23 (0.10)	44 (0.19)	98 (0.42)	



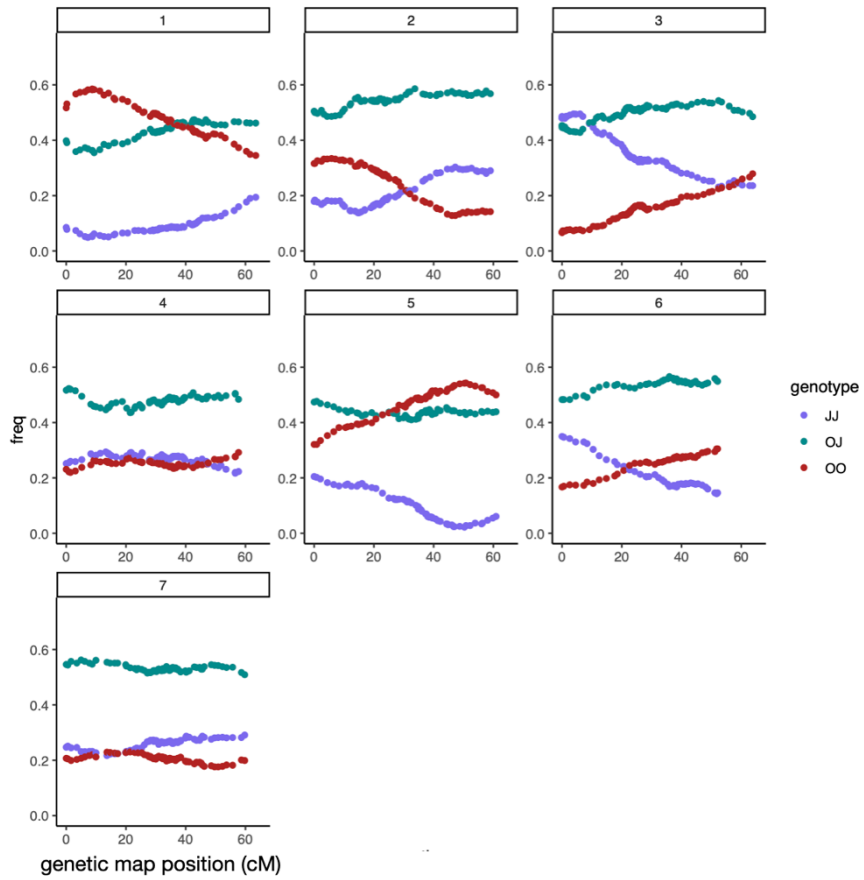
Supplemental Figure 1.5. Violin plots of subtrait values predicted by FON (stamens + staminodes) and whorl across F2 flowers for anther (A), flattening/fringing (B) and fusion (C) subtraits. We randomly chose 1 flower per plant for plants with two flowers measured to maintain independence of each measurement. 21/231 plants were excluded, as total stamens were not counted for them (n = 210). Mean values are plotted for the parents: *A. jonesii*, blue (n = 6); ‘Origami’, red (n = 2). Points are jittered to illustrate the distribution, with more jittering for the parents. p-values between FR scores are associated with the transition from the score beneath it to the score above it.

	anther	fringing	fusion
FON (stamens + staminodes)	0.96** (0.93,0.98)	1.05*** (1.02,1.08)	1.07*** (1.04,1.10)
outer whorl	2.83*** (1.9,4.2)	0.35*** (0.24,0.51)	N/A

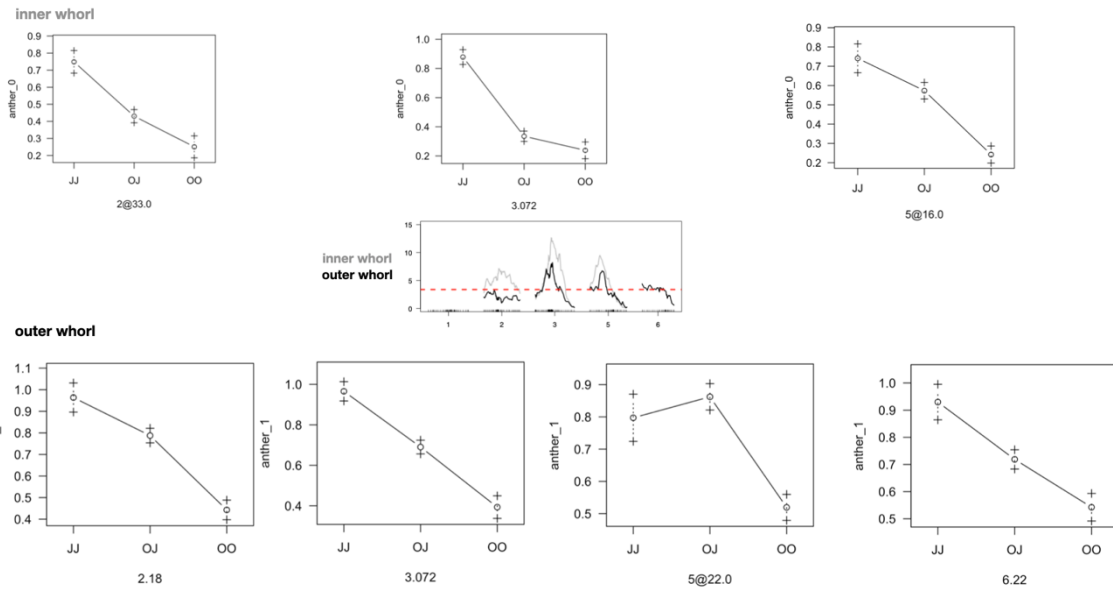
Supplemental Table 1.7. Results of logistic regressions of each subtrait predicted by FON (stamens + staminodes) and whorl. Odds ratios are reported with 95% confidence intervals in parentheses. Asterisks represent significant p-values: **p < 0.01, ***p << 0.001.



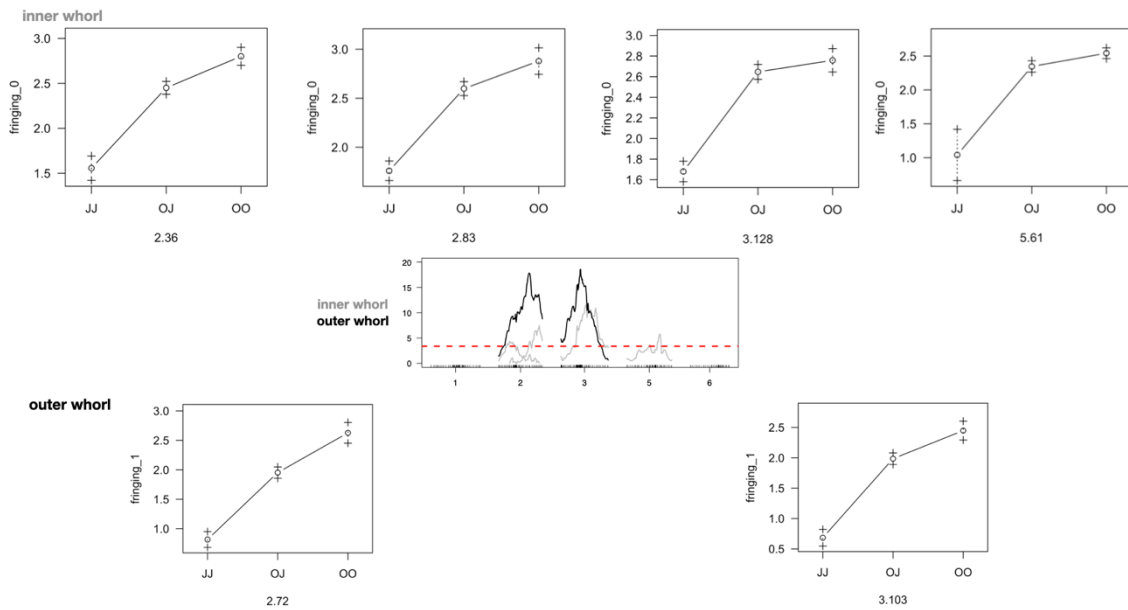
Supplemental Figure 1.6. Genetic position (cM) by physical position (bp) across the 7 *Aquilegia* chromosomes. Points represent markers used in genetic map construction.



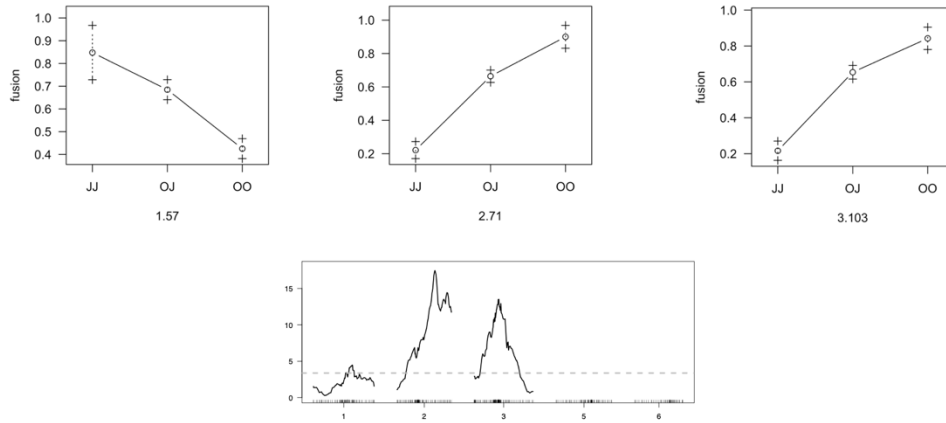
Supplemental Figure 1.7. Genotype frequencies in the F2 population across the 7 *Aquilegia* chromosomes. J, *A. jonesii* allele; O, 'Origami' allele. Points represent markers used in genetic map construction.



Supplemental Figure 1.8. Phenotype by genotype (PxG) effect plots for anther (AN) related QTL. Genotypes are on the x-axis (J = *A. jonesii*, O = 'Origami') and their effects are on the y-axis. The chromosome and marker location of each QTL is listed beneath each graph. QTL map included for reference.



Supplemental Figure 1.9. Phenotype by genotype (PxG) effect plots for fringing (FR) related QTL. Genotypes are on the x-axis (J = *A. jonesii*, O = 'Origami') and their effects are on the y-axis. The chromosome and marker location of each QTL is listed beneath each graph. QTL map included for reference.



Supplemental Figure 1.10. Phenotype by genotype (PxG) effect plots for fusion (FU) related QTL. Genotypes are on the x-axis (J = *A. jonesii*, O = ‘Origami’) and their effects are on the y-axis. The chromosome and marker location of each QTL is listed beneath each graph. QTL map included for reference.

Supplemental Table 1.8. Homologs of candidate genes searched for within and across subtraits

subtrait	whorl	qtl	aq_locus_name	aq_peptid_name	at_best_hit	at_symbol	arabi-defline	GO
anther	both	Q2	Aqcoe2G168200	Aqcoe2G168200.1	AT3G18010.1	WOX1	WUSCHEL related homeobox 1	GO:0003677
anther	outer	Q6	Aqcoe6G031900	Aqcoe6G031900.1	AT5G20240.1	PI	K-box region and MADS-box transcription factor family protein	GO:0006355,GO:0005634,GO:0003700,GO:0046
anther	outer	Q6	Aqcoe6G257100	AP3-1	AT3G54340.1	AP3,ATAP3	K-box region and MADS-box transcription factor family protein	GO:0006355,GO:0005634,GO:0003700,GO:0046
anther	outer	Q3	Aqcoe3G202800	Aqcoe3G202800.1	AT5G63090.1	LOB	Lateral organ boundaries (LOB) domain family protein	
fringing	inner	Q5	Aqcoe5G352300	Aqcoe5G352300.1	AT1G24260.1	AGL9,SEP3	K-box region and MADS-box transcription factor family protein	GO:0046983,GO:0003677,GO:0006355,GO:0005
fusion	NA	Q1	Aqcoe1G419900	Aqcoe1G419900.1	AT3G55950.1	ATCRR3,CCR3	CRINKLY4 related 3	GO:0006468,GO:0005524,GO:0004672
fusion	NA	Q1	Aqcoe2G337000	Aqcoe2G337000.1	AT5G55590.1	QRT1	Pectin lyase-like superfamily protein	GO:0042545,GO:0030599,GO:0005618
fusion	NA	Q1	Aqcoe1G308600	Aqcoe1G308600.1	AT2G20810.1	GAUT10,LGT4	galacturonosyltransferase 10	GO:0016757,GO:0047262
fusion	NA	Q1	Aqcoe1G365400	Aqcoe1G365400.1	AT5G54690.1	GAUT12,JRX8,LGT6	galacturonosyltransferase 12	GO:0016757,GO:0047262
fusion	NA	Q1	Aqcoe1G375000	Aqcoe1G375000.1	AT5G47780.1	GAUT4	galacturonosyltransferase 4	GO:0016757,GO:0047262
adhesion	-	none	Aqcoe7G029100	Aqcoe7G029100.1	AT5G23940.1	DCR,EMB3009,PEL3	HXXXD-type acyl-transferase family protein	GO:0016747
adhesion	-	none	Aqcoe6G082400	Aqcoe6G082400.1	AT1G78240.1	OSU1,QUA2,TS D2	S-adenosyl-L-methionine-dependent methyltransferases superfamily	GO:0008168
adhesion	-	none	Aqcoe7G043400	Aqcoe7G043400.1	AT4G00740.1	QUA3	S-adenosyl-L-methionine-dependent methyltransferases superfamily	GO:0008168
adhesion	-	none	Aqcoe3G134900	Aqcoe3G134900.1	AT3G49720.1	CGR2		
adhesion	-	none	Aqcoe6G316700.1		AT5G65810	CGR3		
adhesion	-	none	Aqcoe1G415600	Aqcoe1G415600.1	AT5G58600.1	PMR5,TBL44	Plant protein of unknown function (DUF828)	

subtrait	whorl	qtl	aq_locus_name	aq_peptid_name	at_best_hit	at_symbol	arabi-defline	GO
ab/adaxial polarity	-	none	Aqcoe1G459000	Aqcoe1G459000.1	AT2G37630.1	AS1,ATMYB91,ATP HAN,MYB91	myb-like HTH transcriptional regulator family protein	GO:0010338,GO:0006351,GO:0005634
ab/adaxial polarity	-	none	Aqcoe2G438700	Aqcoe2G438700.1	AT1G65620.3	AS2	Lateral organ boundaries (LOB) domain family protein	
ab/adaxial polarity	-	none	Aqcoe1G143700	Aqcoe1G143700.1	AT5G60690.1	IFL,IFL1,REV	Homeobox-leucine zipper family protein / lipid-binding START domain-containing protein	GO:0003677,GO:0008289
ab/adaxial polarity	-	none	Aqcoe1G178700	Aqcoe1G178700.1	AT2G34710.1	ATHB-14,ATHB14,PHB,PHB-1D	Homeobox-leucine zipper family protein / lipid-binding START domain-containing protein	GO:0003677,GO:0008289
ab/adaxial polarity	-	none	no matches in <i>Aquilegia</i>	N/A	AT2G46685		miR166/ATBH15	
ab/adaxial polarity	-	none	Aqcoe1G248400	Aqcoe1G248400.2	AT2G33860.1	ARF3,ETT	Transcriptional factor B3 family protein / auxin-responsive factor AUX/IAA-related	GO:0003677,GO:0009725,GO:0006355,GO:0009725,GO:0006355,GO:0009725,GO:0006355,GO:0009725
ab/adaxial polarity	-	none	Aqcoe1G248400	Aqcoe1G248400.2	AT2G33860.1	ARF3,ETT	Transcriptional factor B3 family protein / auxin-responsive factor AUX/IAA-related	GO:0003677,GO:0009725,GO:0006355,GO:0009725,GO:0006355,GO:0009725
ab/adaxial polarity	-	none	Aqcoe1G074300.1		AT2G45190		FILAMENTOUS FLOWER,YABBY1	
ab/adaxial polarity	-	none	Aqcoe1G074300.1		AT1G08465	YABBY2		
ab/adaxial polarity	-	none	Aqcoe7G386400.1		AT2G26580	YABBY5		
ab/adaxial polarity	-	none	Aqcoe3G065300	Aqcoe3G065300.1	AT1G69180.1	CRC	Plant-specific transcription factor YABBY family protein	GO:0007275
ab/adaxial polarity	-	none	Aqcoe3G410900	Aqcoe3G410900.1	AT5G16560.1	KAN,KAN1	Homeodomain-like superfamily protein	
ab/adaxial polarity	-	none	Aqcoe3G169700	Aqcoe3G169700.1	AT1G32240.1	KAN2	Homeodomain-like superfamily protein	
antagonistic with AG	-	none	Aqcoe5G437300	Aqcoe5G437300.1	AT5G41410.1	BEL 1	POX (plant homeobox) family protein	GO:0006355,GO:0003677
antagonistic with AG	-	none	Aqcoe2G233200	Aqcoe2G233200.1	AT5G02030.1	BLH9,BLR,HB-6,LS N,PNY,RPL,VAN	POX (plant homeobox) family protein	GO:0006355,GO:0003677
antagonistic with AG	-	none	Aqcoe1G138800	Aqcoe1G138800.1	AT2G27990.1	BLH8,PNF	BEL1-like homeodomain 8	GO:0006355,GO:0003677
antagonistic with AG	-	none	Aqcoe1G341500	Aqcoe1G341500.1	AT1G62360.1	BUM,BUM1,SHL,STM,WAM,WAM1	KNOX/ELK homeobox transcription factor	GO:0003677,GO:0006355,GO:0005634
antagonistic with AG	-	none	Aqcoe3G280300.1		AT1G70510	KNAT2		
subtrait	whorl	qtl	aq_locus_name	aq_peptid_name	at_best_hit	at_symbol	arabi-defline	GO
anther development	-	none	Aqcoe4G024000	Aqcoe4G024000.1	AT4G18960.1	AG	K-box region and MADS-box transcription factor family protein	GO:0046983,GO:0003677,GO:0006355,GO:0003677
anther development	-	none	Aqcoe7G042600	Aqcoe7G042600.1	AT5G07280.1	EMS1,EXS	Leucine-rich repeat transmembrane protein kinase	GO:0005515,GO:0006468,GO:0005524,GO:0003677
anther development	-	none	Aqcoe1G368600	Aqcoe1G368600.1	AT4G21330.1	DYT1	basic helix-loop-helix (bHLH) DNA-binding superfamily protein	
anther development	-	none	Aqcoe3G100100	Aqcoe3G100100.1	AT3G28470.1	ATMYB35,TDF1	Duplicated homeodomain-like superfamily protein	
anther development	-	none	Aqcoe3G122900	Aqcoe3G122900.1	AT2G16910.1	AMS	basic helix-loop-helix (bHLH) DNA-binding superfamily protein	GO:0046983
anther development	-	none	Aqcoe1G380400	Aqcoe1G380400.1	AT5G56110.1	ATMYB103,ATMYB80,MS188,MYB103	myb domain protein 103	
anther development	-	none	Aqcoe2G003200	Aqcoe2G003200.1	AT3G11440.1	ATMYB65,MYB65	myb domain protein 65	
anther development	-	none	Aqcoe1G085500	Aqcoe1G085500.1	AT3G09090.1	DEX1	defective in exine formation protein (DEX1)	
anther development	-	none	Aqcoe3G100100	Aqcoe3G100100.1	AT3G28470.1	ATMYB35,TDF1	Duplicated homeodomain-like superfamily protein	
anther development	-	none	Aqcoe3G283200	Aqcoe3G283200.1	AT1G23420.1	INO	Plant-specific transcription factor YABBY family protein	GO:0007275
anther development	-	none	Aqcoe5G346200	Aqcoe5G346200.1	AT4G24972.1	TPD1	tapetum determinant 1	
anther development	-	none	Aqcoe7G363100	Aqcoe7G363100.1	AT2G13680.1	ATGSL02,CALS5,GLS2	callose synthase 5	GO:0016020,GO:0006075,GO:0003843,GO:0004545,GO:0015035,GO:0009055
anther development	-	none	Aqcoe3G159700	Aqcoe3G159700.1	AT5G14070.1	ROXY2	Thioredoxin superfamily protein	
anther development	-	none	no protein homolog	matches in <i>Aquilegia</i>	AT4G27330	NZZ/SPL		
anther development	-	none	Aqcoe4G227800	Aqcoe4G227800.1	AT4G20090.1	EMB1025	Pentatricopeptide repeat (PPR) superfamily protein	
anther development	-	none	Aqcoe7G083800	Aqcoe7G083800.1	AT4G37590.1	NPY5	Phototropic-responsive NPH3 family protein	
B-class transcription	-	none	Aqcoe6G257300	AP3-2	AT3G54340.1	AP3,ATAP3	K-box region and MADS-box transcription factor family protein	GO:0006355,GO:0005634,GO:0003700,GO:0005515
floral meristem ID	-	none	Aqcoe0095s0001	Aqcoe0095s0001.1	AT1G30950.1	UFO	F-box family protein	GO:0005515
floral meristem ID	-	none	Aqcoe1G456700	Aqcoe1G456700.1	AT5G03680.1	PTL	Duplicated homeodomain-like superfamily protein	
floral meristem ID	-	none	Aqcoe5G327800	Aqcoe5G327800.1	AT5G61850.1	LFY,LFY3	floral meristem identity control protein LEAFY (LFY)	GO:0006355,GO:0003677

References

- de Almeida AMR, Yockteng R, Schnable J, Alvarez-Buylla ER, Freeling M, Specht CD (2014) Co-option of the polarity gene network shapes filament morphology in angiosperms. *Sci Rep* 4: 6194
- Averof M, Patel NH (1997) Crustacean appendage evolution associated with changes in Hox gene expression. *Nature* 388: 682–686
- Ballerini ES, Min Y, Edwards MB, Kramer EM, Hodges SA (2020) *POPOVICH*, encoding a C2H2 zinc-finger transcription factor, plays a central role in the development of a key innovation, floral nectar spurs, in *Aquilegia*. *Proc Natl Acad Sci USA* 117: 22552–22560
- Bastida JM, Alcántara JM, Rey PJ, Vargas P, Herrera CM (2010) Extended phylogeny of *Aquilegia*: the biogeographical and ecological patterns of two simultaneous but contrasting radiations. *Plant Syst Evol* 284: 171–185
- Bowman JL, Smyth DR, Meyerowitz EM (1991) Genetic interactions among floral homeotic genes of *Arabidopsis*. *Development* 112: 1–20
- Broman KW, Wu H, Sen S, Churchill GA (2003) R/qtl: QTL mapping in experimental crosses. *Bioinformatics* 19: 889–890
- Buzgo M, Soltis PS, Soltis DE (2004) Floral Developmental Morphology of *Amborella trichopoda* (Amborellaceae). *Int J Plant Sci* 165: 925–947
- Cabin Z, Derieg NJ, Garton A, Ngo T, Quezada A, Gasseholm C, Simon M, Hodges SA (2022) Non-pollinator selection for a floral homeotic mutant conferring loss of nectar reward in *Aquilegia coerulea*. *Curr Biol* 32: 1332–1341.e5
- Chanderbali AS, Albert VA, Leebens-Mack J, Altman NS, Soltis DE, Soltis PS (2009) Transcriptional signatures of ancient floral developmental genetics in avocado (*Persea americana*; Lauraceae). *Proc Natl Acad Sci USA* 106: 8929–8934
- Cheng C-Y, Krishnakumar V, Chan AP, Thibaud-Nissen F, Schobel S, Town CD (2017) Araport11: a complete reannotation of the *Arabidopsis thaliana* reference genome. *Plant J* 89: 789–804
- Coen ES, Meyerowitz EM (1991) The war of the whorls: genetic interactions controlling flower development. *Nature* 353: 31–37
- Decraene LPR, Smets EF (2001) Staminodes: Their morphological and evolutionary significance. *Bot Rev* 67: 351–402
- Du J, Anderson CT, Xiao C (2022) Author Correction: Dynamics of pectic homogalacturonan in cellular morphogenesis and adhesion, wall integrity sensing and plant development. *Nat Plants* 8: 721
- Eastwood A (1897) Alice Eastwood semi-centennial publications. Proceedings of the National Academy of Sciences.
- Edwards MB, Choi GPT, Derieg NJ, Min Y, Diana AC, Hodges SA, Mahadevan L, Kramer EM, Ballerini ES (2021) Genetic architecture of floral traits in bee- and hummingbird-pollinated sister species of *Aquilegia* (columbine). *Evolution* 75: 2197–2216
- Eyde RH, Morgan JT (1973) Floral Structure and Evolution in *Lopezieae* (Onagraceae). *Am J Bot* 60: 771
- Filiault DL, Ballerini ES, Mandáková T, Aköz G, Derieg NJ, Schmutz J, Jenkins J, Grimwood J, Shu S, Hayes RD, et al (2018) The *Aquilegia* genome provides insight

- into adaptive radiation and reveals an extraordinarily polymorphic chromosome with a unique history. *Elife* 7: e36426
- Fior S, Li M, Oxelman B, Viola R, Hodges SA, Ometto L, Varotto C (2013) Spatiotemporal reconstruction of the *Aquilegia* rapid radiation through next-generation sequencing of rapidly evolving cp DNA regions. *New Phytol* 198: 579–592
- Géant E, Mouchel-Vielh E, Coutanceau J-P, Ozouf-Costaz C, Deutsch JS (2006) Are Cirripedia hopeful monsters? Cytogenetic approach and evidence for a Hox gene cluster in the cirripede crustacean *Sacculina carcini*. *Dev Genes Evol* 216: 443–449
- Goodstein DM, Shu S, Howson R, Neupane R, Hayes RD, Fazo J, Mitros T, Dirks W, Hellsten U, Putnam N, et al (2012) Phytozome: a comparative platform for green plant genomics. *Nucleic Acids Res* 40: D1178–86
- Huang Y, Guo J, Zhang Q, Lu Z, Liu Y, Others (2017) *Semiaquilegia guangxiensis* (Ranunculaceae), a new species from the limestone areas of Guangxi, China, based on morphological and molecular evidence. *Phytotaxa* 292: 180–188
- Irwin P (1998) Colorado's Best Wildflower Hikes: The Front Range. Big Earth Publishing
- Kim S, Koh J, Yoo M-J, Kong H, Hu Y, Ma H, Soltis PS, Soltis DE (2005) Expression of floral MADS-box genes in basal angiosperms: implications for the evolution of floral regulators. *Plant J* 43: 724–744
- Kramer EM (2009) *Aquilegia*: A New Model for Plant Development, Ecology, and Evolution. *Annu Rev Plant Biol* 60: 261–277
- Kramer EM, Di Stilio VS, Schlüter PM (2003) Complex Patterns of Gene Duplication in the APETALA3 and PISTILLATA Lineages of the Ranunculaceae. *Int J Plant Sci* 164: 1–11
- Kramer EM, Holappa L, Gould B, Jaramillo MA, Setnikov D, Santiago PM (2007) Elaboration of B gene function to include the identity of novel floral organs in the lower eudicot *Aquilegia*. *Plant Cell* 19: 750–766
- Krolikowski KA, Victor JL, Wagler TN, Lolle SJ, Pruitt RE (2003) Isolation and characterization of the Arabidopsis organ fusion gene HOTHEAD. *Plant J* 35: 501–511
- Lolle SJ, Hsu W, Pruitt RE (1998) Genetic analysis of organ fusion in *Arabidopsis thaliana*. *Genetics*
- Luo H, Chen S, Jiang J, Chen Y, Chen F, Teng N, Yin D, Huang C (2011) The expression of floral organ identity genes in contrasting water lily cultivars. *Plant Cell Rep* 30: 1909–1918
- Magallón S, Castillo A (2009) Angiosperm diversification through time. *Am J Bot* 96: 349–365
- Majer C, Hochholdinger F (2011) Defining the boundaries: structure and function of LOB domain proteins. *Trends Plant Sci* 16: 47–52
- Meaders C, Min Y, Freedberg KJ, Kramer E (2020) Developmental and molecular characterization of novel staminodes in *Aquilegia*. *Ann Bot* 126: 231–243
- Meyerowitz EM, Smyth DR, Bowman JL (1989) Abnormal flowers and pattern formation in floral development. *Development* 106: 209–217
- Min Y, Conway SJ, Kramer EM (2022) Quantitative live imaging of floral organ initiation and floral meristem termination in *Aquilegia*. *Development*. doi: 10.1242/dev.200256

- Min Y, Kramer EM (2017) The *Aquilegia* JAGGED homolog promotes proliferation of adaxial cell types in both leaves and stems. *New Phytol* 216: 536–548
- Min Y, Kramer EM (2020) Transcriptome profiling and weighted gene co-expression network analysis of early floral development in *Aquilegia coerulea*. *Sci Rep* 10: 19637
- Mouille G, Ralet M-C, Cavelier C, Eland C, Effroy D, Hématy K, McCartney L, Truong HN, Gaudon V, Thibault J-F, et al (2007) Homogalacturonan synthesis in *Arabidopsis thaliana* requires a Golgi-localized protein with a putative methyltransferase domain. *Plant J* 50: 605–614
- Munz PA (1946) *Aquilegia*: the cultivated and the wild Columbines. *Bailey Hortorium*
- Orr H (1998) Testing natural selection vs. genetic drift in phenotypic evolution using quantitative trait locus data. *Genetics* 149: 2099–2104
- Panikashvili D, Shi JX, Schreiber L, Aharoni A (2009) The *Arabidopsis* DCR encoding a soluble BAHD acyltransferase is required for cutin polyester formation and seed hydration properties. *Plant Physiol* 151: 1773–1789
- Parry CC (1874) Botanical Observations in Western Wyoming. *The American Naturalist* VIII: 211–215
- Qin X-M, Huang Z-P, Lu Y-B, Zhang Q (2020) The complete chloroplast genome of *Semiaquilegia guangxiensis*, a rare and endemic herb in Guangxi, China. *Mitochondrial DNA B Resour* 5: 2324–2325
- Rice DP, Townsend JP (2012) Resampling QTL effects in the QTL sign test leads to incongruous sensitivity to variance in effect size. *G3* 2: 905–911
- Rieseberg LH, Widmer A, Arntz AM, Burke JM (2002) Directional selection is the primary cause of phenotypic diversification. *Proc Natl Acad Sci U S A* 99: 12242–12245
- Sharma B, Kramer E (2013) Sub- and neo-functionalization of *APETALA 3* paralogs have contributed to the evolution of novel floral organ identity in *Aquilegia* (columbine, Ranunculaceae). *New Phytol* 197: 949–957
- Shuai B, Reynaga-Peña CG, Springer PS (2002) The lateral organ boundaries gene defines a novel, plant-specific gene family. *Plant Physiol* 129: 747–761
- Soltis PS, Soltis DE, Kim S, Chanderbali A, Buzgo M (2006) Expression of Floral Regulators in Basal Angiosperms and the Origin and Evolution of ABC-Function. *Advances in Botanical Research*. Academic Press, pp 483–506
- Soza VL, Snelson CD, Hewett Hazelton KD, Di Stilio VS (2016) Partial redundancy and functional specialization of E-class SEPALLATA genes in an early-diverging eudicot. *Dev Biol* 419: 143–155
- Tepfer SS (1953) *Floral anatomy and ontogeny in Aquilegia formosa* var. *truncata* and *Ranunculus repens*. University of California Press
- Tucker SC, Hodges SA (2005) Floral Ontogeny of *Aquilegia*, *Semiaquilegia*, and *Enemion* (Ranunculaceae). *Int J Plant Sci* 166: 557–574
- Voelckel C, Borevitz JO, Kramer EM, Hodges SA (2010) Within and between Whorls: Comparative Transcriptional Profiling of *Aquilegia* and *Arabidopsis*. *PLoS One* 5: e9735
- Walker-Larsen J, Harder LD (2000) The evolution of staminodes in angiosperms: patterns of stamen reduction, loss, and functional re-invention. *Am J Bot* 87: 1367–1384

- Wang W, Chen Z-D (2007) Generic level phylogeny of Thalictroideae (Ranunculaceae) - implications for the taxonomic status of *Paropyrum* and petal evolution. *Taxon* 56: 811–821
- Whittall JB, Hodges SA (2007) Pollinator shifts drive increasingly long nectar spurs in columbine flowers. *Nature* 447: 706–709
- Xie J, Zhao H, Li K, Zhang R, Jiang Y, Wang M, Guo X, Yu B, Kong H, Jiao Y, et al (2020) A chromosome-scale reference genome of *Aquilegia oxysepala* var. *kansuensis*. *Hortic Res* 7: 113
- Xu C, Luo F, Hochholdinger F (2016) LOB Domain Proteins: Beyond Lateral Organ Boundaries. *Trends Plant Sci* 21: 159–167

Chapter II: A complex genetic basis for adaptive dwarfism in a high alpine plant, *Aquilegia jonesii*

Introduction

High alpine environments are especially harsh due to many factors including low temperatures, high winds, and extreme UV radiation. As such, they harbor high levels of biodiversity and endemism (Agakhanjanz and Breckle, 1995; Körner, 1995). Dwarfism is one of the most ubiquitous traits in alpine plants, and because there have been many independent convergent shifts to dwarfism, it is considered adaptive (Billings, 1974; Körner, 1999; Byars et al., 2007; Gonzalo-Turpin and Hazard, 2009; Turesson, 2010). Being dwarf allows plants to withstand heavy wind and snow load and keeps them closer to the ground, which can be an important source of warmth in especially cold and windy conditions (Billings and Mooney, 1968; Körner, 1999). Dwarfism is also important in crops, as it reduces lodging (bending at the base) risk and often results in more branching and more fruit yield, as long as nitrogen is supplemented (Schomburg et al., 2003; Ford et al., 2018; Tan et al., 2018). Extensive research has made significant progress in understanding the anatomical and physiological nature of dwarfism in high alpine plants, but comparatively little is known about the genetic mechanisms controlling these traits in wild species (Bohutínská et al., 2021; Zaborowska et al., 2021).

The genetic basis of alpine adapted traits such as dwarfism, cold/freeze tolerance, UV light tolerance, and epidermal modifications (waxiness or hairiness) have largely been characterized in model systems such as *Arabidopsis* and agricultural crops (Barboza et al., 2013; Weigel and Nordborg, 2015; Bi et al., 2016; Jenkins, 2017; Bohutínská et al., 2021). While *Arabidopsis* is a powerful model taxon, it does not live in extreme alpine

environments, nor do dwarf crop varieties which have been artificially selected for high reproductive yield (Liu et al., 2018; Tan et al., 2018; Wei et al., 2018). Thus, the genetic mechanisms elucidated by these studies provide a starting point for studying these traits in wild systems, but they do not necessarily represent the mechanisms naturally selected in high alpine habitats.

Aquilegia jonesii Parry is an herbaceous perennial that occurs in some of the most extreme alpine environments inhabited by any plants (Parry, 1874). Growing well above the treeline on exposed limestone peaks, *A. jonesii* is the most dwarf, alpine-adapted species of *Aquilegia* (columbine), and among the most alpine adapted plants (Munz, 1946). As columbines grow from a basal rosette, their vegetative stature is determined primarily by leaf tissue. Like all columbines, *A. jonesii* makes ternately compound leaves, though its leaf blades and stalks (petioles and petiolules) are diminutive compared to other species (Fig. 1, (Munz, 1946).

There are many molecular pathways that could be modified to result in a dwarf plant, but most of these would result in deleterious pleiotropic effects to roots and reproductive structures, ultimately rendering the plant maladapted (Ma et al., 2016). Importantly, there are fewer modifications that result in a dwarf plant with normal to high reproductive output, as is imperative for both natural and crop taxa (Luo et al., 2015; Li et al., 2018; Kumar et al., 2020). Research in wild accessions of *Arabidopsis* and crops has consistently shown that dwarfism is caused by modifications to the gibberellic acid (GA) pathway (Peng et al., 1999; Spielmeier et al., 2002). While modifications to most signaling pathways (e.g. auxin, brassinosteroids, strigolactones) ultimately affect plant stature, the GA pathway is by far the most common pathway shown to cause dwarfism, especially in cases where high

reproductive output is maintained (Hedden, 2003; Wang et al., 2017). For example, Barboza et al. (2013) found that semidwarfism in 23 populations of *A. thaliana* across Europe and Asia, from sea level to 2550m, is caused by independent loss-of-function mutations in the same GA biosynthesis gene, *GIBBERELLIN 20-OXIDASE 1 (GA20ox1/GA5)*. In addition to *GA20ox1*, mutations in other GA genes also cause dwarfism in several agricultural varieties, including genes involved in GA biosynthesis (e.g. *GA3ox*), GA metabolism (e.g. *GA2ox*), and DELLA imposed repression (e.g. *RGA, GAI, RGLs*), and perception (e.g. *GID1*) of GA response (Hollender et al., 2016; Wang et al., 2017). Furthermore, the GA pathway is associated with dwarfism in a coastal ecotype of the ecological genetic model species *Mimulus guttatus*. Gould et al. (2017) demonstrated that variation in several locally adapted traits, including dwarfism, between coastal (dwarf) and inland (non-dwarf) ecotypes, is maintained by a chromosomal inversion which includes *GA20ox2* and a QTL outside this inversion that contains *GAI* (Hall et al., 2006; Lowry and Willis, 2010).

The high alpine dwarf, *A. jonesii* gives an opportunity to further explore key genes in adaptive alpine dwarfism. We sought to determine whether dwarfism in *A. jonesii* is due to a simple genetic change, such as a mutation in a GA pathway gene, or if it has a more complex genetic basis involving multiple GA genes and/or other hormonal pathways. To identify regions of the genome harboring causal genes for two whole-plant measurements of plant size and three measurements of leaf size, we used QTL analysis with an F2 population between *A. jonesii* and *A. coerulea* ‘Origami’, which is not dwarf. These analyses reveal that the GA pathway is either uninvolved or plays a small role in the complex genetic basis of adaptive dwarfism in *A. jonesii*.

Methods

** See Chapter I (pages 5-8) for the specifics of the crossing design, genotyping, genetic map, and QTL analysis*

Phenotyping

All plants measured in this study were grown in the same greenhouse. F2 seeds were planted in January 2019 and germinated between February and May of 2019. Sample sizes varied across measurements due to the availability of healthy plants and leaves. We measured 260 plants for both whole-plant measurements, and 144 plants for each leaf size measurement. For plant stature traits, the pollen parent (*A. jonesii*), the maternal parent ('Origami'), the F1, and all F2 plants were measured once. For leaf size traits, one leaf from four *A. jonesii* individuals (not the pollen parent), and two leaves each from the maternal parent, F1, and F2 plants were measured. Plant diameter was measured at the widest diameter of the plant and plant height was measured from the soil to the tip of the highest leaf blade. These whole-plant measurements were taken from mid November to December 2019. Plants in flower were excluded from plant size trait analyses, as the architecture and height of a plant change substantially during flowering. Measurements were only taken from visually healthy plants to avoid measuring variation due to pest impact.

Leaf measurements were taken from scans of fully expanded leaves from January to June 2022. Leaf blades were spread onto a piece of clear tape, then secured to a white piece of paper. We made incisions on leaflets where they overlapped to ensure that all blade tissue was counted. For all plants where two leaves were measured, we used the larger value for each leaf measurement in our analyses to represent the largest and most fully expanded leaf

possible for an individual. Plants varied in the degree of leaf compounding, and thus the number of petiolules. We added the length of all petiolule fragments for the petiolule length measurement. Leaf area was measured in FIJI (Schindelin et al., 2012) using a custom macros. Petiole and petiolule lengths were measured using two custom macros scripts. While temperature, humidity, and light remained relatively constant in the greenhouse, sampling over the course of six months likely introduced environmental variation in leaf size measurements.

We did not have a large enough sample size to statistically compare whole-plant and leaf measurements across *A. jonesii* and ‘Origami’. The *A. jonesii* and ‘Origami’ parents were phenotyped for whole-plant measurements, however as the *A. jonesii* parent was not phenotyped for leaf measurements, we do not know whether the plant stature and leaf size values we observed in the four *A. jonesii* individuals reflect that of the *A. jonesii* parent for this cross. While *A. jonesii* plants can be quite wide in the field, forming prostrate mats, their diameter was restricted in one gallon pots, and thus the diameter measurement represented their small stature (Fig. 2.2).

Candidate gene search

We searched for *Aquilegia* homologs of GA pathway genes in *Arabidopsis* within the 1.5 LOD intervals of all QTL. We compared genes to the ‘Araport11’ *Arabidopsis* genome by keyword using Phytozome (Cheng et al., 2017; <https://phytozome.jgi.doe.gov>). For other pathways, we assembled a list of genes within the 3 marker bins (see Chapter I Methods) at and adjacent to the highest LOD peak for each QTL and scanned the list for homologs of genes known to be involved with plant stature. The top BLAST (‘tblastn’) hit

from *Arabidopsis* to the *Aquilegia coerulea* ‘Goldsmith’ proteome was considered the homolog in *Aquilegia*.

QTLST-EE

We used a simple sign test assuming equal effects of each QTL (QTLST-EE). A QTLST, which accounts for the distribution of QTL effect sizes would be preferable given the inflated false discovery rate of the QTLST-EE when there is high variance in effect sizes (Rice and Townsend, 2012). Although we had enough independent QTL (≥ 6) to perform the test on all traits aggregated as a proxy for dwarfism, most QTL affected multiple traits, making it difficult to determine a single effect size for each QTL. Additionally, our QTL had a relatively small variance in effect sizes (LOD: 3.9 - 8.5, PVE: 5.5 - 12.9) making the QTLST-EE suitable for our analysis.

Results

Phenotypic data

We measured five dwarfism related traits in the parents, F1 and F2 plants. These included two vegetative whole-plant stature measurements ($n = 260$): height and diameter, and three leaf size measurements ($n = 143$): leaf blade area, petiole (1° leaf stalk) length, and total petiolule (2° & 3° leaflet stalks) length. We measured plant diameter (widest part of the rosette) and height (base of the plant to the tip of the tallest leaf) from the greenhouse grown *A. jonesii* pollen parent. For *A. jonesii* leaves, we averaged measurements across four greenhouse grown individuals collected from seed from the same population (Hunt Mtn. Rd, WY) as the pollen parent. All ‘Origami’ measurements were taken from the maternal parent.

There was no overlap in any dwarfism traits between the parents, where *A. jonesii* was smaller than ‘Origami’ in every regard (Figs. 2.1, 2.2).

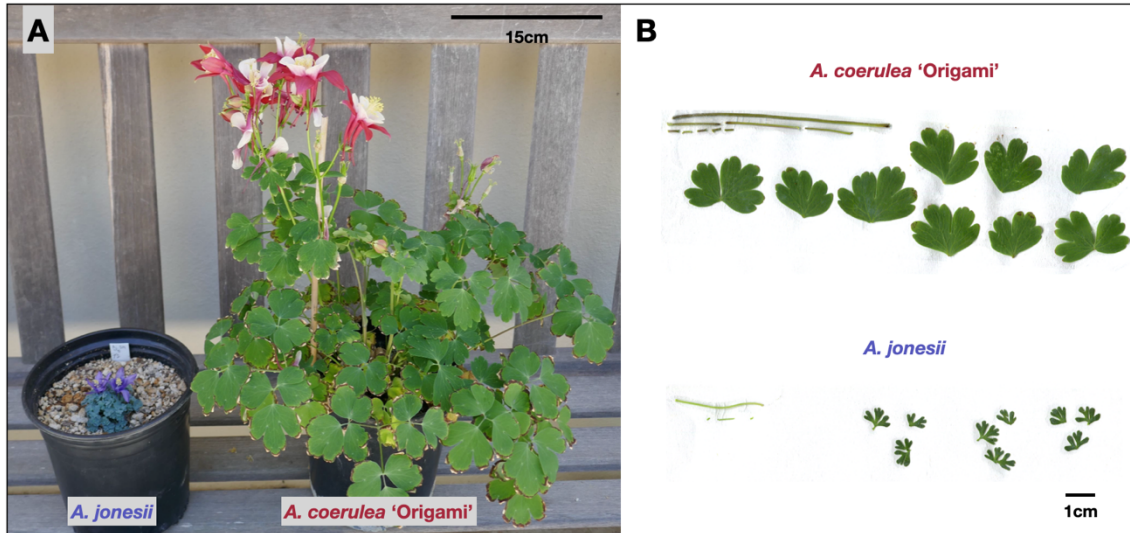


Figure 2.1. Plant stature and leaf comparisons of parents. A Greenhouse grown plants. B Individual leaves dissected into leaf blades, petioles and petioles and then mounted and scanned. Petioles are the top most leaf stalks, and petiolules are beneath them.

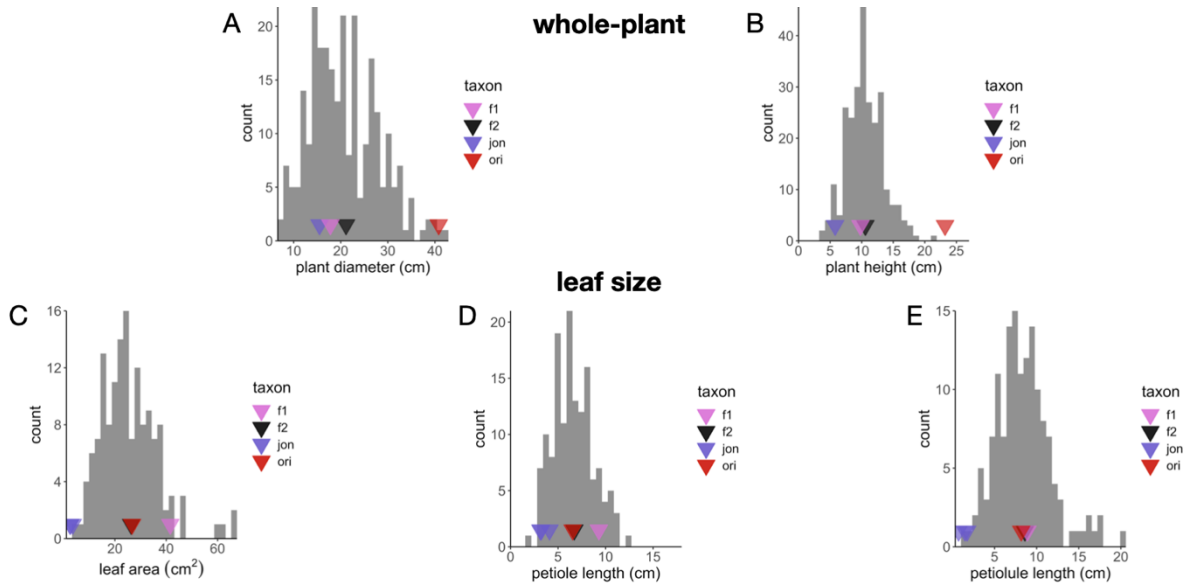


Figure 2.2. Histograms of each dwarfism trait in the F2 population and parents. Arrowheads represent the mean values of individuals, except the black arrow, which is a mean of the F2s. For whole-plant traits, the pollen parent (*A. jonesii*), the maternal parent (‘Origami’), and the F1 were measured. For leaf size traits (n = 143), 3 *A. jonesii* individuals (not the pollen parent), the maternal parent, and the F1 were measured. See Methods for details. Plant stature traits: n_{F2} = 260, leaf size traits: n_{F2} = 143, jon = *A. jonesii*, ori = ‘Origami’.

When we grew *A. jonesii* from seed in the greenhouse it maintained the extreme dwarf phenotype observed in the field. This contrasts ‘Origami’, also grown from seed, which grew much larger (Fig. 2.1), thus indicating a predominantly genetic basis for dwarfism in *A. jonesii*. We did observe some differences between field-grown and greenhouse-grown *A. jonesii* indicating a degree of environmental effects on growth form. For example, in the field, *A. jonesii* primarily grows in sun-exposed habitats with little to no shade, and its leaflets are tightly clustered, vertically oriented, glaucous, and pubescent (Supp. Fig. 2.1). However, when grown in the greenhouse, or when found in the field in shaded crevices, its leaflets are more evenly spread, horizontally oriented, less glaucous and less pubescent (Supp. Fig. 2.1). Greenhouse and shade grown plants also appear to occasionally have longer, more expanded petiolules (see arrows in Supp. Fig. 2.1), but no obvious difference in petiole length.

As measurements were taken over the course of 1-5 months, we examined whether the collection or measurement dates correlated with any trait measurement values. Linear regression revealed that plants measured on the latest date were 2.5cm shorter and had 8.8cm smaller diameters on average. Plants were periodically defoliated to mitigate pest impact, which likely explains this size discrepancy. While significant, the regression models explained relatively little variation in the data (Supp. Fig. 2.2). Collection date did not predict any leaf size measurements (Supp. Fig. 2.2). Given the significant correlations for plant stature traits, we considered the collection date as a potential covariate in multiple QTL models for plant diameter and height.

For plant size traits, F1 and F2 values were generally within the parental values, although the *A. jonesii* parent had a larger diameter than many F2s (Fig. 2.2A). Notably, the

A. jonesii parent was two years older than the F2 population at the time of trait measurement. For all three leaf traits, the mean value of the ‘Origami’ parent was near the mean of the F2s. All traits exhibited unimodal distributions though tests for normality were rejected, except that for petiole length (Fig. 2.2, Supp. Table 2.1).

All significant correlations between traits were positive (Table 2.1, Supp. Fig. 2.3). Spearman’s ρ values for significant correlations ranged from 0.18 - 0.76, with the strongest correlation between plant height and plant diameter (Spearman’s $\rho = 0.76$, $p < 0.001$; Table 2.1, Supp. Fig. 2.3D). The only significant correlation between a plant stature trait and a leaf size trait was between plant height and petiolule length (Spearman’s $\rho = 0.27$, $p = 0.004$, Table 2.1, Supp. Fig. 2.3F). In concert with this correlation, we visually observed that the outer petiolules were often vertically oriented compared to the petioles and inner petiolules (Supp. Fig. 2.4). Thus, overall petiolule length contributes significantly to plant height (Table 2.1, Supp. Fig. 2.3F, Supp. Fig. 2.4). Among leaf size traits, leaf area was weakly correlated with petiole length (Spearman’s $\rho = 0.18$, $p < 0.04$) and more tightly correlated with petiolule length (Spearman’s $\rho = 0.50$, $p < 0.001$; Table 2.1, Supp. Fig. 2.3H,I). Interestingly, petiole and petiolule lengths were not significantly correlated (Spearman’s $\rho = -0.07$, $p = 0.44$; Table 2.1, Supp. Fig. 2.3J).

Table 2.1. Correlation matrix across whole-plant and leaf area traits in F2 plants. Spearman’s ρ values are given with asterisks indicating significance. *: $p < 0.05$, **: $p < 0.01$, ***: $p < 0.001$.

	whole-plant (n = 260)		leaf size (n = 143)		
	plant diameter (cm)	plant height (cm)	leaf area (cm ²)	petiole length (cm)	petiolule length (cm)
plant diameter (cm)	—				
plant height (cm)	0.76***	—			
leaf area (cm ²)	0.01	0.005	—		
petiole length (cm)	0.06	-0.11	0.18*	—	
petiolule length (cm)	0.07	0.27*	0.50***	-0.07	—

As *A. jonesii* is much smaller than ‘Origami’ but makes larger epidermal cells (Chapter III), we explored whether the size of epidermal cells was correlated with the area of leaf blades in 139 F2 plants that had both traits measured. We used the number of leaf blade epidermal cells per mm² as a proxy for cell size and found no correlation between cell size and leaf area (Spearman’s $\rho = 0.082$, $p = 0.34$, Supp. Fig. 2.5).

Genotypic data

** See Chapter I page 15 for genotypic data results*

QTL analysis

Overall, we identified nine independent QTL (non-overlapping 1.5 LOD intervals) across four traits (Table 2.2, Fig. 2.3). Petiole length had no significant QTL. Full models accounted for 12-59 percent variation explained (PVE). All QTL were of moderate or minor effect, defined as having 10-25 PVE and less than 10 PVE, respectively. No QTL overlapped across whole-plant and leaf traits. Plant height was also explained by Q6 (6.1 LOD, 10.8 PVE), as well as a moderate effect QTL on Chr7 (5.8 LOD, 10.2 PVE) that did not overlap with any other traits. Leaf area had both the most QTL and the QTL of greatest effect of any trait (A-Q5; 8.5 LOD, 12.9 PVE), and only one (A-Q5) overlapped with another QTL (PU-Q5), although PU-Q5 covered most of the chromosome. We did not detect any significant interactions between QTL. As the date of measurement was significantly correlated with both plant stature measurements and petiolule length, we considered it as a covariate in both models, although it was excluded from the final models as it never accounted for more than 3 PVE.

Table 2.2. QTL results for each trait. Abbreviations: chr, chromosome; 1.5 LOD int, 1.5 LOD interval; PVE, Percent Variance Explained. For the ‘additive effect’ column, the *A. jonesii* allele has a (-) effect and the ‘Origami’ allele has a (+) effect.

trait	chr	name	1.5 LOD int (cM)	1.5 LOD phys (Mbp)	1.5LOD marker	peak position (cM)	LOD	PVE	total PVE	additive effect	dominance deviation	degree of dominance
diameter	6	D-Q6	18.5 - 37.2	5 - 13	6.11 - 6.33	26.1	6.1	12.1	12.1	3.4	2.8	0.82
height	6	H-Q6	17.6 - 41.2	4.5 - 22	6.1 - 6.37	26.2	6.1	10.8	21.3	1.4	0.6	0.43
height	7	H-Q7	0.5 - 17.2	0.5 - 6.5	7.002 - 7.013	6.2	5.8	10.2		-1.4	-0.4	0.29
leaf area	1	A-Q1	26.1 - 47.5	10 - 39	1.20 - 1.66	38.0	4.5	6.4	59.0	3.5	-1.6	-0.46
leaf area	3	A-Q3.1	0.3 - 10.4	0.3 - 4.5	3.003 - 3.018	7.0	5.8	8.3		1.6	5.3	3.31
leaf area	3	A-Q3.2	29.2 - 34.8	29 - 32	3.125 - 3.129	31.7	5.8	8.3		4.1	3.0	0.73
leaf area	5	A-Q5	47.0 - 58.1	38.5 - 42.5	5.64 - 5.72	48.7	8.5	12.9		7.2	0.6	0.08
leaf area	6	A-Q6	42.3 - 52.1	24 - 30.4	6.39 - 6.49	48.8	3.9	5.5		1.6	4.8	3.00
leaf area	7	A-Q7	20.1 - 27.7	7 - 12.2	7.015 - 7.025	24.0	7.9	11.9		5.5	2.7	0.49
petiolule length	5	PU-Q5.1	0 - 12.5	1 - 4.5	5.01 - 5.09	3.0	4.0	10.1	26.7	0.9	-1.5	-1.67
petiolule length	5	PU-Q5.2	12.5 - 59.8	4.5 - 42.5	5.09 - 5.73	35.8	4.4	11.0		1.9	1.0	0.53

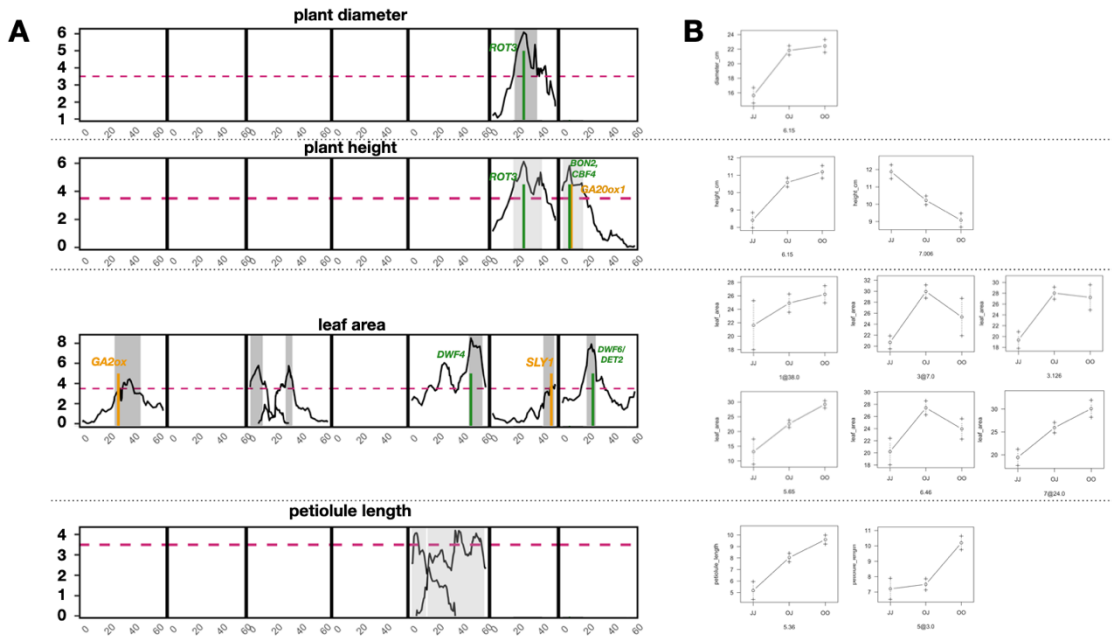


Figure 2.3. QTL maps and effect plots for each dwarfism related trait. A LOD profile reflects the best multiple QTL model associated with each dwarfism trait. Shaded area indicates 1.5 LOD interval for each significant QTL peak. Dashed magenta line represents the significance LOD threshold (3.37) for a ‘scanone’ of each trait. Green line indicates a GA gene, orange line indicates a non-GA growth gene within the 1.5 LOD interval. Commas separate multiple genes near the same locus. Slashes separate synonyms for genes. B Phenotype by genotype (PxG) effect plots for QTL. Genotypes are on the x-axis (J = *A. jonesii*, O = ‘Origami’) and their effects are on the y-axis. The chromosome and marker location of each QTL is listed beneath each plot.

For all QTL except one, we observed parental divergence where F2 plants homozygous for *A. jonesii* alleles were smaller than homozygotes for ‘Origami’ alleles (Table 2.2, Fig. 2.3B). The only exception was H-Q7, where individuals homozygous for the *A. jonesii* allele were taller than individuals heterozygous or homozygous for the ‘Origami’ allele. For leaf area, A-Q3.1, A-Q3.2, and A-Q6 exhibited overdominance, where heterozygotes had a larger mean leaf area than either homozygote genotype. This was consistent with the F1 having a larger leaf area than either parent and most F2 plants. A simple QTL sign test aggregating all independent QTL as dwarfism proxies and assuming equal effects (QTLST-EE; see Methods & Discussion) was significant ($p = 0.03$). Most traits showed additive patterns of inheritance for the parental alleles, although ‘Origami’ alleles were dominant slightly more often than *A. jonesii* alleles (Table 2.2, Fig. 2.3).

Candidate gene search

As the GA pathway has most commonly been associated with adaptive dwarfism, we searched for homologs of genes involved in the GA pathway within the 1.5 LOD interval of QTL. *AtGIBBERELLIN20-OXIDASE 1* (*AtGA20ox1*), *AtGIBBERELLIN2-OXIDASE* (*AtGA2ox*) and *SLEEPY1* (*SLY1*) were GA pathway homologs that colocalized within 1.5 LOD intervals of three QTL. However, *GA2ox* was near the outer edge of A-Q1 and both *GA2ox* and *SLY1* are within the QTLs of smallest effect across all traits (Supp. Table 2.1, Table 2.2, Fig. 2.3). There were no protein coding polymorphisms in any of these genes unique to *A. jonesii* compared to nine other columbine species which are not dwarf, or not nearly as dwarf as *A. jonesii*.

In addition to GA pathway genes, we also searched for candidate genes within the three highest LOD bins for each QTL. Homologs of five genes which cause dwarfism either due to loss of function (LoF) or overexpression (OE) in other systems were within seven different QTL, including three associated with brassinosteroids (BR) and two associated with plant defense (Supp. Table 2.2). There were polymorphisms unique to *A. jonesii* in homologs of two BR biosynthesis genes, *AqDWARF4* (*AqDWF4*) and *AqDWARF6* (*AqDWF6*). About 200bp upstream of the transcriptional start site (TSS) of *AjDWF4* was a ca.1.5kb deletion that does not occur in any other species. The largest deletion observed in several other species was ca.350bp in this region. In *AqDWF6*, there was a missense SNP in the second exon (V61L) unique to *A. jonesii*. There were no amino acid changing polymorphisms in the BR biosynthesis homolog within D/H-Q6, *AqROTUNDIFOLIA3* (*AqROT3*), or in either plant defense homolog within H-Q7 [*AqBON ASSOCIATION PROTEIN 2-LIKE* (*AqBAL/AqBAP2*), *AqC-REPEAT BINDING FACTOR 4* (*AqCBF4*)].

Discussion

Using multiple measures of whole-plant and leaf size, we demonstrate a polygenic and complex genetic basis for adaptive dwarfism in *A. jonesii*. Additionally, the significant QTLST-EE result provides statistical evidence that dwarfism in *A. jonesii* is adaptive. While many of these traits are positively correlated, a lack of shared QTL reveals that they likely evolved via co-selection, rather than pleiotropy or physical linkage. Our findings contrast the majority of previous studies on the genetic basis of dwarfism, which have identified a single GA pathway gene as responsible for dwarfism. To our knowledge, this is the first study to show a complex genetic basis for extreme dwarfism in any species. Our findings

suggest that the evolution of dwarfism via natural selection in high alpine environments may be a more gradual and nuanced process than in green revolution crops and *Arabidopsis*.

As columbines have extremely short internodes and grow from a basal rosette, their stature when not in flower is primarily dictated by leaf tissue. Thus, it is interesting that F2 plant stature measurements were either uncorrelated or weakly correlated with all leaf measurements (Table 2.1, Supp. Fig. 2.3). Particularly noteworthy was the lack of a correlation between plant height and petiole length. Instead, plant height was correlated with petiolule length. The vertical orientation of the outer petiolules is consistent with the significant petiolule-height correlation (Table 2.1, Supp. Figs. 2.3,2.4). Thus, the two QTL controlling plant height (H-Q6 and H-Q7) may harbor genes that control other leaf traits affecting plant stature, such as the angle of the petiolules. Future studies examining plant stature in basal rosette species should incorporate measurements of leaf stalk angles. Additionally, given that petioles of greenhouse grown *A. jonesii* sometimes expand more than field grown plants, studies in *Aquilegia* should measure the effect of environmental variables such as light and temperature on petiolule expansion.

A lack of strong correlation in the phenotypic data and nonoverlapping QTL in the genetic data suggest that different aspects of dwarfism in *A. jonesii* are primarily controlled by different genes. The only QTL that was clearly shared between two traits was on Chr6 between the two traits with the strongest correlation, plant height and plant diameter (Table 2.2, Fig. 2.3). The leaf area model explained more than twice that of any other trait (59 PVE), revealing that it may be under the most strict genetic control and have the least environmental influence of any of the dwarfism related traits we measured. Importantly, our low sample sizes (plant stature traits: $n = 260$, leaf size traits: $n = 143$) make it difficult to

detect small effect QTL (Beavis, 1994; Beavis and Paterson, 1998). Furthermore, with a small sample size, the estimated effect of a given QTL is inherently inflated. QTL effect sizes are calculated only considering the QTL included in the model, ignoring any existing, yet undetected small effect QTL, thus overestimating the effects of QTL in the model (Beavis, 1994; Beavis and Paterson, 1998). In this study, a lack of overlapping QTL across traits suggests that they are controlled by different genes, though small effect-size loci could actually overlap across traits but go undetected in one or the other analysis, especially given the substantial amount of environmental variation in the data. Future studies examining the genetic basis of dwarfism should prioritize obtaining a large sample size to alleviate these issues and thus more comprehensively determine the level of independent genetic control across traits.

The relatively low total PVE of all QTL models is likely due to substantial environmental variation in the data. One of these sources of variation was temporal, as we measured leaves over five months and plant size over one month (Supp. Fig. 2.2). Another likely source of environmental noise in our data was from greenhouse pests, which we were unable to account for. We only measured plants that were visually healthy, however individuals varied in their degree of pest impact over the course of their lives. Some of this impact was random, due to proximity to other infected plants, and there was also likely a genetic component to pest susceptibility that we did not assess. Regardless, pests may have significantly impacted plant stature as they balanced the tradeoff between defense and growth (Huot et al., 2014). Despite the various sources of environmental variation in our data, we still found minor to moderate effect QTL for four out of five traits. To mitigate the large amount of variation in physiological traits, future studies should maximize consistency

in timing of measurements across individuals and/or take measurements at multiple timepoints.

Greenhouse grown *A. jonesii* plants are limited in their width, as they are restricted by pots and *A. jonesii* grows particularly slowly. In contrast, the diameter of field grown plants is not limited by the width of a pot or the length of an experiment. They grow for many years and branch readily, forming attached clonal clumps and thus are relatively wide plants compared to other columbine species (Jouseau, 2005). This is consistent with observations in other taxa where dwarf species branch more than wild type varieties and ecotypes (Wang and Li, 2011; Lowry et al., 2019; Zhang et al., 2020). Furthermore, *A. jonesii* makes solitary flowers on relatively short pedicels, which contrasts the tall, branching inflorescences of most columbine species (Fig. 1A; Munz, 1946). Future studies should map the genetic basis of vegetative branching, inflorescence height, and solitary vs. multiple inflorescences to determine whether they are controlled by the same genes as other alpine dwarf traits.

Most previous work has shown that dwarf alpine plants make the same size or larger cells than non-dwarf relatives, but fewer of them (Körner et al., 1989). Interestingly, in the leaf blades, *A. jonesii* generally makes larger epidermal cells than ‘Origami’ when grown in the greenhouse (Chapter 2). The lack of correlation in the F2s between epidermal cell size and leaf blade area suggests that differences in the area of leaf blades is determined more by cell number rather than cell size (Supp. Fig. 2.5). Importantly, however, as we counted epidermal cells and measured leaf area on different leaves from the same plant, the lack of correlation could be due to environmental variation between leaves. Future studies should

examine the degree to which cell size and cell morphology across various tissues contribute to dwarfism, and the extent to which these traits are environmentally plastic.

It is noteworthy that of the ten genes within any QTL, only two are homologs of GA signaling genes. A homolog of *GA2ox*, which negatively regulates GA signaling by metabolizing bioactive GA, was near the outer edge of the A-Q1 1.5 LOD interval (Supp. Table 2.1) making it a less-likely candidate for underlying the QTL effect. A homolog of *AtSLY1* was within the region of A-Q6 with the highest LOD score. *AtSLY1* is the F-box component of the E3 ubiquitin ligase that degrades the DELLA gene *RGA* and de-represses GA response pathway (Steber et al., 1998; McGinnis et al., 2003). However, this QTL was only marginally significant and had an estimated PVE of only 5.5, suggesting it plays, at most, a small role in leaf area. Both of these genes were within the two QTL of smallest effect (A-Q1, A-Q6). Thus, contrary to most previous studies which have found the GA pathway to be responsible for causing adaptive dwarfism, *A. jonesii*'s dwarfism appears to be caused primarily by other molecular pathways.

With the exception of some wild accessions of *A. thaliana*, most genetic studies that have shown the GA pathway to be responsible for dwarfism have used crop varieties which have been artificially selected for a subset of traits that confer high yield. Importantly, however, these crops would be maladapted to natural environments where selective pressures act without the influence of human inputs such as fertilizer, irrigation, and pesticides (Gooding et al., 2012; Zhao et al., 2012). For example, recent work has shown that the GA pathway controlling dwarfism also interacts with genes controlling nitrogen use efficiency (Li et al., 2018), thus dwarfism and nitrogen use inefficiency have been co-selected in some agricultural varieties. Given the adverse environmental impacts of excess

nitrogen deposition (Guo et al., 2010; Zhang et al., 2015), breeders are attempting to decouple these traits. (Liu et al., 2021) investigated the naturally selected mechanisms of nitrogen use efficiency in wild rice ecotypes with the goal of introgressing beneficial alleles into crop varieties. These breeding efforts will benefit from studies such as this one, which uses a wild plant species whose dwarfism evolved amidst a more holistic suite of natural selective pressures.

While the GA pathway has been most commonly implicated in dwarfism, there are many plant hormones and signaling pathways that affect plant stature and leaf size. For example, brassinosteroids (BR) are involved in both cell division and cell expansion, and mutations in the BR pathway have been shown to cause dwarfism (reviewed by Nolan et al., 2020). In this cross, it was the developmental pathway with the most homologous genes within the regions of QTL with the highest LOD scores (Supp. Table 2.2). One of these was *ROTUNDIFOLIA3 (ROT3)*, a cytochrome P450 that catalyzes several hydroxylation steps in BR biosynthesis to cause leaf expansion, and was within both D-Q6 and H-Q6 (Tsuge et al., 1996; Kim et al., 1998). A lack of polymorphisms unique to *A. jonesii* in *ROT3* suggests that if it is involved in *A. jonesii*'s dwarfism, the change is likely regulatory. In addition, BR biosynthesis genes *DWARF 4 (DWF4)* and *DWARF6/DE-ETIOLATED 2 (DWF6/DET2)*, were both within leaf area QTL (A-Q5 and A-Q7, respectively), and LoF mutations in both genes cause dwarf plants (Choe et al., 1998; Cao et al., 2005; Chung et al., 2010). The large deletion upstream of *AjDWF4* is likely to have some effect on gene expression, and future studies should compare *DWF4* expression between *A. jonesii* and other non-dwarf species which have a smaller deletion using qRT-PCR. The missense mutation unique to *A. jonesii* in *AjDWF6* is unlikely to have a major effect, as valine and leucine are both non-polar

amino acids with highly similar structures. Thus, in addition to *DWF4*, both *DWF6* and *ROT3* expression should be compared between *A. jonesii* and non-dwarf species. The relative prevalence of BR biosynthesis genes within QTL suggests that modifications to this pathway may be largely responsible for alpine adapted dwarfism in *A. jonesii*.

Beyond the BR pathway, our results indicate that other developmental pathways may have been modified to cause dwarfism in *A. jonesii*. Loss-of-function mutations in the two plant defense genes within H-Q7 QTL, *BON-ASSOCIATION PROTEIN 2-LIKE* (*BAL/BAP2*) and C-REPEAT BINDING FACTOR 4 (*CBF4*) both cause dwarfism in *Populus* and *Vitis* (Yang et al., 2006; Yang et al., 2007; Siddiqua and Nassuth, 2011; Tian et al., 2017). Given that *A. jonesii* is dwarf both in the field and in the greenhouse, whatever mechanisms are responsible for dwarfism in *A. jonesii* are highly genetically controlled. Future studies should focus on pathways which are not subject to substantial environmental variation (Supp. Fig. 2.1).

Despite the majority of previous studies reporting a simple genetic basis for dwarfism in *Arabidopsis* and crop species, it is not surprising to find a complex genetic basis for alpine dwarfism in *A. jonesii*. Changes to a single gene of large effect can lead to substantial adaptive phenotypic changes, especially in the case of rapid adaptation due to dynamic selective pressures, such as in crop breeding (Gillespie, 1991; Orr, 2002; Cabin et al., 2022). However, for physiological traits such as stature, studies in systems such as *Drosophila* and humans have uncovered more complex mechanisms, where small changes to multiple genes are responsible for adaptive phenotypic variation (Yang et al., 2010; Turner et al., 2011). During this process, alleles of minor effect that counteract the adapted phenotype may rise in frequency via drift (Orr, 1998). For example, the QTL for plant

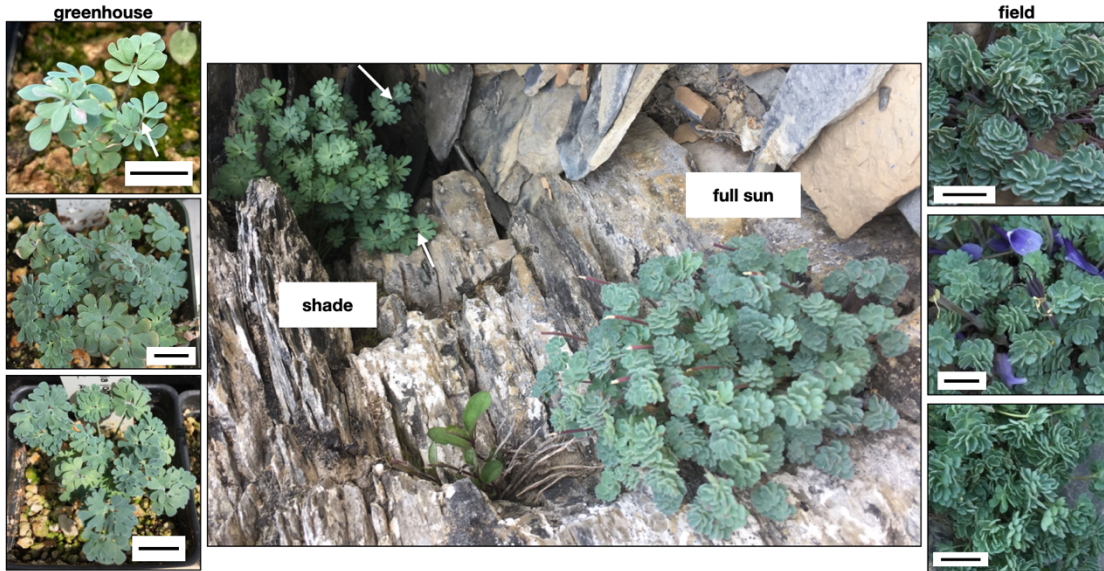
height on Chr7 (H-Q7) was the only QTL out of nine where the *A. jonesii* allele caused taller plants. As dwarfism is considered to be adaptive in all alpine plants, and the QTLST-EE for dwarf traits in *A. jonesii* was significant, H-Q7 likely evolved via drift.

Crossing *A. jonesii* to a non-dwarf columbine variety allowed us to identify regions of the genome harboring genes important for controlling their size differences. However, to identify regions of the genome important for *A. jonesii*'s adaptation to its extreme high alpine environment, *A. jonesii* could be crossed to a more closely related alpine species, such as *A. saximontana*. *A. saximontana* is sister to *A. jonesii* (Whittall and Hodges, 2007), and is relatively small in stature compared to other columbines but not nearly as dwarf as *A. jonesii* (Munz, 1946). A cross such as this one could not only identify genes important for adaptive alpine dwarfism, but also other alpine adapted traits such as glaucousness and pubescence.

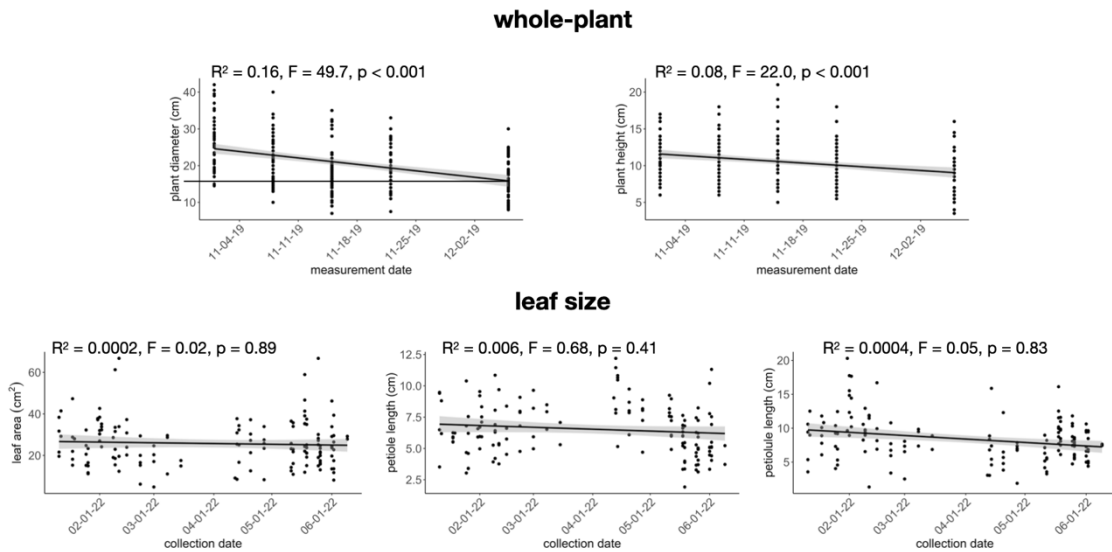
Conclusion

We have demonstrated the first example of a complex genetic basis for plant dwarfism. Furthermore, as *A. jonesii* is the only high alpine species currently represented in a genetic study of naturally selected dwarfism, its complex genetic basis may more accurately represent that of other wild, high alpine species. As genomic tools continue to become available for more taxa, researchers can uncover whether alpine taxa converged on dwarfism via the same mechanisms or different molecular pathways. A better understanding of these mechanisms will strengthen both conservation management strategies and agricultural breeding programs as environmental conditions continue to change at an alarmingly rapid rate (Becker-Scarpitta et al., 2019).

Supplemental Figures and Tables



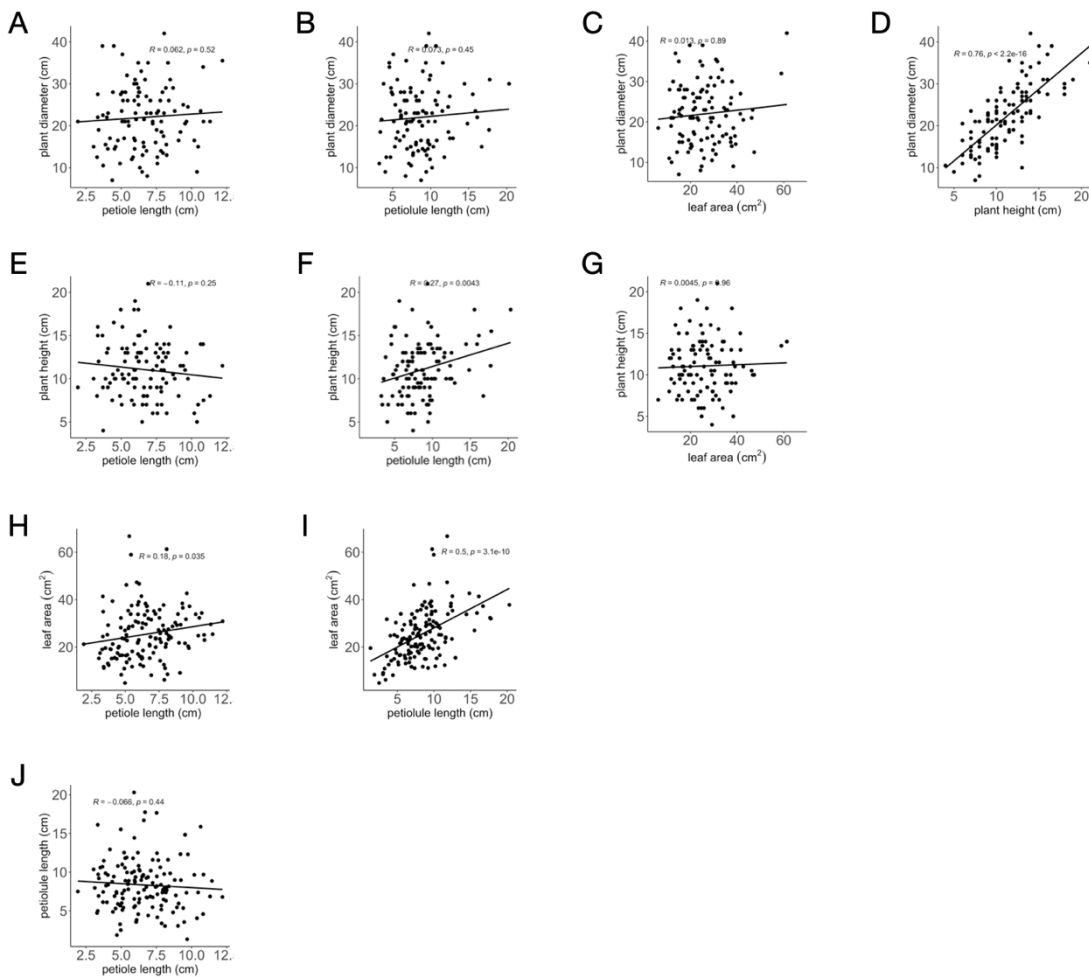
Supplemental Figure 2.1. Morphological differences between greenhouse (left) and field grown *A. jonesii* in full sun (right). The middle photo shows morphological differences between *A. jonesii* plants growing close together in the field, one in full sun and one in partial shade of a rock crevice. Arrows point to petiolules. Scale bars = 1 cm.



Supplemental Figure 2.2. Bivariate plots of each dwarfism related trait predicted by day of collection. R^2 and p-values are from linear regression. Plant stature traits: $n = 255$. Leaf area traits: $n = 141$.

Supplemental Table 2.1. Shapiro-Wilk test of normality for each dwarfism trait. H_0 : data are normally distributed.

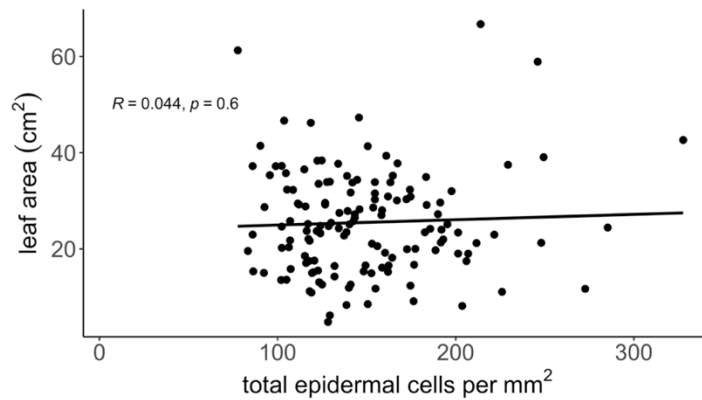
trait	W	p-value	conclusion
diameter	0.98	0.0002	non-normal
height	0.98	0.007	non-normal
leaf area	0.96	0.0002	non-normal
petiole length	0.98	0.06	normal
petiolule length	0.96	0.0009	non-normal



Supplemental Figure 2.3. Bivariate plots between whole-plant and leaf traits with the Spearman correlation values. A-D correlations with plant diameter. D-G correlations with plant height. H-J correlations among leaf size traits. 'R' represents Spearman's ρ values.



Supplemental Figure 2.4. Leaf stalk angles. Petioles (white arrowheads) and inner petiolules (black arrows) are at more horizontal angles. Outer petiolules (white arrows) are at more vertical angles.



Supplemental Figure 2.5. Bivariate plots of leaf area predicted by epidermal cell number per mm^2 as a proxy for size. R^2 and p -values are from linear regression. $n = 139$

Supplemental Table 2.2. Genes involved in GA pathway considered as candidates for dwarfism related traits. Dash indicates no colocalization with QTL.

gene	function	Arabidopsis	Aquilegia	QTL
GA20ox1-4	ga biosynthesis	At4G25420.1	Aqcoe7G054600	H-Q7
GA20ox5	ga biosynthesis	At4G25420.1	Aqcoe6G030000	-
GA3ox	ga biosynthesis	At1G15550.1	Aqcoe2G173400	-
GA3ox	ga biosynthesis	At1G15550.1	Aqcoe7G198700	-
GA3ox	ga biosynthesis	At1G15550.1	Aqcoe7G198600	-
GA3ox	ga biosynthesis	At1G15550.1	Aqcoe7G198500	-
GA3ox	ga biosynthesis	At1G15550.1	Aqcoe7G199100	-
GA3ox	ga biosynthesis	At1G15550.1	Aqcoe7G198100	-
GA2ox	ga metabolism	At1G30040.1	Aqcoe1G189900	A-Q1
GAI1	DELLA (GA repressor)	At1G14920.1	Aqcoe3G003900	-
RGA	DELLA (GA repressor)	At2G01570	Aqcoe3G418400	-
RGA	DELLA (GA repressor)	At2G01570	Aqcoe7G205100	-
GID1A	DELLA de-repression	At3G05120.1	Aqcoe2G319700	-
SLY1	DELLA de-repression	At4G24210.1	Aqcoe6G307300	A-Q6

Supplemental Table 2.3. Non-GA genes involved in plant growth within QTL. Abbreviations: mk, marker; chr, chromosome; pos, genetic position; start/end, physical location; Aq, *Aquilegia coerulea*; At, *Arabidopsis thaliana*; abbv, abbreviation; GO, gene ontology

qtl	mk	chr	pos (cM)	lod	start	end	Aq_gene_id	At_id	At_abbrev	At_name	source	hormone/process	GO
diameter	6.15	Q6	26.17	6.28	7217767	7229404	Aqcoe6G130300	AT4G36380.1	ROT3	Cytochrome P450 superfamily protein	Kim 1998 et al. Tsuge et al. 1996	cytochrome p450 leaf expansion w/ BR	GO:0055114, GO:0020037, GO:0016705, GO:0005506
height	6.15	Q6	26.17	6.28	7217767	7229404	Aqcoe6G130300	AT4G36380.1	ROT3	Cytochrome P450 superfamily protein	Kim 1998 et al. Tsuge et al. 1996	cytochrome p450 leaf expansion w/BR	GO:0055114, GO:0020037, GO:0016705, GO:0005506
height	7.006	Q7	6.23	5.59	2506328	2508626	Aqcoe7G042700	AT2G45760.1	BAL,BAP2	BON association protein 2	Yang et al. 2006, Yang et al. 2007	negative regulator of plant defense response, lof mutants are dwarf	GO:0005515
height	7.006	Q7	6.23	5.59	2880273	2881299	Aqcoe7G049000	AT5G51990.1	CBF4,DREB1D	C-repeat-binding factor 4	Siddiqua & Nauseth 2011, Tian et al. 2017	ERF/AP2 disease resistance TF; OE causes dwarfism, in poplar, dwarfism and increased SI in vitis	GO:0006355, GO:0003700
area	5.65	Q5	48.74	8.51	38578748	38581337	Aqcoe5G389600	AT3G50660.1	DWF4	Cytochrome P450 superfamily protein	Choe et al. 1998	dwarf due to lack of cell elongation; BR biosynthesis	GO:0055114, GO:0020037, GO:0016705, GO:0005506
area	7.02	Q7	25.28	7.19	9698750	9699641	Aqcoe7G149300	AT2G38050.1	DWF6, DET2	3-oxo-5-alpha-steroid 4-dehydrogenase family protein	Chung et al. 2010, Cao et al. 2005	BR biosynthesis; mutants are dwarf	NA
petiolule	5.18	Q5	25.03	2.67	8523890	8531673	Aqcoe5G151400	AT1G45249.1	ABF2,AREB1	abscisic acid responsive elements-binding factor 2	Paixao et al. 2019	OE were dwarf; ABA	GO:0043565, GO:0006355, GO:0003700
petiolule	5.18	Q5	25.03	2.67	8537976	8545312	Aqcoe5G151500	AT5G67030.1	ABA1,IBS3,LO56,NPQ2,ZEP	zeaxanthin epoxidase (ZEP) (ABA1)	Razem & Davis 2022	mutants were dwarf	GO:0005515, GO:0071949
petiolule	5.18	Q5	25.03	2.67	8723608	8724489	Aqcoe5G154300	AT5G42750.1	BKI1	BRI1 kinase inhibitor 1	Wang & Chory 2006	regulates bri, so maybe	NA

References

- Agakhanjanz O, Breckle SW (1995) Origin and Evolution of the Mountain Flora in Middle Asia and Neighbouring Mountain Regions. *In* FS Chapin, C Körner, eds, Arctic and Alpine Biodiversity: Patterns, Causes and Ecosystem Consequences. Springer Berlin Heidelberg, Berlin, Heidelberg, pp 63–80
- Ballerini ES, Min Y, Edwards MB, Kramer EM, Hodges SA (2020) *POPOVICH*, encoding a C2H2 zinc-finger transcription factor, plays a central role in the development of a key innovation, floral nectar spurs, in *Aquilegia*. *Proc Natl Acad Sci USA* 117: 22552–22560
- Barboza L, Effgen S, Alonso-Blanco C, Kooke R, Keurentjes JJB, Koornneef M, Alcazar R (2013) Arabidopsis semidwarfs evolved from independent mutations in GA20ox1, ortholog to green revolution dwarf alleles in rice and barley. *Proceedings of the National Academy of Sciences* 110: 15818–15823
- Beavis WD (1994) The power and deceit of QTL experiments: lessons from comparative QTL studies. Corn and sorghum industry research conference
- Beavis WD, Paterson AH (1998) Molecular dissection of complex traits. CRC, New York
- Becker-Scarpitta A, Vissault S, Vellend M (2019) Four decades of plant community change along a continental gradient of warming. *Glob Chang Biol* 25: 1629–1641
- Bi H, Luang S, Li Y, Bazanova N, Morran S, Song Z, Perera MA, Hrmova M, Borisjuk N, Lopato S (2016) Identification and characterization of wheat drought-responsive MYB transcription factors involved in the regulation of cuticle biosynthesis. *J Exp Bot* 67: 5363–5380
- Billings WD (1974) Adaptations and Origins of Alpine Plants. *Arct Alp Res* 6: 129
- Billings WD, Mooney HA (1968) The ecology of arctic and alpine plants. *Biol Rev Camb Philos Soc* 43: 481–529
- Bohutínská M, Vlček J, Yair S, Laenen B, Konečná V, Fracassetti M, Slotte T, Kolář F (2021) Genomic basis of parallel adaptation varies with divergence in Arabidopsis and its relatives. *Proc Natl Acad Sci USA*. doi: 10.1073/pnas.2022713118
- Broman KW, Wu H, Sen S, Churchill GA (2003) R/qtl: QTL mapping in experimental crosses. *Bioinformatics* 19: 889–890
- Byars S, Papst W, Hoffmann A (2007) Local adaptation and cogradient selection in the alpine plant, *Poa hiemata*, along a narrow altitudinal gradient. *Evolution* 61: 2925–2941
- Cabin Z, Derieg NJ, Garton A, Ngo T, Quezada A, Gasseholm C, Simon M, Hodges SA (2022) Non-pollinator selection for a floral homeotic mutant conferring loss of nectar reward in *Aquilegia coerulea*. *Curr Biol* 32: 1332–1341.e5
- Cao S, Xu Q, Cao Y, Qian K, An K, Zhu Y, Binzeng H, Zhao H, Kuai B (2005) Loss-of-function mutations in DET2 gene lead to an enhanced resistance to oxidative stress in Arabidopsis. *Physiol Plant* 123: 57–66
- Cheng C-Y, Krishnakumar V, Chan AP, Thibaud-Nissen F, Schobel S, Town CD (2017) Araport11: a complete reannotation of the Arabidopsis thaliana reference genome. *Plant J* 89: 789–804
- Choe S, Dilkes BP, Fujioka S, Takatsuto S, Sakurai A, Feldmann KA (1998) The DWF4 Gene of Arabidopsis Encodes a Cytochrome P450 That Mediates Multiple 22 α -Hydroxylation Steps in Brassinosteroid Biosynthesis. *Plant Cell* 10: 231–243

- Chung HY, Fujioka S, Choe S, Lee S, Lee YH, Baek NI, Chung IS (2010) Simultaneous suppression of three genes related to brassinosteroid (BR) biosynthesis altered campesterol and BR contents, and led to a dwarf phenotype in *Arabidopsis thaliana*. *Plant Cell Rep* 29: 397–402
- Edwards MB, Choi GPT, Derieg NJ, Min Y, Diana AC, Hodges SA, Mahadevan L, Kramer EM, Ballerini ES (2021) Genetic architecture of floral traits in bee- and hummingbird-pollinated sister species of *Aquilegia* (columbine). *Evolution* 75: 2197–2216
- Filiault DL, Ballerini ES, Mandáková T, Aköz G, Derieg NJ, Schmutz J, Jenkins J, Grimwood J, Shu S, Hayes RD, et al (2018) The *Aquilegia* genome provides insight into adaptive radiation and reveals an extraordinarily polymorphic chromosome with a unique history. *Elife* 7: e36426
- Ford BA, Foo E, Sharwood R, Karafiatova M, Vrána J, MacMillan C, Nichols DS, Steuernagel B, Uauy C, Doležel J, et al (2018) Rht18 semidwarfism in wheat is due to increased GA 2-oxidaseA9 expression and reduced GA content. *Plant Physiol* 177: 168–180
- Gillespie JH (1991) *The Causes of Molecular Evolution*. Oxford University Press
- Gonzalo-Turpin H, Hazard L (2009) Local Adaptation Occurs along Altitudinal Gradient despite the Existence of Gene Flow in the Alpine Plant Species *Festuca eskia*. *J Ecol* 97: 742–751
- Gooding MJ, Addisu M, Uppal RK, Snape JW, Jones HE (2012) Effect of wheat dwarfing genes on nitrogen-use efficiency. *J Agric Sci* 150: 3–22
- Goodstein DM, Shu S, Howson R, Neupane R, Hayes RD, Fazo J, Mitros T, Dirks W, Hellsten U, Putnam N, et al (2012) Phytozome: a comparative platform for green plant genomics. *Nucleic Acids Res* 40: D1178–86
- Gould BA, Chen Y, Lowry DB (2017) Pooled ecotype sequencing reveals candidate genetic mechanisms for adaptive differentiation and reproductive isolation. *Mol Ecol* 26: 163–177
- Guo JH, Liu XJ, Zhang Y, Shen JL, Han WX, Zhang WF, Christie P, Goulding KWT, Vitousek PM, Zhang FS (2010) Significant acidification in major Chinese croplands. *Science* 327: 1008–1010
- Hall MC, Basten CJ, Willis JH (2006) Pleiotropic quantitative trait loci contribute to population divergence in traits associated with life-history variation in *Mimulus guttatus*. *Genetics* 172: 1829–1844
- Hedden P (2003) The genes of the Green Revolution. *Trends Genet* 19: 5–9
- Hollender CA, Hadiarto T, Srinivasan C, Scorza R, Dardick C (2016) A brachytic dwarfism trait (dw) in peach trees is caused by a nonsense mutation within the gibberellic acid receptor PpeGID1c. *New Phytol* 210: 227–239
- Huot B, Yao J, Montgomery BL, He SY (2014) Growth-defense tradeoffs in plants: a balancing act to optimize fitness. *Mol Plant* 7: 1267–1287
- Jenkins GI (2017) Photomorphogenic responses to ultraviolet-B light. *Plant Cell Environ* 40: 2544–2557
- Jouseau M (2005) *Aquilegia jonesii*: Threatened - Or is it? *Rock Garden Quarterly* 63: 163–171

- Kim G-T, Tsukaya H, Uchimiya H (1998) The ROTUNDIFOLIA3 gene of Arabidopsis thaliana encodes a new member of the cytochrome P-450 family that is required for the regulated polar elongation of leaf cells. *Genes Dev* 12: 2381–2391
- Körner C (1995) Alpine Plant Diversity: A Global Survey and Functional Interpretations. *In* FS Chapin, C Körner, eds, *Arctic and Alpine Biodiversity: Patterns, Causes and Ecosystem Consequences*. Springer Berlin Heidelberg, Berlin, Heidelberg, pp 45–62
- Körner C (1999) *Alpine Plant Life*. Springer Berlin Heidelberg
- Körner C, Neumayer M, Menendez-Riedl SP, Smeets-Scheel A (1989) Functional Morphology of Mountain Plants 1) Dedicated to Prof. H. Meusel, on the occasion of his 80th birthday. *Flora* 182: 353–383
- Kumar A, Sandhu N, Venkateshwarlu C, Priyadarshi R, Yadav S, Majumder RR, Singh VK (2020) Development of introgression lines in high yielding, semi-dwarf genetic backgrounds to enable improvement of modern rice varieties for tolerance to multiple abiotic stresses free from undesirable linkage drag. *Sci Rep* 10: 13073
- Li S, Tian Y, Wu K, Ye Y, Yu J, Zhang J, Liu Q, Hu M, Li H, Tong Y, et al (2018) Modulating plant growth–metabolism coordination for sustainable agriculture. *Nature* 560: 595–600
- Liu F, Wang P, Zhang X, Li X, Yan X, Fu D, Wu G (2018) The genetic and molecular basis of crop height based on a rice model. *Planta* 247: 1–26
- Liu Y, Wang H, Jiang Z, Wang W, Xu R, Wang Q, Zhang Z, Li A, Liang Y, Ou S, et al (2021) Genomic basis of geographical adaptation to soil nitrogen in rice. *Nature* 590: 600–605
- Lowry DB, Popovic D, Brennan DJ, Holeski LM (2019) Mechanisms of a locally adaptive shift in allocation among growth, reproduction, and herbivore resistance in *Mimulus guttatus*. *Evolution* 73: 1168–1181
- Lowry DB, Willis JH (2010) A widespread chromosomal inversion polymorphism contributes to a major life-history transition, local adaptation, and reproductive isolation. *PLoS Biol.* doi: 10.1371/journal.pbio.1000500
- Luo Y, Dong X, Yu T, Shi X, Li Z, Yang W, Widmer A, Karrenberg S (2015) A Single Nucleotide Deletion in Gibberellin 20-oxidase 1 Causes Alpine Dwarfism in Arabidopsis. *Plant Physiol* 168: 930–937
- Ma Y, Xue H, Zhang L, Zhang F, Ou C, Wang F, Zhang Z (2016) Involvement of Auxin and Brassinosteroid in Dwarfism of Autotetraploid Apple (*Malus × domestica*). *Sci Rep* 6: 26719
- McGinnis KM, Thomas SG, Soule JD, Strader LC, Zale JM, Sun T-P, Steber CM (2003) The Arabidopsis SLEEPY1 gene encodes a putative F-box subunit of an SCF E3 ubiquitin ligase. *Plant Cell* 15: 1120–1130
- Munz PA (1946) *Aquilegia: the cultivated and the wild Columbines*. Bailey Hortorium
- Nolan TM, Vukašinović N, Liu D, Russinova E, Yin Y (2020) Brassinosteroids: Multidimensional Regulators of Plant Growth, Development, and Stress Responses. *Plant Cell* 32: 295–318
- Orr H (2002) The population genetics of adaptation: the adaptation of DNA sequences. *Evolution* 56: 1317–1330
- Orr H (1998) Testing natural selection vs. genetic drift in phenotypic evolution using quantitative trait locus data. *Genetics* 149: 2099–2104

- Parry CC (1874) Botanical Observations in Western Wyoming. *The American Naturalist* VIII: 211–215
- Peng J, Richards DE, Hartley NM, Murphy GP, Devos KM, Flintham JE, Beales J, Fish LJ, Worland AJ, Pelica F, et al (1999) “Green revolution” genes encode mutant gibberellin response modulators. *Nature* 400: 256–261
- Razem FA, Davis AR (2002) Stomatal frequency, maturity and index on developing bracts of four abscisic acid mutants and wild-type plants of *Arabidopsis thaliana*. *Environ Exp Bot* 48: 247–256
- Rice DP, Townsend JP (2012) Resampling QTL effects in the QTL sign test leads to incongruous sensitivity to variance in effect size. *G3* 2: 905–911
- Roca Paixão JF, Gillet F-X, Ribeiro TP, Bournaud C, Lourenço-Tessutti IT, Noriega DD, Melo BP de, de Almeida-Engler J, Grossi-de-Sa MF (2019) Improved drought stress tolerance in *Arabidopsis* by CRISPR/dCas9 fusion with a Histone AcetylTransferase. *Sci Rep* 9: 8080
- Schindelin J, Arganda-Carreras I, Frise E, Kaynig V, Longair M, Pietzsch T, Preibisch S, Rueden C, Saalfeld S, Schmid B, et al (2012) Fiji: an open-source platform for biological-image analysis. *Nat Methods* 9: 676–682
- Schomburg FM, Bizzell CM, Lee DJ, Zeevaart JAD, Amasino RM (2003) Overexpression of a novel class of gibberellin 2-oxidases decreases gibberellin levels and creates dwarf plants. *Plant Cell* 15: 151–163
- Siddiqua M, Nassuth A (2011) *Vitis* CBF1 and *Vitis* CBF4 differ in their effect on *Arabidopsis* abiotic stress tolerance, development and gene expression. *Plant Cell Environ* 34: 1345–1359
- Spielmeyer W, Ellis MH, Chandler PM (2002) Semidwarf (*sd-1*), “green revolution” rice, contains a defective gibberellin 20-oxidase gene. *Proceedings of the National Academy of Sciences* 99: 9043–9048
- Steber CM, Cooney SE, McCourt P (1998) Isolation of the GA-response mutant *sly1* as a suppressor of *ABI1-1* in *Arabidopsis thaliana*. *Genetics* 149: 509–521
- Tan P-H, Zhang L, Yin S-X, Teng K (2018) Heterologous expression of a novel *Poa pratensis* gibberellin 2-oxidase gene, *PpGA2ox*, caused dwarfism, late flowering, and increased chlorophyll accumulation in *Arabidopsis*. *Biol Plant* 62: 462–470
- Tian Q, Chen J, Wang D, Wang H-L, Liu C, Wang S, Xia X, Yin W (2017) Overexpression of a *Populus euphratica* CBF4 gene in poplar confers tolerance to multiple stresses. *Plant Cell Tissue Organ Cult* 128: 391–407
- Tsuge T, Tsukaya H, Uchimiya H (1996) Two independent and polarized processes of cell elongation regulate leaf blade expansion in *Arabidopsis thaliana* (L.) Heynh. *Development* 122: 1589–1600
- Turesson G (2010) The genotypical response of the plant species to the habitat. *Hereditas* 3: 211–350
- Turner TL, Stewart AD, Fields AT, Rice WR, Tarone AM (2011) Population-based resequencing of experimentally evolved populations reveals the genetic basis of body size variation in *Drosophila melanogaster*. *PLoS Genet* 7: e1001336
- Wang X, Chory J (2006) Brassinosteroids regulate dissociation of BKI1, a negative regulator of BRI1 signaling, from the plasma membrane. *Science* 313: 1118–1122
- Wang Y, Li J (2011) Branching in rice. *Curr Opin Plant Biol* 14: 94–99

- Wang Y, Zhao J, Lu W, Deng D (2017) Gibberellin in plant height control: old player, new story. *Plant Cell Rep* 36: 391–398
- Wang ZY, Seto H, Fujioka S, Yoshida S, Chory J (2001) BRI1 is a critical component of a plasma-membrane receptor for plant steroids. *Nature* 410: 380–383
- Weigel D, Nordborg M (2015) Population Genomics for Understanding Adaptation in Wild Plant Species. *Annu Rev Genet* 49: 315–338
- Wei L, Zhang X, Zhang Z, Liu H, Lin Z (2018) A new allele of the *Brachytic2* gene in maize can efficiently modify plant architecture. *Heredity* 121: 75–86
- Whittall JB, Hodges SA (2007) Pollinator shifts drive increasingly long nectar spurs in columbine flowers. *Nature* 447: 706–709
- Xie J, Zhao H, Li K, Zhang R, Jiang Y, Wang M, Guo X, Yu B, Kong H, Jiao Y, et al (2020) A chromosome-scale reference genome of *Aquilegia oxysepala* var. *kansuensis*. *Hortic Res* 7: 113
- Yang H, Li Y, Hua J (2006) The C2 domain protein BAP1 negatively regulates defense responses in *Arabidopsis*. *Plant J* 48: 238–248
- Yang H, Yang S, Li Y, Hua J (2007) The *Arabidopsis* BAP1 and BAP2 genes are general inhibitors of programmed cell death. *Plant Physiol* 145: 135–146
- Yang J, Benyamin B, McEvoy BP, Gordon S, Henders AK, Nyholt DR, Madden PA, Heath AC, Martin NG, Montgomery GW, et al (2010) Common SNPs explain a large proportion of the heritability for human height. *Nat Genet* 42: 565–569
- Zaborowska J, Łabiszak B, Perry A, Cavers S, Wachowiak W (2021) Candidate Genes for the High-Altitude Adaptations of Two Mountain Pine Taxa. *IJMS* 22: 3477
- Zhang X, Davidson EA, Mauzerall DL, Searchinger TD, Dumas P, Shen Y (2015) Managing nitrogen for sustainable development. *Nature* 528: 51–59
- Zhang X, He L, Zhao B, Zhou S, Li Y, He H, Bai Q, Zhao W, Guo S, Liu Y, et al (2020) Dwarf and Increased Branching 1 controls plant height and axillary bud outgrowth in *Medicago truncatula*. *J Exp Bot* 71: 6355–6365
- Zhao X, Zhou Y, Min J, Wang S, Shi W, Xing G (2012) Nitrogen runoff dominates water nitrogen pollution from rice-wheat rotation in the Taihu Lake region of China. *Agric Ecosyst Environ* 156: 1–11

Chapter III: A simple genetic basis for amphistomaty and stomatal density in an alpine columbine, *Aquilegia jonesii*

Introduction

Environmental stressors are amplified in alpine environments. Wind speed, snow load, light exposure, and other factors are all generally more intense in high elevations than in the lowlands (Billings and Mooney, 1968). Alpine plants have adopted a myriad of mechanisms to mitigate these conditions and make the most of short growing seasons, photosynthesizing and reproducing before returning to dormancy (Körner, 1999). For herbaceous plants above the treeline in rocky landscapes, physiological evidence suggests that photosynthesis is rarely limited by light availability but rather due to the rate of laminar CO₂ diffusion from stomatal pores to the cells doing photosynthesis (Parkhurst, 1978; Gutschick, 1984; Parkhurst and Mott, 1990; Beerling and Kelly, 1996). Accordingly, many plants from alpine and other high light environments such as deserts make stomata on both leaf surfaces (amphistomaty; Parkhurst and Mott, 1990; Peat and Fitter, 1994; Jordan et al., 2014; McKown et al., 2014b; Muir, 2015; Bucher et al., 2017).

The strikingly high frequency of amphistomatous species in alpine environments suggests that it is adaptive, despite the fact that a direct fitness advantage has yet to be measured (Mott et al., 1982). Furthermore, the direct physiological advantages measured in CO₂ diffusion, photosynthetic rate, and water use efficiency suggest that amphistomaty is indeed adaptive (Mott and O'leary, 1984; Beerling and Kelly, 1996; McKown et al., 2014a). However, there may also be direct costs of adaxial (usually upper) stomatal production through increased susceptibility to water loss and foliar pathogens (Gutschick, 1984; Foster and Smith, 1986; McKown et al., 2014b; Buckley et al., 2015). Thus, amphistomaty would

be optimally adaptive when plants can independently control their stomatal aperture on each leaf surface in response to changes in light, temperature, and water availability (Jordan et al., 2014; Muir et al., 2015; Richardson et al., 2017). Many alpine plants are exposed to high light and high winds and often orient their leaves vertically, which mitigates their transpiration rate and susceptibility to foliar fungal pathogens (Ehleringer, 1988; Körner et al., 1989; Muir, 2018). Dorsiventral stomatal patterning (DSP) can be highly variable within closely related clades, and can even be environmentally plastic within species and ecotypes (Metcalf et al., 1950; Körner et al., 1986; Körner et al., 1989; Mott and Michaelson, 1991; Weyers and Lawson, 1997; Gornall and Guy, 2007; McKown et al., 2014a; Muir, 2018). This abundant intra- and interspecific variation in DSP indicates that it can evolve readily as plants adapt to their environments.

Patterns of amphistomaty across environments have been well characterized, however relatively little is known about the molecular mechanisms underlying the production of stomata on the adaxial surface of leaves. Research on the genetic basis of DSP has been carried out using non-alpine plants including *Arabidopsis*, crops, an amphibious species (*Callitriche*), and a wild tomato species (*Solanum pennellii*; Dong and Bergmann, 2010; Muir et al., 2014; Doll et al., 2021; Wall et al., 2022). The genetic basis of DSP has also been examined in Poplar (*Populus tremuloides*), which occupies a wide variety of habitats, including subalpine, although it is not a particularly high alpine taxon (McKown et al., 2014b; McKown et al., 2019). *Aquilegia jonesii* Parry is an herbaceous high alpine species that occurs on limestone peaks throughout the Northern Rocky Mountains in full sun exposure with a short growing season (Parry, 1874). It exhibits common adaptations to alpine environments such as dwarfism and making leaves that are both glaucous and

pubescent (Parry, 1874). Similar to many plants exposed to long periods of high light, *A. jonesii* often has relatively monofacial leaves compared to other columbine species, which are oriented vertically (Fig. 1A,B). With an annotated *Aquilegia* reference genome and the ability to make interspecific hybrids, *A. jonesii* presents an opportunity to study the genetic basis of DSP in a high alpine plant (Filiault et al., 2018).

The canonical stomatal development pathway is relatively well-understood at a molecular level. The development of guard cells that make stomatal openings requires the activity of a paralogous family of basic helix-loop-helix (bHLH) transcription factors (MacAlister et al., 2007). *SPEECHLESS* (*SPCH*), *MUTE*, and *FAMA* (known as the SMF genes) drive stomatal lineage asymmetric cell division (ACD) to form a small meristemoid cell, promote the differentiation from meristemoid to guard mother cell (GMC), and drive division of the GMC to form two guard cells, respectively (Ohashi-Ito and Bergmann, 2006; MacAlister et al., 2007; Pillitteri et al., 2007). Complete loss of function of any of these genes abolishes stomatal development, thus they are considered master stomatal regulators. The regulation of these genes in canonical stomatal development and their responses to environmental inputs are relatively well understood, however less is known about the genetic basis of DSP specifically. The two studies which have mapped regions of the genome associated with DSP in natural systems have identified that variation in *SPCH* can cause differential DSP, including amphistomaty (Muir et al., 2014; McKown et al., 2019).

We examined DSP in *A. jonesii* and leveraged the annotated *Aquilegia* reference genome to map the genetic basis of DSP in a cross with a non-alpine horticultural columbine, *A. coerulea* ‘Origami’, henceforth referred to as ‘Origami’. We compared DSP in *A. jonesii*, ‘Origami’, and their hybrid offspring. In *A. jonesii* specifically, we used field

and greenhouse specimens to determine whether presence/absence of amphistomaty is environmentally plastic. Histological analysis allowed us to compare parental cellular morphology and polarity in the leaf lamina. We then used QTL analysis to find regions of the genome associated with qualitative measures of amphistomaty and quantitative measures of stomatal production. Using a list of genes known to be involved in stomatal development and leaf polarity, we explored candidate genes colocalizing with QTL to determine whether DSP appears to be associated with variation in polarity factors and/or stomatal development genes themselves. High coverage whole genome sequence (WGS) allowed us to further explore candidate genes by comparing the frequency of polymorphisms across wild species with differential DSP. Our analyses reveal a simple genetic basis for the presence/absence of amphistomaty and stomatal production on both leaf surfaces and identify a strong candidate gene for driving these processes.

Methods

** See Chapter I (pages 5-8) for the specifics of the crossing design, genotyping, genetic map, and QTL analysis*

Phenotyping

We characterized presence/absence of amphistomaty in both wild and greenhouse plants, but only counted epidermal cells from greenhouse grown plants for environmental consistency. We did not have a large enough sample size to statistically compare total SI (SI_T) across *A. jonesii*, ‘Origami’, and the F1. As the *A. jonesii* parent was not phenotyped,

we do not know whether the SI numbers we observed in the six *A. jonesii* individuals we measured reflect that of the *A. jonesii* parent for this cross.

Amphistomaty was determined from microscope images of epidermal leaf impressions made from the fully expanded leaves of mature, ca. two-year-old F2 plants from October 2021 to January 2022. Impressions were taken from the parents, F1, and other columbine plants at maturity in July 2022. For the parents, multiple leaf impressions per plant were taken on the same day. Leaf impressions were generated by applying a thin layer of clear nail polish, allowing the nail polish to dry, applying a piece of clear tape to the nail polish, peeling it off, and adhering it to a microscope slide. Microscope slides were imaged with a light microscope at 100x magnification. We navigated around the adaxial side of each leaf peel and scored amphistomaty as a binary trait - “1” for amphistomatous plants and “0” for hypostomatous plants. To determine the consistency of amphistomaty within plants, we randomly selected five plants and took epidermal peels from 5 leaves per plant, all collected on the same day. Each plant was consistent across all leaves in presence/absence of amphistomaty, but highly variable in stomatal index (SI, see below). As presence/absence of amphistomaty was the main focus of this study, we phenotyped both sides of one leaf per F2 plant (n = 235). The same leaf was used for both the abaxial and adaxial peels. *Aquilegia* (columbine) leaves are multiply ternately compound, so to maximize consistency we took impressions from the middle-most leaflet, proximal to the petiolule and away from any major veins.

Stomata and pavement cells were counted from the same slides used for amphistomaty determination. We determined through a pilot study that we could capture a relatively accurate representation of a leaf’s SD/SI/E by averaging counts from three

0.15mm² square sections of an epidermal peel. In our pilot study, we measured from five different 0.15mm² sections of a leaf, then downsampled the data to three sections and did not see a significant difference in stomatal index/density values. Three images were generated per leaf surface, and on each image we overlaid a 0.15mm² box, only moving the box to avoid vasculature and leaf edges. Otherwise, the placement of the measured zones was random. We counted both stomatal and pavement cells in the box using the Cell Counter plugin in FIJI (Fiji Version 2.9.0/1.53t; Schindelin et al., 2012), counting cells that touched any part of either the left and/or the top side of the box, and did not count cells that touched any part of either the right and/or the bottom side of the box. If a cell touched the bottom and left sides, or the top and right sides, it was not counted. SD/SI/E were calculated for each of the three sections per leaf, and these values were averaged to yield the SD/SI/E for each plant. Total SI/SD/E were calculated by adding the averaged counts from both sides of the leaf.

$$\text{Stomatal Index} = \frac{\# \text{ stomata}}{\# \text{ stomata} + \text{ pavement cells}} \times 100$$

While temperature, humidity, and light remained relatively constant in the greenhouse, sampling over the course of four months likely introduced variation in epidermal count measurements, although amphistomaty was constant. Linear regressions revealed that the day of leaf impression was not a significant predictor of any SI or SD measures.

Microscope images were taken with an Olympus S97809 microscope camera (Olympus U-CMAD3 adapter) on an Olympus BX61 compound light microscope (Olympus BX-UCB control box) with program PictureFrame V2.0, Optronics©.

Histology

Mature leaves were harvested, photographed, measured, and from *A. jonesii* and *A. coerulea* ‘Kirigami’ (nearly identical to ‘Origami’) individuals. See Meaders et al. (2020) for histology protocol.

Narrowing the causal region for Q5

We identified 10 individuals with cross-over events within the 1.5 LOD region of Q5 that changed from homozygous ‘Origami’ to heterozygous, or vice versa. We scanned the number of reads that contained ‘Origami’ and *A. jonesii* SNP alleles, and identified the approximate location of recombination. Five plants were amphistomatous and five were hypostomatous, allowing us to narrow the region to just 170 Mb (42,804,151 - 42,975,649bp; Supp. Fig. 3.6). This region harbors 24 annotated genes including the ortholog to *AtSPEECHLESS*, *Aqcoe5g450000* (Supp. Fig. 3.6).

Candidate gene analysis

We searched for homologs of genes known to be involved in stomatal development or leaf polarity. Genes were searched in the *Arabidopsis* genome by gene id using Phytozome (Araport11, Cheng et al., 2017; <https://phytozome.jgi.doe.gov>) and compared to the *Aquilegia* proteome using the ‘Protein Homologs’ tool. Results were filtered based on sequence similarity and alignment length, and we used the top hit as the homolog for each gene.

Phylogeny

We blasted the protein sequence (tblastn) of each SMF gene against *Aquilegia coerulea*, *Solanum lycopersicum*, and *Populus tremuloides*. We took the top hit of each gene and labeled it after its homolog in *Arabidopsis*. A non-SMF bHLH protein (At3G56980) was used as an outgroup (MacAlister and Bergmann, 2011). We aggregated the amino acid sequences of each top hit from Phytozome and used MAFFT version 7 (Kato and Standley, 2013) to align them. Maximum likelihood analysis was performed using IQtree2 version v.2.2.2.6 (Minh et al., 2020) with the amino acid model -s and 1000 bootstraps. A midpoint rooted tree was created with iTOL (Interactive Tree of Life; Letunic and Bork, 2021).

SPCH promoter polymorphism analysis

We visualized >10x sequence data of 10 columbine species (all species from Filiault et al., 2018) plus *A. jonesii* from .bam files using Integrative Genomics Viewer (IGV; Robinson et al., 2011). SNPs and indels were compared across taxa to identify polymorphisms unique to and homozygous in *A. jonesii* compared to the nine other columbine species examined. Heterozygous polymorphisms were removed from consideration.

Results

Abbreviations

AM	amphistomaty
SI	stomatal index
SD	stomatal density
SR	stomatal ratio
E	epidermal cells/mm ²
Q-	QTL
AM	amphistomatous
HY	hypostomatous
AB	abaxial
AD	adaxial

Phenotypic

We characterized aspects of dorsiventral stomatal patterning (DSP) in the parent taxa, F1, and F2 plants. *A. jonesii* is the most dwarf species in the genus with tightly clustered, vertically oriented leaves and leaflets (Fig. 3.1A, Munz, 1946). Though the specific *A. jonesii* plant used as the pollen parent was not phenotyped, all 32 *A. jonesii* from field collections across 12 populations were amphistomatous as were 6 plants grown in the UCSB greenhouses (Fig. 3.1A-C, Table 3.1). The ‘Origami’ maternal parent had horizontally oriented leaves and was hypostomatous (Fig. 3.1D-F, Table 3.1). The F1 was amphistomatous (Table 3.1, Fig. 3.2A), revealing dominance for amphistomaty. This dominance dynamic was reflected in F2 plants, where amphistomaty (n = 124; 57%) was

significantly more common than hypostomaty ($n = 92$; 43%; $X^2 = 4.74$, $p = 0.03$). We also phenotyped presence/absence of amphistomaty in 9 other species of *Aquilegia* and related genera, and only *A. jonesii* and *A. scopulorum* are amphistomatous, where the others are hypostomatous. We examined whether amphistomaty in *A. jonesii* could be due to a partial loss of dorsiventral leaf polarity. Histological analysis shows that *A. jonesii* and 'Origami' leaves are both similarly polar, with two layers of subepidermal palisade parenchyma cells on the adaxial side and spongy mesophyll and vasculature occupying the rest of the laminar space to the abaxial epidermis (Fig 3.1C,F).

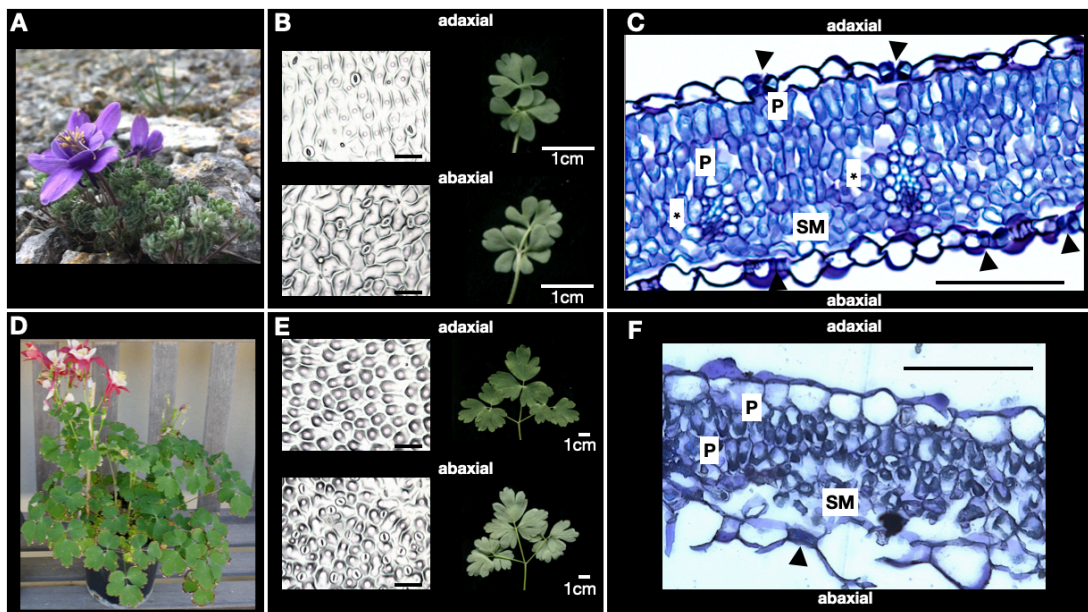


Figure 3.1. Parental phenotypes. A-C *A. jonesii*. D,E 'Origami'. F *A. laramiensis* (hypostomatous). A,D Whole plant. *A. jonesii* individual is from the field (Iceberg Lake, Glacier National Park). 'Origami' individual is greenhouse grown. B,E 100x images of leaf epidermal peels from ab- and adaxial leaf surfaces of each parent. Scans of ab- and adaxial leaf surfaces. C 400x confocal microscope images (put magnification) of histological cross sections of *A. jonesii*. F Compound light microscope image of *A. laramiensis* histological cross section. AB: abaxial, AD: adaxial, P: palisade parenchyma, SM: spongy mesophyll; arrowheads indicate stomata, asterisks indicate vascular bundles. Scale bars = 100 μ m unless otherwise indicated.

Table 3.1. Mean values for dorsiventral stomatal patterning (DSP) traits. Standard deviations are given in parentheses. See bottom of Results section for abbreviations.

class	DSP	n	SR	SI _T	SI _{AB}	SI _{AD}	SD _T	SD _{AB}	SD _{AD}	E _T	E _{AB}	E _{AD}
AjAM	amphi	3	0.24 (0.04)	34.2 (5.7)	25.8 (3.5)	8.4 (2.4)	94 (22)	71.1 (7.8)	23.0 (9.0)	81.8 (11)	40.9 (4.2)	40.9 (7.3)
AjBB19	amphi	2	0.23 (0.03)	29.9 (0.07)	23.1 (1)	6.8 (1.0)	141.3 (3.8)	96.0 (11.3)	45.3 (15.1)	156.6 (10.5)	62.7 (4.4)	93.9 (14.8)
AjBB22	amphi	2	0.36 (0.03)	23.1 (1)	14.7 (0.1)	8.4 (1.2)	118.0 (20)	78.0 (8.5)	40.0 (11.3)	151 (17.5)	80.3 (7.2)	70.7 (10.3)
AjBB40	amphi	2	0.36 (0.05)	23.3 (0.7)	14.9 (1.5)	8.4 (0.8)	124.7 (8.5)	95.3 (14.1)	29.3 (5.7)	148.8 (3.4)	98.3 (3.5)	50.5 (6.9)
AjBB42	amphi	2	0.27 (0.01)	24.3 (2.7)	17.9 (2.2)	6.5 (0.5)	106.7 (25)	80.0 (20.7)	26.7 (3.8)	127.7 (12.9)	66.9 (8.9)	60.8 (4.0)
AjBB50	amphi	2	0.39 (0.01)	24.0 (0.03)	14.7 (0.3)	9.2 (0.3)	132.7 (20)	75.3 (8.5)	57.3 (11.3)	172.4 (28.0)	78.4 (9.1)	94.0 (19.0)
origami	hypo	3	0	23.3 (2.1)	23.3 (2.0)	0	156.4 (20.4)	156.4 (20.4)	0	197.1 (30)	101.9 (17)	95.1 (14)
F1	amphi	3	0.17 (0.07)	31.0 (1.6)	25.6 (1.9)	5.4 (2.2)	159.7 (9.2)	135.6 (20.4)	24.1 (11.9)	145.3 (13)	79.3 (9)	66.0 (8)
F2 _{AM}	amphi	124	0.23 (0.06)	32.0 (3.8)	24.4 (2.5)	7.6 (0.3)	156.9 (45)	123.2 (37)	33.7 (15)	144.1 (45)	76.2 (24)	68.0 (24)
F2 _{HY}	hypo	92	0	27.0 (2.4)	27.0 (2.4)	0	169.2 (50)	169.2 (50)	0	164.5 (48)	94.7 (30)	69.8 (22)

We calculated stomatal index (SI) on both leaf surfaces. SI is less prone to variation in cell size than stomatal density (SD), as it is a count of the proportion of stomata per epidermal cell (see Methods). Despite accounting for epidermal cell size variation, there was substantial variation across leaves in the ‘Origami’ parent, the F1 and 6 *A. jonesii* plants we measured both in SI and SD (Table 3.1, Fig. 3.2, Supp. Fig. 3.1). This was likely due to environmental variation associated with different timing of measurements and/or the physiological status of plants. Regardless, F1 values always overlapped either the ‘Origami’ parent values or some of the *A. jonesii* measurements, or both, indicating that the parental alleles may have different degrees of dominance across DSP traits (Table 3.1, Fig. 3.2, Supp. Fig. 3.1). Without the *A. jonesii* parent, we cannot make statements about transgressive variation among the F2 plants. Dominance dynamics in DSP traits were revealed in the F2 population.

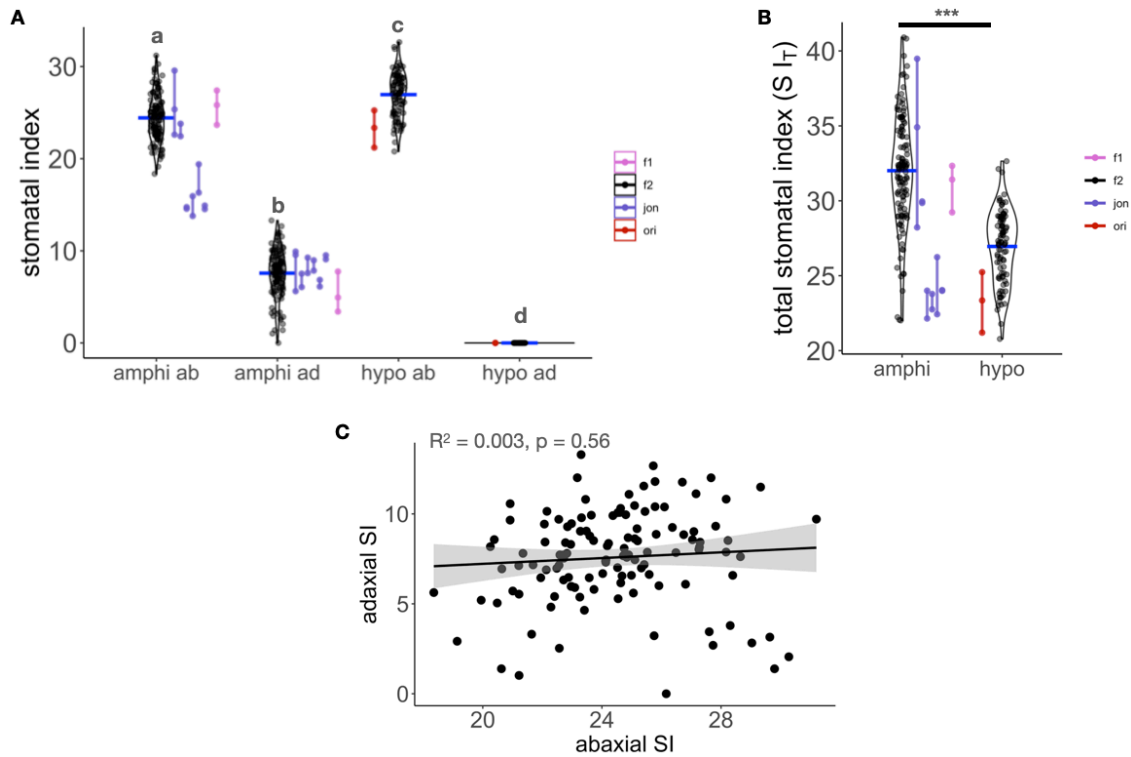


Figure 3.2. Distributions of SI in F2 population and parents, and correlation between SI_{AB} and SI_{AD} in F2_{AM} plants. A,B Violin plots of SI predicted by F2 DSP groups, parents, and F1. Points are jittered to illustrate the distribution. Mean F2 values are indicated by horizontal blue bars. A SI distributions by leaf side; ab: abaxial, ad: adaxial. Measurements from different leaves of the same individual are connected with a vertical line. DSP groups that differ significantly have different lower case letter above (Kruskal-Wallis & Wilcoxon post hoc rank sum). B Total SI distributions by DSP. Black line indicates statistical comparison between F2 DSP groups (t-test). ***: $p < 0.001$. C Linear regression of SI_{AD} and SI_{AB} in F2_{AM} plants with best fit line (solid black) and 95% CI (grey shadow).

In the F2 population, the SI values of the ab- and adaxial leaf surfaces of amphi- and hypostomatous plants all differed significantly (Kruskal-Wallis $X^2 = 375.5$, $p < 0.001$; Fig. 3.2A). Although the difference in mean was small and there was nearly complete overlap in the range of measurements, hypostomatous plants ($\bar{x} = 27.0$, $s = 2.4$) had significantly higher SI_{AB} than amphistomatous plants ($\bar{x} = 24.4$, $s = 2.5$; Kruskal-Wallis chi-squared = 375.6, $p < 0.001$, Wilcoxon post hoc rank sum, $p < 0.001$; Fig. 3.2A, Table 3.1). Within amphistomatous plants, SI_{AB} ($\bar{x} = 24.4$, $s = 2.5$) was significantly higher and did not overlap with the SI_{AD} values ($\bar{x} = 7.6$, $s = 0.3$; Kruskal-Wallis chi-squared = 375.6, $p < 0.001$,

Wilcoxon post hoc rank sum, $p < 0.001$; Fig. 3.2A). Combining measurements for both leaf surfaces revealed that amphistomatous F2 plants ($\bar{x} = 32.0$, $s = 3.8$) had significantly higher SI_T than hypostomatous F2 plants ($\bar{x} = 27.0$, $s = 2.4$; $t = 12.0$, $p < 0.001$) due to a larger mean gain in SI_{AD} (+ 7.6) than the mean loss in SI_{AB} (-2.6; Fig. 3.2B). The mean stomatal ratio ($SR = SI_{AD}/SI_{AB}$) for amphistomatous F2 plants ($\bar{x} = 0.23$, $s = 0.26$) was similar to *A. jonesii* ($\bar{x} = 0.23-0.39$, $s = 0.01-0.05$; Table 3.1). Both SI and SD were correlated with SR on the adaxial side, but not the abaxial side, indicating that dorsiventral stomatal distribution (SR) is determined by the adaxial side alone (Table 3.2). Interestingly, among amphistomatous plants, SI_{AB} and SI_{AD} were not significantly correlated (Spearman's $\rho = 0.1$, $p = 0.6$; Fig. 3.2C).

Table 3.2. Correlation matrix across DSP traits in F2 plants. Spearman's ρ values are given with asterisks indicating significance. *: $p < 0.05$, **: $p < 0.01$, ***: $p < 0.001$

	SR	SI _{AD}	SD _{AD}	SI _{AB}	SD _{AB}	SI _T	SD _T	E _{AD}	E _{AB}	E _T
SR	—									
SI _{AD}	0.95***	—								
SD _{AD}	0.67***	0.66***	—							
SI _{AB}	-0.18	0.1	-0.05	—						
SD _{AB}	-0.11	-0.08	0.48***	0.27***	—					
SI _T	0.53***	0.74***	0.42***	0.28***	-0.28***	—				
SD _T	0.13	0.15	0.71***	0.11	0.91***	0	—			
E _{AD}	-0.07	-0.14	0.61***	-0.20**	0.63***	-0.23***	0.73***	—		
E _{AB}	-0.07	-0.13	0.47***	-0.05	0.94***	-0.38***	0.91***	0.74***	—	
E _T	-0.07	-0.14	0.56***	-0.12	0.86***	-0.33***	0.89***	0.92***	0.94***	—

In contrast to SI_T , SD_T was significantly greater in hypostomatous plants ($x = 169.2$, $s = 50$) than amphistomatous plants ($x = 156.9$, $s = 45$), though the distributions overlapped nearly completely (Table 3.1, Supp. Fig. 3.1B). The disparity between SD_T and SI_T is

explained by a smaller cell size in hypostomatous plants. With more epidermal cells per mm² (E_T - F2_{HY}: $\bar{x} = 164.5$, $s = 48$, F2_{AM}: $\bar{x} = 144.1$, $s = 45$), and thus smaller cells, SD is inflated compared to SI in hypostomatous plants (Table 3.1, Fig. 3.2B, Supp. Figs. 3.1B,3.2B). This dynamic was reflected in the parent taxa, where ‘Origami’ generally had greater E_T than *A. jonesii* (Supp. Fig. 3.2). In both amphi- and hypostomatous plants, abaxial epidermal cells were smaller than adaxial, where the abaxial side of hypostomatous plants were the smallest on average (Table 3.1, Supp. Fig. 3.2).

Genotypic

** See Chapter I page 15 for genotypic data results*

QTL analysis and candidate gene identification for DSP

The model for amphistomaty as a simple binary trait identified a single QTL on Chr5 (AM-Q5), which had the highest LOD (52.7) and percent variance explained (PVE: 68.2) of any leaf epidermal patterning trait (Table 3.3, Fig. 3.3A). At AM-Q5, all homozygous *A. jonesii* (AM-Q5_{JJ}) and heterozygous (AM-Q5_{OJ}) plants were amphistomatous, and 91/98 homozygous ‘Origami’ (AM-Q5_{OO}) plants were hypostomatous (Fig. 3.3B, Supp. Table 3.1). The 7 AM-Q5_{OO} plants which were amphistomatous had significantly lower SI_{AD} (Kruskal-Wallis X²: 87.6, $p < 0.001$, pairwise Wilcoxon rank sum with BH adjustment: $p < 0.001$) and greater SI_{AB} (Kruskal-Wallis X²: 57.4, $p < 0.001$, pairwise Wilcoxon rank sum with BH adjustment: $p < 0.001$) than AM-Q5_{OJ} and AM-Q5_{JJ} plants (Fig. 3.4, Supp. Fig. 3.3). One plant (167) had zero stomata in the randomly chosen leaf sections used to score

SI_{AD}, but was observed to have sparse adaxial stomata outside the measured leaf sections, so it was scored as amphistomatous with an SI_{AD} of zero.

Table 3.3. QTL results for each trait. Abbreviations: chr, chromosome; 1.5 LOD int, 1.5 LOD interval; PVE, Percent Variance Explained. Additive effects are in terms of the ‘Origami’ allele.

trait	chr	name	1.5 LOD int (cM)	1.5LOD marker	peak position (cM)	LOD	PVE	total PVE	additive effect	dominance deviation	degree of dominance
AM	5	AM-Q5	58.1 - 60.9	5.72 - 5.74	60.0	52.7	68.2	68.2	-8.6	8.6	-1.00
SR	5	SR-Q5	58.1 - 60.9	5.72 - 5.74	60.0	16.7	47.3	47.3	-0.11	0.06	-0.55
SI _{AD}	5	SI _{AD} -Q5	58.1 - 60.9	5.72 - 5.74	59.8	11.4	35.3	35.3	-3.8	2.0	-0.53
SD _{AD}	5	SD _{AD} -Q5	58.1 - 60.9	5.72 - 5.74	59.8	6.8	23.1	23.1	-17.5	11.5	-0.66
SI _{AB}	5	SI _{AB} -Q5	58.1 - 60.9	5.72 - 5.74	60.9	14.6	26.9	26.9	1.8	-0.9	-0.50
SD _{AB}	1	SD _{AB} -Q1	22.9 - 33.5	1.17 - 1.32	25.7	6.7	10.6	30.8	20.9	-9.7	-0.46
SD _{AB}	5	SD _{AB} -Q5	58.1 - 60.9	5.72 - 5.74	60.9	14.0	24.2	-	32.7	-12.6	-0.39

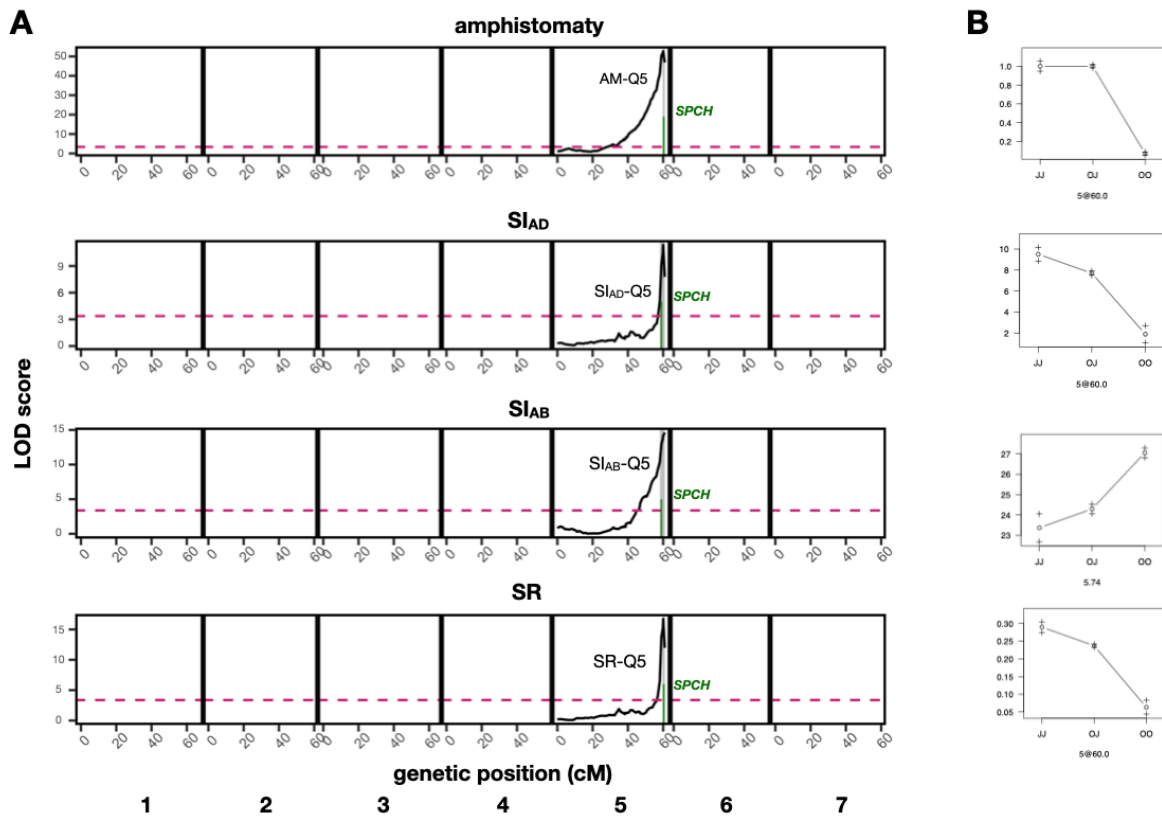


Figure 3.3. QTL maps for amphistomaty, SI and SR and their effect plots. A LOD profile reflects the best multiple QTL model associated with each trait. Shaded area indicates 1.5 LOD interval for the QTL peak. Dashed magenta line represents the significance LOD threshold (3.37) for a ‘scanone’ of amphistomaty. Green line indicates a candidate gene within the 1.5 LOD interval. Black numbers under the bottom plot indicate chromosomes. B Phenotype by genotype (P x G) effect plots for QTL. Genotypes are on the x-axis (J = *A. jonesii*, O = ‘Origami’) and their effects are on the y-axis. The chromosome and marker location of each QTL is listed beneath each plot.

The models for SR, as well as SI and SD on both leaf surfaces also identified QTLs at the same position on Chr5 as for amphistomaty but with lower LOD scores (6.8 - 16.7) and PVE (23.1 - 47.3; Table 3.1, Fig. 3.3, Supp. Fig. 3.3). Notably, the genotype effect plots for SI_{AD} and SI_{AB} are in opposite directions (Fig. 3.3B). This is further illustrated when comparing the SI values across the leaf surfaces for amphistomatous F2 plants by genotype at AM-Q5 (Fig. 3.4). Within each genotype, there is a positive correlation (though only significant for AM-Q5_{JJ} and AM-Q5_{OJ} plants) indicating other factors influence SI on both surfaces in a similar manner. In contrast, mean values for the three genotypes show a negative relationship. (Fig. 3.4).

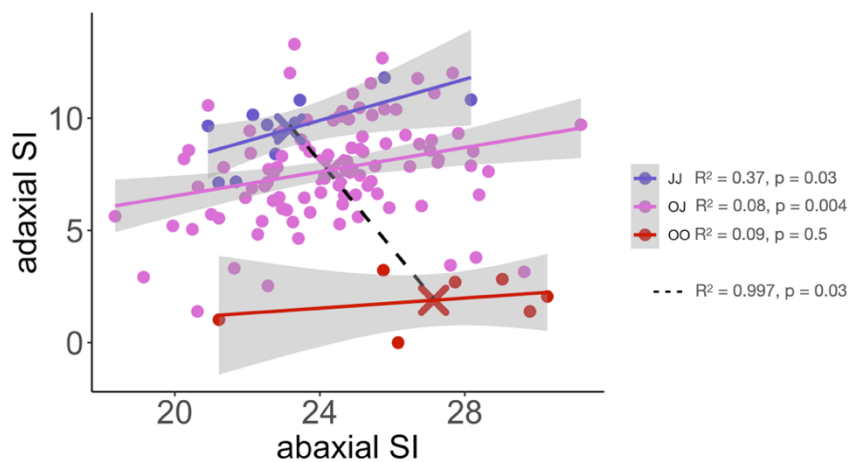


Figure 3.4. Bivariate plot of SI_{AB} and SI_{AD} in $F2_{AM}$ plants. Best fit line colors correspond to each genotype with corresponding 95% CI (grey shadow) calculated from linear regression. Dashed line is best fit from linear regression of the mean values of the three genotype groups.

SD_{AB} had an additional and unique stomatal QTL on Chr1 (SD_{AB} -Q1; Table 3.3, Supp. Fig. 3.3). Interestingly, E_{AB} also had a significant QTL at the same position as SD_{AB} -Q1 with a nearly identical LOD profile (Supp. Fig. 3.3, Supp. Table 3.2). SD_{AB} and E_{AB} were highly correlated, with a Spearman correlation coefficient of 0.94 ($p \ll 0.001$, Table 3.2).

Because the Q5 locus was so strongly associated with all DSP traits, we sought to narrow the window likely to be harboring causal element(s). We identified 10 individuals

with recombination events within the 1.5 LOD interval of AM-Q5 from the initial analysis (5 were amphistomatous and 5 were hypostomatous) and determined more refined recombination break points. This allowed us to narrow the region controlling amphistomaty to a ca. 170kb region (42,804,151 - 42,975,649) with 24 genes annotated in the *Aquilegia* genome, 18 of which had distinct homologs in *Arabidopsis*, including an ortholog of *AtSPEECHLESS*, *Aqcoe5G450000* (Supp. Fig. 3.4). *AqSPCH* was the only homolog of genes known to be associated with stomatal development and/or ab/adaxial polarity within this causal interval of Q5 (Supp. Table 3.3).

Homologs of three genes within SD_{AB}-Q1, are involved with stomatal development and ab/adaxial polarity in *Arabidopsis* (Supp. Fig. 3.3, Supp. Table 3.3). These include *MAP KINASE 6 (MPK6)* and *BRASSINOSTEROID INSENSITIVE 2 (BIN2)*, which are involved in stomatal development, and *AtPHABULOSA (AtPHB)/AtPHAVOLUTA (AtPHV)* which is involved in ab/adaxial leaf polarity establishment (McConnell et al., 2001; Gudesblat et al., 2012; Houbaert et al., 2018). The top BLAST hits for *AtPHB* and *AtPHV* in *Aquilegia* were the same gene (*Aqcoe1G178700*).

AjSPCH is orthologous with SPCH in other taxa

We gathered amino acid sequences of the SMF bHLH proteins from *Aquilegia* and three plant species where SPCH has been shown to be involved with adaxial stomatal development (*Arabidopsis thaliana*, *Solanum lycopersicum*, and *Populus trichocarpa*; Supp. Fig. 3.5). Similar to previous studies, a maximum likelihood (ML) tree of amino acid sequences identified three monophyletic clades, corresponding to each SMF protein (Supp. Fig. 3.6). Also consistent with previous findings, *SPCH* and *MUTE* form sister clades with

89% bootstrap support. *Aqcoe5G450000* was orthologous to *AtSPCH*, thus henceforth we refer to *Aqcoe5G450000* as *AqSPCH*.

SPCH sequence analysis

Using deep coverage whole genome sequence of one individual from each species, we searched for polymorphisms unique to *A. jonesii* compared to nine other hypostomatous columbine species. We examined the *AqSPCH* genic region and 3.5kb upstream of the translational start site (TSS). In the coding region, there were only 2 exonic SNPs unique to and homozygous in *A. jonesii*, and both would cause synonymous amino acid coding mutations. This reveals that if variation in *AqSPCH* is responsible for amphistomaty, it is likely cis-regulatory (Fig. 3.5). There were four intronic SNPs unique to *A. jonesii* and one 1bp deletion in the second intron. Upstream of the TSS, we found three SNPs, two insertions (5bp & 9bp), and one deletion (9bp) unique to *A. jonesii* (Fig. 3.5). Both insertions are within 1kb of the TSS and the deletion was 3.2kb upstream of the TSS. We did not find evidence that these polymorphisms were within DNA binding motifs of transcription factors known to interact with *SPCH* (Supp. Table 3.4).

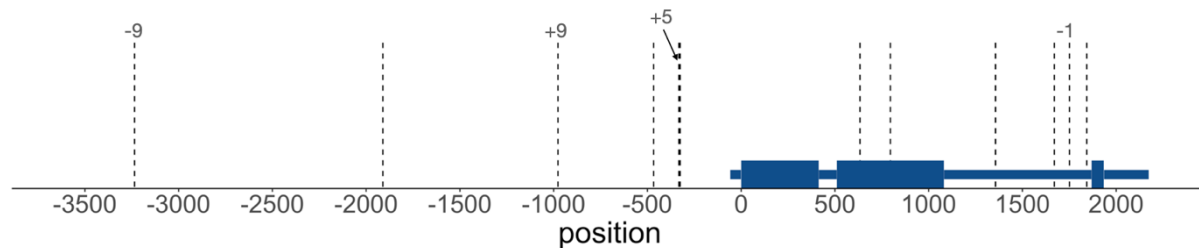


Figure 3.5. Polymorphisms fixed and unique to *A. jonesii*, 3.5kb upstream and within *AqSPCH*. Position 0 is the translational start site. Exons are indicated with thick blue bars and introns and UTR are indicated with thin blue bars. Dashed lines without numbers represent SNP positions, and dashed lines with numbers represent INDELS, with the number of bases added or deleted indicated above. The arrow points to a 5bp insertion which is 6bp upstream of an unrelated SNP.

Discussion

We discovered the presence of amphistomaty in an alpine columbine (*A. jonesii*) with a simple genetic basis revealed by QTL analysis. *AqSPCH*, a master control gene for stomatal development, co-localizes with a major effect QTL for amphistomaty, SI, and SD (Q5). A lack of protein coding polymorphisms in *AqSPCH* unique to *A. jonesii* suggests that cis-regulatory variation in *AqSPCH* causes production of adaxial stomata. Similar to previous studies, we found that stomatal density has some level of independent control on either leaf surface. Given the high occurrence of amphistomaty in both alpine and herbaceous plants exposed to high light, amphistomaty in *A. jonesii* is likely an adaptation to its environment. To our knowledge, this is the first study to map both amphistomaty and stomatal index using QTL analysis in a high alpine plant.

Dorsiventral stomatal patterning has a simple genetic basis in Aquilegia

A single major effect QTL on Chr5 (Q5) primarily controls both the production and density of stomata on both leaf surfaces (Table 3.3, Figure 3.3, Supp. Fig. 3.3). This contrasts previous QTL and GWAS studies mapping SD on both leaf surfaces, where there was always at least one locus unique to either the ab- or adaxial side (Muir et al., 2015; McKown et al., 2019). Other than SD_{AB}-Q1, we did not detect any other QTL unique to one leaf surface, which is likely because these traits are largely, if not fully controlled by Q5. Alternatively, there may be small-effect QTL specific to one leaf surface that we did not detect due to sample size and/or environmental variation. The fact that there were seven amphistomatous individuals with homozygous ‘Origami’ genotypes at Q5 with low SI_{AD} suggests that there may be small effect QTL and/or environmental effects epistatic to Q5

that we did not detect. Regardless, it is clear that stomatal patterning on both leaf surfaces is primarily controlled by the same major locus (Q5) in a high alpine species of *Aquilegia*. This is the first study to identify a single region to be primarily responsible for amphistomaty, as well as stomatal index and stomatal density on both leaf surfaces.

In addition to having a major effect, Q5 was conveniently located on the end of the chromosome where the recombination rate is high, which allowed us to narrow the causal region to just 170kb. Of the 24 annotated genes in the causal region for amphistomaty (AM-Q5), *AqSPCH* is the only one to have been previously implicated in stomatal development, thus making it an exceptionally strong candidate for the gene underlying Q5 for all DSP traits. Two studies to date have identified multiple loci associated with DSP traits in wild species, and both found orthologs of *AtSPCH* as the most strongly associated loci. Using introgression lines (IL) of a wild species of *Solanum*, the QTL most highly associated with SR (15.9 PVE; using SD_{AD}/SD_{AB}) included an ortholog of *AtSPCH*, as well as nine other QTL of lesser effects (Muir et al., 2014). Similarly, in a GWAS study of *Populus*, McKown et al. (2019) found that SNPs in an ortholog of *AtSPCH* were the most strongly associated with SR and several other stomatal traits, though they also found another 279 significantly associated genes. Together, these results suggest that variation in *SPCH* orthologs is a common target for major changes in stomatal patterning across angiosperms, including *A. jonesii*.

Interestingly, at Q5, *A. jonesii* alleles cause increased stomatal deposition on the adaxial side and decreased stomatal deposition on the abaxial side (Fig. 3.4). This could be explained by variation in multiple loci within Q5 that have opposing effects, either in two different genes, or in two loci within the same gene (Liu et al., 2015). It could also be caused

by a single variant which has opposite effects on either leaf surface, although we are unaware of an example of this. More likely, there may be a negative feedback dynamic between leaf surfaces, where the production of adaxial stomata negatively regulates abaxial stomatal development. Mott and Michaelson (1991) found that exposing *Ambrosia cordifolia* to high light induced amphistomaty, and continued exposure caused increased adaxial SD and decreased abaxial SD, with no change in total SI. Furthermore, when comparing high and low elevation species in the genus *Ranunculus*, (Körner et al., 1986) found an increase in adaxial SD and a decrease in abaxial SD in high elevation species. McKown et al. (2019) found significant GWAS SNPs associated with increased SD_{AD} , but found no relationship between SD on either leaf surface, revealing a lack of negative feedback in *Populus*. In *A. jonesii*, there could be a gene(s) within SD_{AB} -Q1 or a different undetected QTL which act additively or epistatically to the gene(s) driving Q5. Our sample size may have been too small to detect all QTL and/or epistatic interactions responsible for establishing the dynamics of stomatal deposition on either leaf surface. Regardless, little is known about how gene expression restricts stomatal development to a particular leaf surface, and *A. jonesii* is a powerful model for exploring this phenomenon.

The QTL on Chr1 for SD_{AB} (SD_{AB} -Q1) also harbors two genes involved in canonical stomatal development. *MAP KINASE 6* (*MPK6*) and *BRASSINOSTEROID INSENSITIVE 2* (*BIN2*) are both known to directly phosphorylate SPCH, resulting in its degradation. Importantly, while these stomatal development genes could be involved in controlling SD_{AB} , Q1 could just as likely harbor genes that control E_{AB} , as these traits are highly correlated and both are affected by Q1. This is supported by the lack of association between Q1 and SI_{AB} ,

which controls for epidermal cell size/number. Thus, Q1 may have a larger direct role in controlling epidermal cell size than SD_{AB} .

Cis-regulatory variation in SPCH likely drives DSP in Aquilegia

Research on SPCH regulation has elucidated a myriad of post-transcriptional mechanisms, including miRNAs and several proteins involved in the degradation or stabilization of SPCH through kinase activity (Pillitteri et al., 2011; Zhang et al., 2015; Zhang et al., 2016; Houbaert et al., 2018; Chen et al., 2020; Guo et al., 2021). In contrast, relatively little is known about the mechanisms of SPCH regulation at the transcriptional level (Chen et al., 2020). While the exact mechanisms of regulation remain unclear, multiple studies using wild plant species have implicated differential SPCH expression in driving amphistomaty and adaxial stomatal density (McKown et al., 2019, Doll et al., 2021). Thus, additional studies on these species will likely help elucidate cis-regulatory controls of SPCH.

In addition to finding that SNPs in *PtSPCH* were highly associated with SR, (McKown et al., 2019) also presented evidence that plants with different *PtSPCH* alleles have differential levels and timing of *PtSPCH* expression. Furthermore, a recent study in *Callitriche* found that differences in stomatal lineage asymmetric cell division (ACD) patterns on both leaf surfaces were governed partially by different expression levels of SPCH, and not by protein coding changes (Doll et al., 2021). These results together suggest that variation in SPCH expression can cause amphistomaty and increased SD, similar to the implications of our study. If *AqSPCH* is indeed the gene driving Q5 in *Aquilegia*, a lack of protein coding variants unique to *A. jonesii* (Fig. 3.5) suggests that pre-translational cis-

regulation of *AjSPCH* leads to amphistomaty and concurrent changes in other DSP traits. Like most plant taxa, *Aquilegia* has only one copy of *SPCH*, and its function is imperative for stomatal formation on either leaf surface (Supp. Fig. 3.6; MacAlister et al., 2007; MacAlister and Bergmann, 2011; Harris et al., 2020), further supporting the hypothesis that differential DSP is most likely due to a regulatory change. Further investigation of differences in *AqSPCH* transcription, transcript stability, and protein interactions will help elucidate the mechanism of the evolution of amphistomaty in *A. jonesii*. Future studies should examine whether the parental alleles indeed confer differential *SPCH* expression on either leaf surface, and if these expression differences are caused by the same or different regulatory loci, such as different regions of the promoter, introns, or downstream regulatory regions.

While the regulation of *SPCH* at the transcriptional level is relatively poorly understood compared to post-transcriptional *SPCH* regulation, several genes have been shown to regulate *SPCH* expression in *Arabidopsis*. These include *SPCH* itself and one of its paralogs (*FAMA*), other transcription factors such as HD-ZIP IV (*ML1* & *HDG2*), *C2H2* (*IDD16*), *RETINOBLASTOMA RELATED 1* (*RBR1*), and DNA methylation via the histone protein H3K27me3 (Kutter et al., 2007; Weimer et al., 2012; Peterson et al., 2013; Takada et al., 2013; Lau et al., 2014; Matos et al., 2014; Yang et al., 2014; Qi et al., 2019). Analysis of protein-DNA interactions using methods such as DAP-seq, EMSA, and/or Y1H could clarify whether any of these genes interact with the *AqSPCH* promoter, and whether these interactions differ between the *A. jonesii* and ‘Origami’ alleles.

A potential mechanism for the transition to amphistomaty would be if *SPCH* gained regulation by adaxial polarity factors (Muir 2014). Importantly, while these polarity factors

may be associated with the stomatal lineage pathway (i.e. membrane polarity), they may also act further upstream in establishing upstream general dorsiventral leaf polarity. In *Arabidopsis*, dorsiventral leaf polarity is established through antagonistic interactions between ab- and adaxial specific genes, where adaxialization genes such as *AtPHABULOSA* (*AtPHB*) and *AtPHAVOLUTA* (*AtPHV*) repress abaxial genes (Siegfried et al., 1999; McConnell et al., 2001; Machida et al., 2015). In addition to implicating *PtSPCH* in several DSP traits, McKown et al. (2019) found that the leaf polarity factor *PtPHB* was associated with increased SD_{AD} . Thus, SD_{AD} in *Populus trichocarpa* may have evolved via modifications in the direct or indirect interactions between *AtSPCH* and genes that establish overall leaf polarity. Given their antagonistic function in establishing adaxialization, and occurrence within a QTL for SD_{AB} in our study (SD_{AB} -Q1; Supp. Table 3.3, Supp. Fig. 3.3), *AqPHB/PHV* could interact directly or indirectly with *AjSPCH* to cause amphistomaty. Although *A. jonesii* clearly has some level of dorsiventral polarity in the cellular morphology of the leaf lamina, similar to ‘Origami’ and other hypostomatous columbines (Krokhmal, 2015), a partial loss of polarity at the molecular level could explain its production of adaxial stomata. Cis-regulation of stomatal development by interactions between polarity factors and *SPCH*, both upstream and within the stomatal lineage pathways should be further studied using *A. jonesii*.

If *AqSPCH* transcription levels do not differ between *A. jonesii* and hypostomatous columbines on the adaxial leaf surface, DSP traits in *A. jonesii* could be caused by intronic variation or by synonymous SNPs (Fig. 3.4). Differential transcript splicing due to intronic variation could have significant impacts on *SPCH* protein synthesis and/or function (Schmucker et al., 2000; Syed et al., 2012). Additionally, while synonymous SNPs do not

change the polypeptide sequence, they can affect translational efficiency via codon bias (reviewed by Parvathy et al., 2022). If *AqSPCH* is responsible for *A. jonesii*'s DSP, an absence of differential expression of *AjSPCH* and *AoSPCH* on either leaf surface would indicate that one of these post-transcriptional mechanisms may govern DSP in *Aquilegia*.

Amphistomaty in A. jonesii is likely an adaptation to its alpine environment

A. jonesii possesses traits associated with amphistomatous plants, as an herb that lives in a high alpine environment far above the tree line with little to no shade and a short growing season. Furthermore, when observing nine columbine species and related taxa across the Northern Hemisphere, *A. jonesii* and *A. scopulorum* were the only amphistomatous species observed. From field observations, these species live in especially high light environments compared to other columbines, however this should be quantitatively characterized. Additionally, functional studies examining the role of *AjSPCH* in amphistomaty should also include *A. scopulorum* to determine whether its amphistomaty evolved via the same mechanism as *A. jonesii* or whether the two species converged via different pathways.

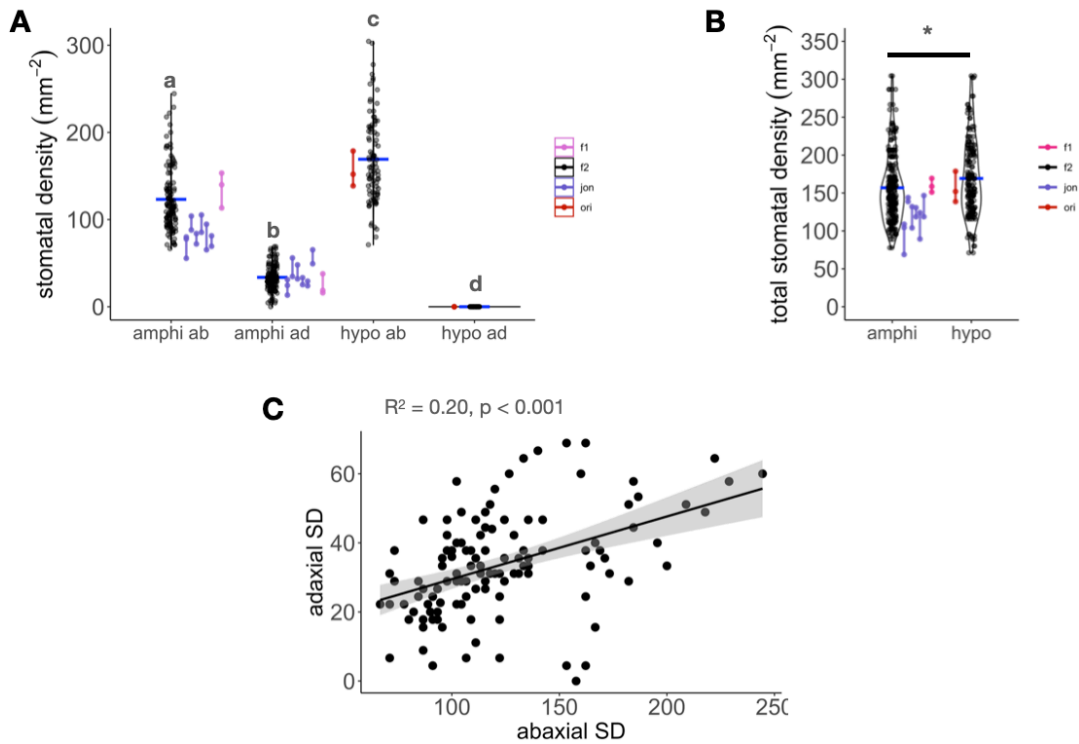
It has been demonstrated that amphistomaty is especially adaptive when stomata on both sides of the leaf can be independently controlled depending on environmental conditions (Richardson et al., 2017). Thus, it would be interesting to compare stomatal response to environmental stressors on either leaf surface, both in stomatal density and stomatal aperture. Both *A. jonesii* and *A. scopulorum* grow in particularly sun-exposed habitats, where the other columbine species observed have some degree of partial shade from tree canopies or nearby boulders. Future studies should compare CO₂ diffusion,

photosynthetic efficiency, and stomatal responses to stressors such as light and desiccation between amphi- and hypostomatous plants. These studies can help quantify the selective advantages associated with amphistomaty and DSP traits in high alpine environments.

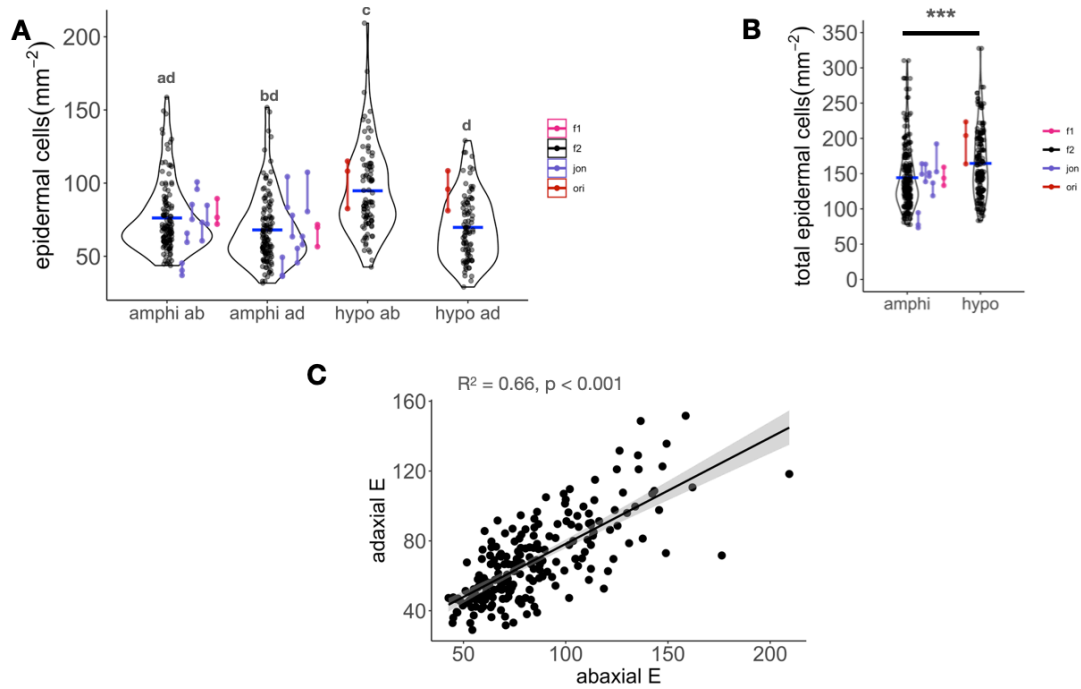
Conclusion

Previous work has found that *SPCH* plays a major role in controlling adaxial stomatal density. However, our study represents the first evidence that cis-regulation of *SPEECHLESS* is largely responsible for amphistomaty and stomatal index on both leaf surfaces, and largely responsible for stomatal density on both leaf surfaces. *A. jonesii* is a strong model for determining the mechanism(s) of *SPCH* regulation and the impacts of DSP on fitness in alpine plants.

Supplemental Figures and Tables



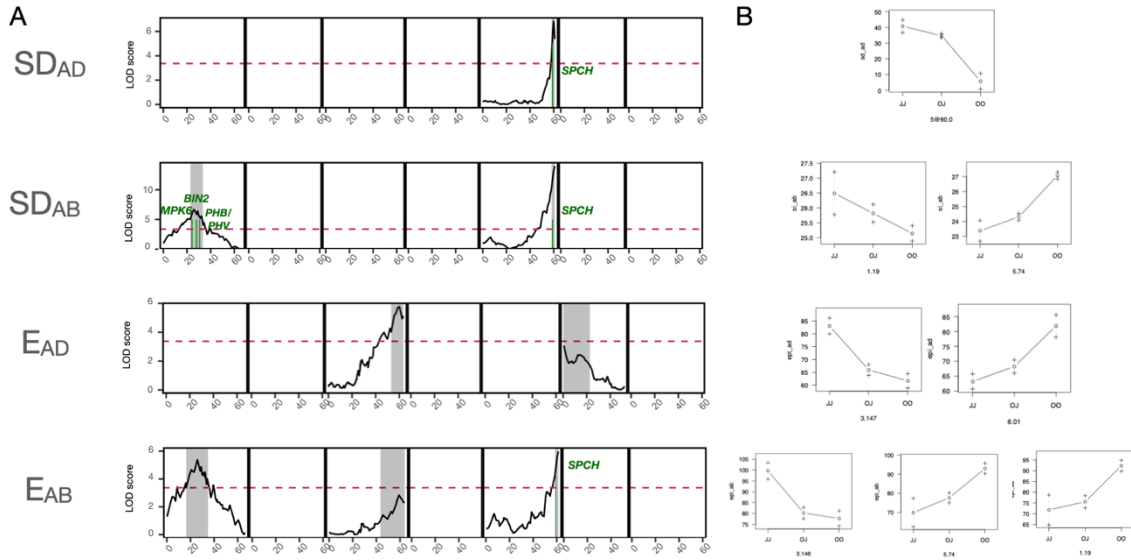
Supplemental Figure 3.1. Distributions of SD in F2 population and parents, and correlation between SD_{AB} and SD_{AD} in F2AM plants. A,B Violin plots of SD predicted by F2 DSP groups, parents, and F1. Points are jittered to illustrate the distribution. Mean F2 values are indicated by horizontal blue bars. A SD distributions by leaf side; ab: abaxial, ad: adaxial. Measurements from different leaves of the same individual are connected with a vertical line. DSP groups that differ significantly have different lower case letter above (Kruskal-Wallis & Wilcoxon post hoc rank sum). B Total SD distributions by DSP. Black line indicates statistical comparison between F2 DSP groups (t-test). ***: $p < 0.001$. C. Linear regression of SD_{AD} and SD_{AB} in F2AM plants with best fit line (solid black) and 95% CI (grey shadow).



Supplemental Figure 3.2. Distributions of E in F2 population and parents, and correlation between E_{AB} and E_{AD} in all F2 plants. A,B Violin plots of E predicted by F2 DSP groups, parents, and F1. Points are jittered to illustrate the distribution. Mean F2 values are indicated by horizontal blue bars. A E distributions by leaf side; ab: abaxial, ad: adaxial. Measurements from different leaves of the same individual are connected with a vertical line. DSP groups that differ significantly have different lower case letter above (Kruskal-Wallis & Wilcoxon post hoc rank sum). B Total E distributions by DSP. Black line indicates statistical comparison between F2 DSP groups (t-test). ***: $p < 0.001$. C. Linear regression of E_{AD} and E_{AB} in all F2 plants with best fit line (solid black) and 95% CI (grey shadow).

Supplemental Table 3.1. Numbers of plants in each genotype/phenotype at AM-Q5.

	JJ	OJ	OO	total
amphistomatous	11	101	7	119
hypostomatous	0	0	91	91



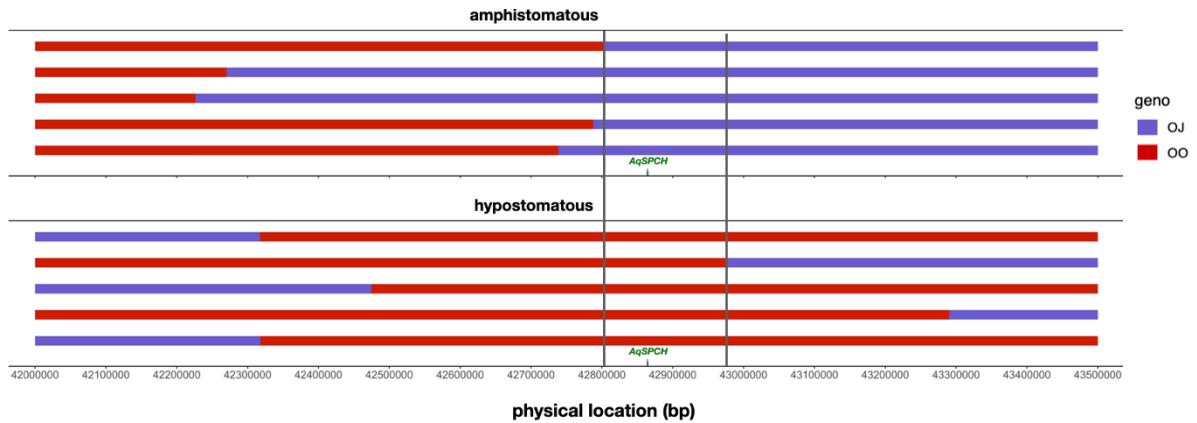
Supplemental Figure 3.3. QTL maps for SD & E, and effect plots for each QTL. A LOD profiles reflect the best multiple QTL models associated with each trait. Shaded areas indicate 1.5 LOD interval for the QTL peak. Dashed magenta line represents the significance LOD threshold (3.37) for a ‘scanone’ of amphistomaty. Green line indicates a candidate gene within QTL 1.5 LOD interval. B Phenotype by genotype (PxG) effect plots for each QTL in each trait. Genotypes are on the x-axis (J = *A. jonesii*, O = ‘Origami’) and their effects are on the y-axis. The chromosome and marker location of each QTL is listed beneath each plot.

Supplemental Table 3.2. QTL results for SD and E. Abbreviations: chr, chromosome; 1.5 LOD int, 1.5 LOD interval; PVE, Percent Variance Explained. Additive effects are in terms of the ‘Origami’ allele.

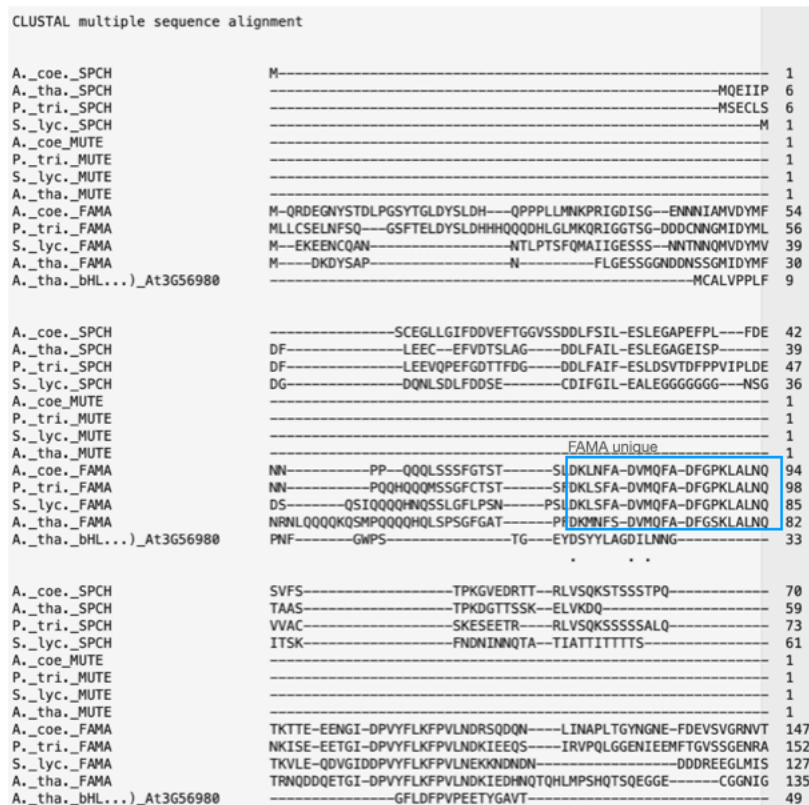
trait	chr	name	1.5 LOD int (cM)	1.5LOD marker	peak position (cM)	LOD	PVE	total PVE	additive effect	dominance deviation	degree of dominance
SD _{AD}	5	SD _{AD} -Q5	58.1 - 60.9	5.72 - 5.74	59.8	6.8	23.1	23.1	-17.5	11.5	-0.66
SD _{AB}	1	SD _{AB} -Q1	22.9 - 33.5	1.17 - 1.32	25.7	6.7	10.6	30.8	20.9	-9.7	-0.46
SD _{AB}	5	SD _{AB} -Q5	58.1 - 60.9	5.72 - 5.74	60.9	14.0	24.2		32.7	-12.6	-0.39
E _{AD}	3	E _{AD} -Q3	53.4 - 63.8	3.143 - 3.149	60.3	5.8	10.8	18.2	-10.3	-5.3	0.51
E _{AD}	6	E _{AD} -Q6	0.0 - 22.6	6.01 - 6.13	0.0	3.3	6.1		8.3	-5.7	-0.69
E _{AB}	1	E _{AB} -Q1	16.3 - 34.9	1.14 - 1.36	25.7	5.4	9.0	26.0	11.4	-4.8	-0.42
E _{AB}	3	E _{AB} -Q3	43.3 - 63.8	3.137 - 3.149	58.9	2.8	4.6		-8.0	-5.5	0.69
E _{AB}	5	E _{AB} -Q5	58.1 - 60.9	5.72 - 5.74	60.9	6.0	10.1		13.3	-3.2	-0.24

Supplemental Table 3.3. Genes involved in stomatal development and leaf polarity considered as candidates for DSP traits. Dash indicates no colocalization with QTL.

gene	Arabidopsis	Aquilegia	QTL
<i>SPCH</i>	At5G53210.1	Aqcoe5G450000	Q5
<i>MPK6</i>	AT2G43790.1	Aqcoe1G154900	SD _{AB} -Q1
<i>BIN2</i>	AT4G18710.1	Aqcoe1G221700	SD _{AB} -Q1
<i>PHB</i>	AT2G34710	Aqcoe1G178700	SD _{AB} -Q1
<i>PHV</i>	AT1G30490	Aqcoe1G178700.1	SD _{AB} -Q1
<i>YDA</i>	AT1G63700.1	Aqcoe7G030000	-
<i>TMM</i>	AT1G80080.1	Aqcoe0768s0001	-
<i>ER</i>	AT2G26330	Aqcoe7G111900	-
<i>BAK1</i>	AT4G33430	Aqcoe6G053300.1	-
<i>BIR1</i>	AT5G48380.1	Aqcoe2G437900	-
<i>SERK1</i>	AT1G71830.1	Aqcoe6G053300.1	-
<i>SERK2</i>	AT1G34210.1	Aqcoe6G053300.1	-
<i>SERK4</i>	AT2G13790	Aqcoe6G053300.1	-
<i>MKK4</i>	AT1G51660.1	Aqcoe7G329700	-
<i>MKK5</i>	AT3G21220	Aqcoe3G413900.1	-
<i>MKK7</i>	AT1G18350.1	Aqcoe3G413900.1	-
<i>MKK9</i>	AT1G73500.1	Aqcoe3G413900	-
<i>MPK3</i>	AT3G45640.1	Aqcoe1G488300.1	-
<i>BASL</i>	AT5G60880.1	Aqcoe7G067300	-
<i>POLAR</i>	AT4G31805	Aqcoe7G359500.1	-
<i>SCRM</i>	AT3G26744.4	Aqcoe5G338900	-
<i>PP2A-4</i>	AT3G58500.1	Aqcoe1G050400	-
<i>CDKA-1</i>	AT3G48750.1	Aqcoe7G241000.1	-
<i>SDD 1</i>	AT1G04110.1	Aqcoe5G013600.1	-
<i>ERL1/2</i>	AT5G62230.1	Aqcoe7G062000	-
<i>EPF1</i>	AT2G20875.1	Aqcoe1G319600	-
<i>ML1</i>	AT5G61960	Aqcoe5G325800.1	-
<i>HDG2</i>	AT1G05230.2	Aqcoe4G229500	-
<i>EPFL9/STOMAGEN</i>	AT4G12970.1	Aqcoe2G409200	-
<i>EPFL5</i>	AT3G22820	Aqcoe5G048200.1	-
<i>EPFL6</i>	AT2G30370.1	Aqcoe1G400100	-
<i>NCED1</i>	AT3G63520.1	Aqcoe2G021000.1	-
<i>ZEP</i>	AT5G67030.1	Aqcoe5G151500	-
<i>ABA2</i>	AT1G52340.1	Aqcoe2G032700.1	-
<i>FLP</i>	AT1G14350.2	Aqcoe3G332500	-
<i>MUTE</i>	AT3G06120	Aqcoe2G332800	-
<i>FAMA</i>	AT3G24140.1	Aqcoe2G399200.1	-
<i>ICE2/SCRM2</i>	AT1G12860	Aqcoe5G338900.1	-
<i>FK</i>	AT3G52940	Aqcoe1G111200	-
<i>AAO3</i>	AT2G27150	Aqcoe1G068500.1	-
<i>FIL</i>	AT2G45190	Aqcoe1G074300.1	-
<i>YABBY2</i>	AT1G08465	Aqcoe1G074300.1	-
<i>YABBY5</i>	AT2G26580	Aqcoe7G386400.1	-
<i>CRC</i>	AT1G69180.1	Aqcoe3G065300	-
<i>LUG</i>	AT4G32551	Aqcoe7G397900.1/Aqcoe7G200300.1	-



Supplemental Figure 3.4. Estimated location of recombination break points of F2 plants within the initial 1.5 LOD region for AM-Q5. 5 F_{2AM} and 5 F_{2HY} individuals with recombination events within AM-Q5. Location of *AqSPCH* is indicated on the x-axes. Vertical grey bars indicate the narrowed 170kb region (42,804,151-42,975,649) associated with amphistomaty. geno = genotype; OO = homozygous ‘Origami’, JJ = homozygous *A. jonesii*.



```

A._coe_SPCH -----DFE-----NEVE-----ASPTI---CRKRRRKLFEPTPT--- 95
A._tha_SPCH -----DYE-----NESP-----KRRKQRLERKEEDE 81
P._tri_SPCH -----DFD-----ETNNELE-----TSP-----KSKRQKIAASAAA--- 99
S._lyc_SPCH -----DEIT-----GLVS-----EEGKRRKLSIQKSTGS 85
A._coe_MUTE -----
P._tri_MUTE -----
S._lyc_MUTE -----
A._tha_MUTE -----
A._coe_FAMA -----SLV-----EEEEPHVSENNMQLGFLGGT---SLQ-KNP---GSEVKHAKRPRSVKTT--- 193
P._tri_FAMA -----GMVGEERGIGEDDEEARISSDNNVQLQFLGDQ---DLQNKNP I---PEAKNNAKRPRRTIKTS--- 207
S._lyc_FAMA -----GGK-----EKSE-----NNNNNVE-----KNQE-GKSNNAKRPR-IKTS--- 160
A._tha_FAMA -----NVFLEEKEDODDD---NDNNVQLRFIGGEEEDRENKNVTKEKVKSKRKRARTSKTS--- 189
A._tha_bHL...)_At3G56980 -----AVTQHNSFGVSVSSE 65

```

```

-----SDEVGQDGGQQRLLHITVERNRRKQMNHEHLGVLRLTLPMSF-YVVRGDAQSII 145
A._tha_SPCH -----EEEDGDGEAEEDNKQDGGQQRMSHVTVERNRRKQMNHEHLTVLRSMLPCF-YVVRGDAQSII 140
P._tri_SPCH -----IASSDQEVNPDGGQQRISHITVERNRRKQMNHELSVLRSLMPCF-YVVRGDAQSII 153
S._lyc_SPCH -----CATL-----QEEETIENKISHITVERNRRKQMNHELSVLRSLMPCF-YAKRGDAQSII 137
A._coe_MUTE -----MSHIAVERNRRKQMNHELVLRSLTPCF-YIKKSDAQSII 39
P._tri_MUTE -----MSHIAVERNRRKQMNHELVLRSLTPCF-YIKRGDAQSII 39
S._lyc_MUTE -----MSHIAVERNRRKQMNENLVLRSLTPCF-YIKRGDAQSII 39
A._tha_MUTE -----MSHIAVERNRRKQMNHELSLRSLTPCF-YIKRGDAQSII 39
A._coe_FAMA -----EVEVSQRTHTHIAVERNRRKQMNHELVLRSLMPGS-YVVRGDAQSII 239
P._tri_FAMA -----EVEVSQRTHTHIAVERNRRKQMNHELVLRSLMPGS-YVVRGDAQSII 253
S._lyc_FAMA -----EVEVSQRTHTHIAVERNRRKQMNHELVLRSLMPGS-YVVRGDAQSII 206
A._tha_FAMA -----EVEVSQRTHTHIAVERNRRKQMNHELVLRSLMPGS-YVVRGDAQSII 235
A._tha_bHL...)_At3G56980 -----GNEI-----DNNPVVVKKLNNHNASERDRRRKINLSFSSLRSCLPASGQSKLSIPATV 118

```

```

A._coe_SPCH -----GGVVVDYIKELQVQLQSLEAKKQRK---VY---SDV-----LSPRVSSPRPTMASALS 192
A._tha_SPCH -----GGVVEYISELQVQLQSLEAKKQRK---TY---AEV-----LSPRVSPRPS 181
P._tri_SPCH -----GGVVVDYINELQVQLQSLEAKKQRK---VY---SEV-----LSPRVSSPRPPL 195
S._lyc_SPCH -----GGVVVDYINELQVQLQSLEAKKQRK---VY---SEV-----LSPRVL-----PPQLVPTIS 180
A._coe_MUTE -----GGAIEFIKELHQILQLSLEAKKQRK---SL---SPS-----PVP 71
P._tri_MUTE -----GGAIEFIKELHQVLQALESKKQRK---SSL---SPS-----PGPCLS 75
S._lyc_MUTE -----AGVIEFIKELHLVLQSLEAKKQRK---SL---SPS-----PGPT 72
A._tha_MUTE -----GGVIEFIKELQVQLQVLESKQRK---TL---NRP-----SFPYDH 74
A._coe_FAMA -----GGAIEFVRELEQLLQCLLESQKRRR---LY---NGEAPRPMGD---PNSLP IQ 283
P._tri_FAMA -----GGAIEFVRELEQLLQCLLESQKRRR---LM---DDS-----SLAIQ 287
S._lyc_FAMA -----GGAIEFVRELEQLLQCLLESQKRRR---IY---GDTPT-RPLGDSSTPPSPMNQNP 255
A._tha_FAMA -----GGAIEFVRELEQLLQCLLESQKRRR---IL---GET-G-RDMTTTTSSSPITVA 283
A._tha_bHL...)_At3G56980 -----SRSLSKYIPELQEQVKKLIKKEEL---LVQISGQRNTEC 154

```

```

A._coe_SPCH -----PRPLASSLSPRKPLSPRVSL-----PVSPTPTPTSPYK---PRLQ----- 232
A._tha_SPCH -----PPV-----LSPRKPLSPRINHQQIHHLHLF---PISPTPTPTSPYRAIPPQLPLIPOPPL 236
P._tri_SPCH -----SPRKPLSPRLNL-----PNSPTPTPTSPYK---PRLQ----- 226
S._lyc_SPCH -----PRLLTPTSPRKPLSPRML-----PISPTPTPTSPYK---PNAN----- 220
A._coe_MUTE -----SPR-P-----IQL-----TPL----- 81
P._tri_MUTE -----P-----SPRAP---LQL-----ITSSLHPDHHPF----- 97
S._lyc_MUTE -----TPR-P---LQL-----SPTPESS----- 86
A._tha_MUTE -----QTIEP-----SSLGAATTRV----- 89
A._coe_FAMA -----QP-QP-----PLFPMPSPDQIKF----- 302
P._tri_FAMA -----QPAQP-----AFFSPMLPNDQMKL----- 307
S._lyc_FAMA -----SAINP-----HHHQ5---PILFPLP---NEYNI----- 277
A._tha_FAMA -----NOAQP-----LIITGNV---TELEG----- 300
A._tha_bHL...)_At3G56980 -----YVKQP-----PKAV----- 163

```

```

A._coe_SPCH -----YGHLS-----PTIITTSHEPSTATISTTPS---FDSV-KEL A-ANSKSIADVEVKF 278
A._tha_SPCH -----RSYSSLASCSLGDPFPSYSSASSSSPSVSNHE---SSVI-NELV-ANSKSAIADVEVKF 292
P._tri_SPCH -----QGYIS-----PT-MATSLPSPTSSSSSS-INDNI-NELI-ANSKSAIADVEVKF 272
S._lyc_SPCH -----ANKPPEPSPTSSNSS-IDSHVNNELA-ANSKSAIADVEVKF 260
A._coe_MUTE -----PISPG-----TKNL-KELG-ACCNSPVADVEAKI 108
P._tri_MUTE -----PFGNI-----ENDL-KELGAACNSPIADVEAKI 125
S._lyc_MUTE -----PFITH-----NNNF-KELG-ACCNSPVADVEARI 113
A._tha_MUTE -----PFSRIENVMTSTF-KEVG-ACCNSPVADVEAKI 121
A._coe_FAMA -----GEYD-----DTGL-LEET-AENKSLADVEVKV 328
P._tri_FAMA -----VDF-----ETGL-REET-AENKSLADVEVKL 332
S._lyc_FAMA -----L-----EDEI-QEEV-AESKSLADVEVKL 299
A._tha_FAMA -----L-----GGL-REET-AENKSLADVEVKI 322
A._tha_bHL...)_At3G56980 -----ANYIS-----TVSATRL-GDNEV-MVQI-SSSKIHNFISNVL 198

```

```

A._coe_SPCH -----S-GAN-----VLVKTISPRIPGQALKIITALEGHSLEIHSVSISSTD-DTMINSFTIKIG 331
A._tha_SPCH -----S-GAN-----VLLKTVSHKIPGQVMKIIAALEDLAL EILQVNIINTVD-ETMLNSFTIKIG 345
P._tri_SPCH -----S-GPN-----VLLKTVSPRIPGQAVKIVSALEGLALEIHSVISTVDHETMLNSFTIKIG 326
S._lyc_SPCH -----SGAGAN-----VILKTVSPRIPGQAVKIIAALEQLALEIHSVISTID-GTMLNSFTIKIG 315
A._coe_MUTE -----S-GSN-----VVLKVLSTRNRGQITKIIVAVLEKFSFEVLHLNLISSME-DTVLYSFVCIKIG 161
P._tri_MUTE -----S-GSN-----VILKVISRRIPGQIVRIISVLENLSFEIHLNLISSME-DTVLYSFVCIKIG 178
S._lyc_MUTE -----C-GSN-----VMLRTISKRIPGQIVKIINVLEKLSFEIHLNLISSME-DTVLYSFVCIKIG 166
A._tha_MUTE -----S-GSN-----VVLRVVSRRIVGQVKIISVLEKLSFOVLHLNLISSME-ETVLYFFVVKIG 174
A._coe_FAMA -----L-GFD-----ALIKILSRRRPGQLIKTIAALEDLQNLILHTNITIE-QTVLYSFVNVKIA 381
P._tri_FAMA -----L-GFD-----AMIKILSRRRPGQLIKTIAALEDLQNLILHTNITID-QTVLYSFVNVKIA 385
S._lyc_FAMA -----L-GFD-----AMIKILSRRRPGQLIKTIAALEDQMLILHTNITIE-QTVLYSFVNVKIA 352
A._tha_FAMA -----L-GFD-----AMIKILSRRRPGQLIKTIAALEDLHLSILHTNITIME-QTVLYSFVNVKII 375
A._tha_bHL...)_At3G56980 -----S-GLEEDRFVLDMSSSRSGERLFYTLHLQVEKIENYKLNCEELS-QRMLLYL 250

```

	SMF domain	
A._coe._SPCH	IECKLSAEELAHEIQQTFC-----	350
A._tha._SPCH	IECQLSAEELAQQIQQTFC-----	364
P._tri._SPCH	IECQLSAEDLAQQIQQTFC-----	345
S._lyc._SPCH	IECQLSAEELAHQIQQTFC-----	334
A._coe._MUTE	LECQLSVEELALEVQQSFT-----	180
P._tri._MUTE	LECQVSVEELAVEVQQSFF---QDTIITYTEL-----	206
S._lyc._MUTE	LECQLSVEELALEVQKSFT---SSDVLGINEI-----	195
A._tha._MUTE	LECHLSLEELTLEVQKSFV---SDEVIVSTN-----	202
A._coe._FAMA	SESRFTAEDIASSVQIFTFIHASSTL-----	408
P._tri._FAMA	SDSGFTAEDIASSVQIFNFIHANSI-----	412
S._lyc._FAMA	GETRYTADDIANSIQIFSFIAEAIAPYDIN-----	383
A._tha._FAMA	SETRFTAEDIASSIQITSEFIHANTNISGSSNLGNIVFT-----	414
A._tha._bHL...)_At3G56980	-----EECGNS-----YI-----	258
	:.....: :.....:	

Supplemental Figure 3.5. AA alignments with specific domains highlighted.

References

- Ballerini ES, Min Y, Edwards MB, Kramer EM, Hodges SA (2020) *POPOVICH*, encoding a C2H2 zinc-finger transcription factor, plays a central role in the development of a key innovation, floral nectar spurs, in *Aquilegia*. *Proc Natl Acad Sci USA* 117: 22552–22560
- Beerling DJ, Kelly CK (1996) Evolutionary comparative analyses of the relationship between leaf structure and function. *New Phytol* 134: 35–51
- Billings WD, Mooney HA (1968) The ecology of arctic and alpine plants. *Biol Rev Camb Philos Soc* 43: 481–529
- Broman KW, Wu H, Sen S, Churchill GA (2003) R/qtl: QTL mapping in experimental crosses. *Bioinformatics* 19: 889–890
- Bucher SF, Auerswald K, Grün-Wenzel C, Higgins SI, Garcia Jorge J, Römermann C (2017) Stomatal traits relate to habitat preferences of herbaceous species in a temperate climate. *Flora* 229: 107–115
- Buckley TN, John GP, Scoffoni C, Sack L (2015) How Does Leaf Anatomy Influence Water Transport outside the Xylem? *Plant Physiol* 168: 1616–1635
- Chen L, Wu Z, Hou S (2020) SPEECHLESS Speaks Loudly in Stomatal Development. *Front Plant Sci* 11: 114
- Danecek P, Bonfield JK, Liddle J, Marshall J, Ohan V, Pollard MO, Whitwham A, Keane T, McCarthy SA, Davies RM, et al (2021) Twelve years of SAMtools and BCFtools. *Gigascience*. doi: 10.1093/gigascience/giab008
- Doll Y, Koga H, Tsukaya H (2021) The diversity of stomatal development regulation in *Callitriche* is related to the intrageneric diversity in lifestyles. *Proc Natl Acad Sci USA*. doi: 10.1073/pnas.2026351118
- Dong J, Bergmann DC (2010) Stomatal patterning and development. *Curr Top Dev Biol* 91: 267–297
- Dow GJ, Bergmann DC, Berry JA (2014) An integrated model of stomatal development and leaf physiology. *New Phytol* 201: 1218–1226
- Edwards MB, Choi GPT, Derieg NJ, Min Y, Diana AC, Hodges SA, Mahadevan L, Kramer EM, Ballerini ES (2021) Genetic architecture of floral traits in bee- and hummingbird-pollinated sister species of *Aquilegia* (columbine). *Evolution* 75: 2197–2216
- Ehleringer JR (1988) Changes in leaf characteristics of species along elevational gradients in the Wasatch front, Utah. *Am J Bot* 75: 680–689
- Fanourakis D, Giday H, Milla R, Pieruschka R, Kjaer KH, Bolger M, Vasilevski A, Nunes-Nesi A, Fiorani F, Ottosen C-O (2015) Pore size regulates operating stomatal conductance, while stomatal densities drive the partitioning of conductance between leaf sides. *Ann Bot* 115: 555–565
- Filiault DL, Ballerini ES, Mandáková T, Aköz G, Derieg NJ, Schmutz J, Jenkins J, Grimwood J, Shu S, Hayes RD, et al (2018) The *Aquilegia* genome provides insight into adaptive radiation and reveals an extraordinarily polymorphic chromosome with a unique history. *Elife* 7: e36426
- Foster JR, Smith WK (1986) Influence of stomatal distribution on transpiration in low-wind environments. *Plant Cell Environ* 9: 751–759

- Gornall JL, Guy RD (2007) Geographic variation in ecophysiological traits of black cottonwood (*Populus trichocarpa*). *Can J Bot* 85: 1202–1213
- Gudesblat GE, Schneider-Pizoń J, Betti C, Mayerhofer J, Vanhoutte I, van Dongen W, Boeren S, Zhiponova M, de Vries S, Jonak C, et al (2012) SPEECHLESS integrates brassinosteroid and stomata signalling pathways. *Nat Cell Biol* 14: 548–554
- Guo X, Park CH, Wang Z-Y, Nickels BE, Dong J (2021) A spatiotemporal molecular switch governs plant asymmetric cell division. *Nat Plants* 7: 667–680
- Gutschick VP (1984) Photosynthesis model for C3 leaves incorporating CO₂ transport, propagation of radiation, and biochemistry. II: Ecological and agricultural utility. *Photosynthetica* 18: 569–595
- Harris BJ, Harrison CJ, Hetherington AM, Williams TA (2020) Phylogenomic Evidence for the Monophyly of Bryophytes and the Reductive Evolution of Stomata. *Curr Biol* 30: 2001–2012.e2
- Houbaert A, Zhang C, Tiwari M, Wang K, de Marcos Serrano A, Savatin DV, Urs MJ, Zhiponova MK, Gudesblat GE, Vanhoutte I, et al (2018) POLAR-guided signalling complex assembly and localization drive asymmetric cell division. *Nature* 563: 574–578
- Jordan GJ, Carpenter RJ, Brodribb TJ (2014) Using fossil leaves as evidence for open vegetation. *Palaeogeogr Palaeoclimatol Palaeoecol* 395: 168–175
- Katoh K, Standley DM (2013) MAFFT multiple sequence alignment software version 7: improvements in performance and usability. *Mol Biol Evol* 30: 772–780
- Kim E-J, Lee S-H, Park C-H, Kim T-W (2018) Functional role of BSL1 subcellular localization in brassinosteroid signaling. *J Plant Biol* 61: 40–49
- Kim E-D, Dorrity MW, Fitzgerald BA, Seo H, Sepuru KM, Queitsch C, Mitsuda N, Han S-K, Torii KU (2022) Dynamic chromatin accessibility deploys heterotypic cis/trans-acting factors driving stomatal cell-fate commitment. *Nat Plants* 8: 1453–1466
- Körner C (1999) *Alpine Plant Life*. Springer Berlin Heidelberg
- Körner C, Bannister P, Mark AF (1986) Altitudinal variation in stomatal conductance, nitrogen content and leaf anatomy in different plant life forms in New Zealand. *Oecologia* 69: 577–588
- Körner C, Neumayer M, Menendez-Riedl SP, Smeets-Scheel A (1989) Functional Morphology of Mountain Plants 1) Dedicated to Prof. H. Meusel, on the occasion of his 80th birthday. *Flora* 182: 353–383
- Krokhmal I (2015) Functional morphology of the vegetative organs of ten *Aquilegia L.* species. *Annali di Botanica* 5: 17–29
- Kutter C, Schöb H, Stadler M, Meins F Jr, Si-Ammour A (2007) MicroRNA-mediated regulation of stomatal development in *Arabidopsis*. *Plant Cell* 19: 2417–2429
- Kutuzov MA, Andreeva AV (2002) Protein Ser/Thr phosphatases with kelch-like repeat domains. *Cell Signal* 14: 745–750
- Lau OS, Davies KA, Chang J, Adrian J, Rowe MH, Ballenger CE, Bergmann DC (2014) Direct roles of SPEECHLESS in the specification of stomatal self-renewing cells. *Science* 345: 1605–1609
- Letunic I, Bork P (2021) Interactive Tree Of Life (iTOL) v5: an online tool for phylogenetic tree display and annotation. *Nucleic Acids Res* 49: W293–W296
- Liu M, Watson LT, Zhang L (2015) Predicting the combined effect of multiple genetic variants. *Hum Genomics* 9: 18

- Liu Y, Yan J, Qin Q, Zhang J, Chen Y, Zhao L, He K, Hou S (2020) Type one protein phosphatases (TOPPs) contribute to the plant defense response in Arabidopsis. *J Integr Plant Biol* 62: 360–377
- MacAlister CA, Bergmann DC (2011) Sequence and function of basic helix-loop-helix proteins required for stomatal development in Arabidopsis are deeply conserved in land plants. *Evol Dev* 13: 182–192
- MacAlister CA, Ohashi-Ito K, Bergmann DC (2007) Transcription factor control of asymmetric cell divisions that establish the stomatal lineage. *Nature* 445: 537–540
- Machida C, Nakagawa A, Kojima S, Takahashi H, Machida Y (2015) The complex of ASYMMETRIC LEAVES (AS) proteins plays a central role in antagonistic interactions of genes for leaf polarity specification in Arabidopsis. *Wiley Interdiscip Rev Dev Biol* 4: 655–671
- Matos JL, Lau OS, Hachez C, Cruz-Ramírez A, Scheres B, Bergmann DC (2014) Irreversible fate commitment in the Arabidopsis stomatal lineage requires a FAMA and RETINOBLASTOMA-RELATED module. *Elife*. doi: 10.7554/eLife.03271
- McConnell JR, Emery J, Eshed Y, Bao N, Bowman J, Barton MK (2001) Role of PHABULOSA and PHAVOLUTA in determining radial patterning in shoots. *Nature* 411: 709–713
- McKown AD, Guy RD, Quamme L, Klápště J, La Mantia J, Constabel CP, El-Kassaby YA, Hamelin RC, Zifkin M, Azam MS (2014a) Association genetics, geography and ecophysiology link stomatal patterning in *Populus trichocarpa* with carbon gain and disease resistance trade-offs. *Mol Ecol* 23: 5771–5790
- McKown AD, Klápště J, Guy RD, Corea ORA, Fritsche S, Ehling J, El-Kassaby YA, Mansfield SD (2019) A role for SPEECHLESS in the integration of leaf stomatal patterning with the growth vs disease trade-off in poplar. *New Phytol* 223: 1888–1903
- McKown AD, Klápště J, Guy RD, Geraldine A, Porth I, Hannemann J, Friedmann M, Muchero W, Tuskan GA, Ehling J, et al (2014b) Genome-wide association implicates numerous genes underlying ecological trait variation in natural populations of *Populus trichocarpa*. *New Phytol* 203: 535–553
- Meaders C, Min Y, Freedberg KJ, Kramer E (2020) Developmental and molecular characterization of novel staminodes in Aquilegia. *Ann Bot* 126: 231–243
- Metcalf CR, Chalk L, Others (1950) Anatomy of the Dicotyledons: leaves, stem, and wood, in relation to taxonomy, with notes on economic uses. *Anatomy of the Dicotyledons: leaves, stem, and wood, in relation to taxonomy, with notes on economic uses.*
- Minh BQ, Schmidt HA, Chernomor O, Schrempf D, Woodhams MD, von Haeseler A, Lanfear R (2020) Corrigendum to: IQ-TREE 2: New Models and Efficient Methods for Phylogenetic Inference in the Genomic Era. *Mol Biol Evol* 37: 2461
- Mott KA, Gibson AC, O’Leary JW (1982) The adaptive significance of amphistomatic leaves. *Plant Cell Environ* 5: 455–460
- Mott KA, Michaelson O (1991) Amphistomy as an adaptation to high light intensity in ambrosia cordifolia (compositae). *Am J Bot* 78: 76–79
- Mott KA, O’leary JW (1984) Stomatal Behavior and CO₂ Exchange Characteristics in Amphistomatous Leaves. *Plant Physiol* 74: 47–51

- Muir CD (2015) Making pore choices: repeated regime shifts in stomatal ratio. *Proc Biol Sci* 282: 20151498
- Muir CD (2018) Light and growth form interact to shape stomatal ratio among British angiosperms. *New Phytol* 218: 242–252
- Muir CD, Conesa MÀ, Galmés J (2015) Independent evolution of ab- and adaxial stomatal density enables adaptation. *bioRxiv*
- Muir CD, Pease JB, Moyle LC (2014) Quantitative genetic analysis indicates natural selection on leaf phenotypes across wild tomato species (*Solanum* sect. *Lycopersicon*; *Solanaceae*). *Genetics* 198: 1629–1643
- Munz PA (1946) *Aquilegia: the cultivated and the wild Columbines*. Bailey Hortorium
- Nakamura M, Katsumata H, Abe M, Yabe N, Komeda Y, Yamamoto KT, Takahashi T (2006) Characterization of the class IV homeodomain-Leucine Zipper gene family in *Arabidopsis*. *Plant Physiol* 141: 1363–1375
- Ohashi-Ito K, Bergmann DC (2006) *Arabidopsis* FAMA controls the final proliferation/differentiation switch during stomatal development. *Plant Cell* 18: 2493–2505
- Parkhurst DF (1978) The Adaptive Significance of Stomatal Occurrence on One or Both Surfaces of Leaves. *J Ecol* 66: 367
- Parkhurst DF, Mott KA (1990) Intercellular Diffusion Limits to CO₂ Uptake in Leaves : Studies in Air and Helox. *Plant Physiol* 94: 1024–1032
- Parry CC (1874) Botanical Observations in Western Wyoming. *The American Naturalist* VIII: 211–215
- Parvathy ST, Udayasuriyan V, Bhadana V (2022) Codon usage bias. *Mol Biol Rep* 49: 539–565
- Peat HJ, Fitter AH (1994) A comparative study of the distribution and density of stomata in the British flora. *Biol J Linn Soc Lond* 52: 377–393
- Peterson KM, Shyu C, Burr CA, Horst RJ, Kanaoka MM, Omae M, Sato Y, Torii KU (2013) *Arabidopsis* homeodomain-leucine zipper IV proteins promote stomatal development and ectopically induce stomata beyond the epidermis. *Development* 140: 1924–1935
- Pillitteri LJ, Peterson KM, Horst RJ, Torii KU (2011) Molecular profiling of stomatal meristemoids reveals new component of asymmetric cell division and commonalities among stem cell populations in *Arabidopsis*. *Plant Cell* 23: 3260–3275
- Pillitteri LJ, Sloan DB, Bogenschutz NL, Torii KU (2007) Termination of asymmetric cell division and differentiation of stomata. *Nature* 445: 501–505
- Qi S-L, Lin Q-F, Feng X-J, Han H-L, Liu J, Zhang L, Wu S, Le J, Blumwald E, Hua X-J (2019) IDD16 negatively regulates stomatal initiation via trans-repression of SPCH in *Arabidopsis*. *Plant Biotechnol J* 17: 1446–1457
- Richardson F, Brodribb TJ, Jordan GJ (2017) Amphistomatic leaf surfaces independently regulate gas exchange in response to variations in evaporative demand. *Tree Physiol* 37: 869–878
- Robinson JT, Thorvaldsdóttir H, Winckler W, Guttman M, Lander ES, Getz G, Mesirov JP (2011) Integrative genomics viewer. *Nat Biotechnol* 29: 24–26
- Salisbury EJ (1927) I. On the causes and ecological significance of stomatal frequency, with special reference to the woodland flora. *Philos Trans R Soc Lond* 216: 1–65

- Schindelin J, Arganda-Carreras I, Frise E, Kaynig V, Longair M, Pietzsch T, Preibisch S, Rueden C, Saalfeld S, Schmid B, et al (2012) Fiji: an open-source platform for biological-image analysis. *Nat Methods* 9: 676–682
- Schmucker D, Clemens JC, Shu H, Worby CA, Xiao J, Muda M, Dixon JE, Zipursky SL (2000) *Drosophila* Dscam is an axon guidance receptor exhibiting extraordinary molecular diversity. *Cell* 101: 671–684
- Siegfried KR, Eshed Y, Baum SF, Otsuga D, Drews GN, Bowman JL (1999) Members of the YABBY gene family specify abaxial cell fate in *Arabidopsis*. *Development* 126: 4117–4128
- Syed NH, Kalyna M, Marquez Y, Barta A, Brown JWS (2012) Alternative splicing in plants--coming of age. *Trends Plant Sci* 17: 616–623
- Takada S, Takada N, Yoshida A (2013) ATML1 promotes epidermal cell differentiation in *Arabidopsis* shoots. *Development* 140: 1919–1923
- Uhrig RG, Labandera A-M, Moorhead GB (2013) *Arabidopsis* PPP family of serine/threonine protein phosphatases: many targets but few engines. *Trends Plant Sci* 18: 505–513
- Wall S, Violet-Chabrand S, Davey P, Van Rie J, Galle A, Cockram J, Lawson T (2022) Stomata on the abaxial and adaxial leaf surfaces contribute differently to leaf gas exchange and photosynthesis in wheat. *New Phytol* 235: 1743–1756
- Weimer AK, Nowack MK, Bouyer D, Zhao X 'ai, Harashima H, Naseer S, De Winter F, Dissmeyer N, Geldner N, Schnittger A (2012) Retinoblastoma related1 regulates asymmetric cell divisions in *Arabidopsis*. *Plant Cell* 24: 4083–4095
- Weyers JDB, Lawson T (1997) Heterogeneity in Stomatal Characteristics. *In* JA Callow, ed, *Advances in Botanical Research*. Academic Press, pp 317–352
- Yang K, Jiang M, Le J (2014) A new loss-of-function allele 28y reveals a role of ARGONAUTE1 in limiting asymmetric division of stomatal lineage ground cell. *J Integr Plant Biol* 56: 539–549
- Zhang Y, Guo X, Dong J (2016) Phosphorylation of the Polarity Protein BASL Differentiates Asymmetric Cell Fate through MAPKs and SPCH. *Curr Biol* 26: 2957–2965
- Zhang Y, Wang P, Shao W, Zhu J-K, Dong J (2015) The BASL polarity protein controls a MAPK signaling feedback loop in asymmetric cell division. *Dev Cell* 33: 136–149